TECHNISCHE UNIVERSITÄT MÜNCHEN

Lehrstuhl für Entwicklungsgenetik

Generation and analysis of a Pink1 deficient mouse model for Parkinson's disease

Anne Henriette Janice Röthig

Vollständiger Abdruck der von der Fakultät Wissenschaftszentrum Weihenstephan für Ernährung, Landnutzung und Umwelt der Technischen Universität München zur Erlangung des akademischen Grades eines

Doktors der Naturwissenschaften

genehmigten Dissertation.

Vorsitzender:	Univ.-Prof. Dr. K. Schneitz
Prüfer der Dissertation:	1. Univ.-Prof. Dr. W. Wurst
	2. Univ.-Prof. Dr. A. Gierl

Die Dissertation wurde am 08.03.2010 bei der Technischen Universität München eingereicht und durch die Fakultät Wissenschaftszentrum Weihenstephan für Ernährung, Landnutzung und Umwelt am 29.07.2010 angenommen.

Für meine Eltern

TABLE OF CONTENTS

1 ABSTRACT

Parkinson's disease (PD) is the most common neurodegenerative movement disorder with a typical onset in the 7th decade of life. The pathological hallmarks of the disease are the preferential loss of the dopaminergic neurons of the substantia nigra pars compacta and the presence of Lewy bodies in surviving neurons. Clinically the disease is characterized by severe motor symptoms as rigidity, resting tremor, bradykinesia, and postural instability (Abou-Sleiman *et al.*, 2006b). To find out more about the role of the PD-linked gene *Pink1* in the pathogenesis of the disorder, in this research project a knockout mouse model for the *Pink1* (*PARK6*) gene was successfully generated and analyzed. To find out important regions of Pink1 function, a detailed expression analysis of Pink1 during murine embryonic development and in the adult brain was performed. It revealed that Pink1 is ubiquitously expressed, with an age of onset around E9.0. From E10.0 on, Pink1 starts to show a differential expression pattern, with remarkably high levels of Pink1 in some areas of the organism including the developing heart, liver, kidney, and neural tissues. In the adult brain, strong expression of Pink1 can be seen in the striatum and substantia nigra pars compacta. Pink1 deficient mice emerged to be viable and fertile without any obvious signs of abnormality in body weight, posture, morbidity or mortality. Analysis of Pink1 function in mitochondria revealed no changes in mitochondrial morphology, but an impairment of complex I activity in the absence of Pink1. Pink1 mutant mice were further analyzed with regard to characteristical features of PD and it was found that they exhibit normal levels of striatal dopamine and do not show reduced numbers of nigral dopaminergic neurons or motor dysfunctions. Furthermore, Pink1 deficient mice show a slight increase in levels of cortical serotonin. Regarding PD-specific non-motor symptoms, Pink1 mutants exhibit no signs of anxiety or depression-like behavior. However, they display a deficit in social discrimination, which does not result from memory dysfunctions, but rather from an impairment in olfaction, which is one of the early-indicative symptoms known from Parkinson's disease patients. Taken together, the generated Pink1 knockout mouse line does not recapitulate typical

parkinsonian symptoms. However, it provides a genetic link of complex I impairment and PD. Moreover, the observed deficiency in cognitive function and olfaction might characterize this mouse line as a very promising model for the study of early-indicative, non-motor symptoms of Parkinson's disease.

Zusammenfassung

Die Parkinson'sche Krankheit (Parkinson's disease, PD) ist die prävalenteste, neurodegenerative, motorische Krankheit der Welt. Sie tritt typischerweise in der 7. Dekade des Lebens auf. Die charakteristischen pathologischen Symptome der Krankheit sind der bevorzugte Verlust der dopaminergen Neuronen der Substantia Nigra pars compacta und die Entstehung von Proteineinschlüssen, genannt Lewy bodies, in den überlebenden Nervenzellen. Klinische Charakteristika der Krankheit sind schwere motorische Beeinträchtigungen wie Rigidität, Ruhetremor, Bradykinesie und Haltungsinstabilität (Abou-Sleiman *et al.*, 2006b). Um mehr über die Funktion des Parkinson-assoziierten Gens *Pink1* in der Pathogenese der Krankheit herauszufinden, wurde in dieser Arbeit erfolgreich ein *Pink1* (*PARK6*) Knockout Mausmodell generiert und analysiert. Zunächst wurde eine detaillierte Expressionsanalyse von Pink1 während der Embryonalentwicklung und im adulten Maushirn durchgeführt, um die Regionen zu entdecken, die von besonderer Wichtigkeit für die Funktion von Pink1 sind. Dabei wurde herausgefunden, dass Pink1 ab dem Embryonalstadium E9.0 ubiquitär exprimiert ist. Ab E10.0 beginnt das Expressionsmuster von Pink1 spezifischer zu werden und einige Bereiche des Organismus weisen auffallend starke Pink1 Expression auf. Dazu gehören unter anderem das sich entwickelnde Herz, Leber, Nieren und neurales Gewebe. Im adulten Maushirn wurde unter anderem starke Expression von Pink1 im Striatum und in der Substantia Nigra pars compacta detektiert. Pink1 defiziente Mäuse stellten sich als überlebensfähig und fruchtbar heraus. Sie weisen keine offensichtlichen Zeichen von Abnormalität bezüglich des Körpergewichts, der Haltung, der Morbidität und der Sterblichkeit auf. Die Analyse der Funktion von Pink1 in Mitochondrien zeigte, dass die mitochondriale Morphologie in Abwesenheit von Pink1 nicht verändert ist. Es wurde jedoch eine Beeinträchtigung der Aktivität von Complex I festgestellt. Eine weitere Analyse der Pink1 Mutanten bezüglich Parkinson-charakteristischer Symptome zeigte unveränderte Mengen an striatialem Dopamin, eine unveränderte Anzahl an dopaminergen Neuronen der Substantia Nigra und unverändertes motorisches Verhalten. Des Weiteren wurde eine schwache Erhöhung der

festgestellt. Darüber hinaus wurden die Pink1 Mutanten bezüglich Parkinson-spezifischer nicht-motorischer Symptome untersucht. Dabei zeigte sich, dass Pink1-defiziente Mäuse keine Anzeichen von Angstverhalten oder Depression aufweisen. Allerdings zeigen sie eine Störung des Sozialverhaltens. Pink1 Knockouts konnten nicht zwischen einer bekannten und einer unbekannten Maus unterscheiden. Die Ursache für diesen Phänotyp ist jedoch nicht eine Störung des Erinnerungsvermögens sondern eine olfaktorische Dysfunktion, welche als eins der früh auftretenden, nicht motorischen Symptome der Parkinson'schen Krankheit bekannt ist. Zusammenfassend lässt sich feststellen, dass die in dieser Arbeit generierte Pink1 Knockout Mauslinie nicht die charakteristischen Symptome der Parkinson'schen Krankheit aufwies. Es konnte jedoch eine genetische Verbindung zwischen Defiziten der Complex I-Aktivität und der Parkinson'schen Krankheit hergestellt werden. Darüber hinaus charakterisiert die beobachtete Störung der kognitiven Funktion und Olfaktion diese Mauslinie als vielversprechendes Modell um frühe, nicht-motorische Symptome der Parkinson'schen Krankheit zu untersuchen.

2 INTRODUCTION

2.1 Morbus Parkinson

Morbus Parkinson, also called Parkinson's disease (PD) was first described by James Parkinson in 1817 (Jefferson, 1973). It is a major neurodegenerative, progressive movement disorder with mainly late onset and a prevalence of 1.8% in individuals over 65 years (de Rijk *et al.*, 2000). However even juveniles and children can be affected. Clinical characteristics of PD are severe and progressing motor disturbances like bradykinesia, tremor at rest, muscle rigidity, and impaired balance. These motoric manifestations appear late in the progress of the disease, when about 60-70% of the dopamine fibers in the caudate putamen and at least 50% of the dopaminergic neurons in the substantia nigra pars compacta are already lost (Orth & Schapira, 2002; Terzioglu & Galter, 2008). In addition to the motor symptoms, other, non-motoric dysfunctions were implicated in Morbus parkinson, which include insomnia, depression, anxiety, slowness of thinking, dementia, hallucination, decreased motivation, olfactory dysfunction, and autonomic and cognitive impairments (Hughes *et al.*, 2000; Juri *et al.*, 2008; Madeley *et al.*, 1991; Matuja & Aris, 2008; Mindham, 1970; Verbaan *et al.*, 2007; Verbaan *et al.*, 2008). Over a long period of time, these non-motor impairments were not regarded as associated to the disease, and they usually manifest themselves rather early compared to the characteristic motor dysfunctions (Poewe, 2008). The neuropathological hallmarks of PD are predominantly characterized by the loss of the neuromelanine containing dopaminergic neurons of the substantia nigra pars compacta (Forno, 1996). This leads to an intense depletion of dopamine in the striatum, a central component of the basal ganglia that is responsible for induction and control of movement. The surviving neurons may contain Lewy bodies, which are eosinophilic, intracytoplasmic, proteinaceous inclusions mainly consisting of α-synuclein. Furthermore dystrophic neurites called Lewy neurites can be found in the brainstem and cortical areas of PD patients (Jellinger, 2003; Spillantini *et al.*, 1997). Beyond the dopaminergic nigrostriatal system, several other brain areas are affected in PD patients. These include for example the noradrenergic

neurons of the locus coeruleus, the serotonergic raphe nuclei of the brain stem, the dopaminergic VTA neurons, and in later stages of the disease also the dorsal vagal nucleus, the hypothalamus, olfactory bulb, and large parts of the cortex (Ansari & Johnson, 1975; Belin & Westerlund, 2008; Braak *et al.*, 2003; Doty *et al.*, 1988). Up to now PD is known to be non-curable with slow but irreversible disease progression. Different drug treatments were found to ameliorate the symptoms, but they are not capable of arresting or slowing down the pace of neurodegeneration. Although there is fairly good knowledge of the pathology and pathophysiology of the disease, the molecular pathways that lead to PD with all its multifaceted symptoms are unidentified so far. There is evidence that the disease may result from either environmental exposures, hereditary deficiencies, or a combination of both. Based on the discovery of parkinsonism-inducing toxins and the study of post mortem PD brains, the following molecular mechanisms were implied in the pathology of the disease.

2.1.1 Molecular mechanisms implied in Parkinson's disease

2.1.1.1 Protein degradation and the ubiquitin proteasome system (UPS)

Impaired protein folding results in an increase in misfolded proteins, which are generally cytotoxic and need to be removed by protein degradation. This can either happen via the autophagy-lysosomal pathway, or the ubiquitin-proteasome system (UPS). The autophagy-lysosomal pathway is able to degrade oligomers and aggregates of proteins as well as cell organelles. Damaged proteins are encircled by double-membrane bound autophagosomes, which then fuse with lysosomes to form autophagosome-lysosomes. These include acidic hydrolases originating from the lysosomes that digest the incorporated proteins (Rubinsztein, 2006). In the UPS, wrongly folded or damaged proteins get polyubiquitinated by the ubiquitination enzymes, E1, E2, and E3. Polyubiquitination at specific sites targets eukaryotic proteins for ATP-dependent proteolytic degradation via the 26S proteasome (Tanaka *et al.*, 2004). This degradation pathway predominantly

removes short-lived nuclear and cytosolic proteins, and misfolded proteins in the endoplasmic reticulum (Rubinsztein, 2006). One important factor for nigral neuron death is deficient protein degradation and dysfunctional regulation of the UPS (McNaught *et al.*, 2001; Olanow, 2007; Vu & Sakamoto, 2000). The presence of Lewy bodies in PD brain is strong evidence of impaired protein degradation. In addition, impairment of the 26S proteasomal activity was shown in PD substantia nigra (McNaught & Jenner, 2001). Furthermore, the 26S proteasome is an ATP-dependent enzyme. Hence, its function is affected by disturbances in the energy production of a cell, which takes place inside the mitochondria.

2.1.1.2 Mitochondrial impairment and oxidative stress

Impaired mitochondrial function seems to be another important factor in the pathogenesis of PD. Mitochondria are plenteous cell organelles that can be found in every eukaryotic cell. Their most important function in cell biology is the production of energy. This occurs via an electron transport chain of complexes I-V of the mitochondrial respiratory chain, where oxidative phosphorylation of ADP to ATP takes place (Schapira, 2007). PD patients were shown to exhibit decreased activity of complex I of the mitochondrial respiratory chain (Schapira *et al.*, 1989), and a decrease in complex I proteins (Hattori *et al.*, 1991; Mizuno *et al.*, 1989). Another important function of mitochondria is the mediation of apoptotic cell death signals. Additionally, some neurotoxin-studies showed that dopaminergic neurons are more susceptible than other neurons. These studies included neurotoxins like 6-OHDA, MPTP (Schober, 2004), rotenone (Betarbet *et al.*, 2000; Bossy-Wetzel *et al.*, 2004), paraquat (Castello *et al.*, 2007), or maneb (Schober, 2004), which induce distinct features of PD in animal models. All of these toxins affect mitochondria. They cause mitochondrial dysfunction in such that they inhibit complexes I or III of the mitochondrial respiratory chain (see Figure 1), leading to oxidative stress. Oxidative stress is another substantial influence on nigral neurodegeneration (Gotz *et al.*, 1990). Reactive oxygen species (ROS) are radicals generated by a myriad of biochemical reactions. An important

portion of ROS is formed e.g. in the mitochondria. Inside these cell organelles, the main part of the total oxygen consumption occurs. 1-4% of these oxygen molecules are partially reduced in mitochondria and thus form ROS, which are then able to oxidize macromolecules as e.g. lipids, proteins, or nucleic acids. The consequence of these oxidations can be cellular dysfunction, mutagenesis, and cell death (Nakabeppu *et al.*, 2007). Under normal conditions, the ROS are eliminated by intracellular antioxidant systems. If these systems are impaired as a result of aging or disease, insufficient scavenging of ROS results in oxidative stress. Many senescent organisms show for example a decline in reduced glutathione during aging, protein carbonyl concentrations increase with age in all human tissues, and oxidative damage to mitochondrial DNA increases up to 15-fold compared to nuclear DNA (Lotharius & Brundin, 2002). During aging, it seems that all tissues undergo a progressive increase in oxidative stress that could be due to a failing capacity to scavenge free radicals. In certain neurodegenerative diseases, this age-dependent increase in ROS seems to be heightened (Lotharius & Brundin, 2002). Different indicators of oxidative stress were also proven to manifest in various symptoms related to PD: High levels of iron (Dexter *et al.*, 1989b; Youdim *et al.*, 1989), lipid peroxides (Dexter *et al.*, 1989a), hydroxynonenal-modified proteins (Yoritaka *et al.*, 1996), 8-hydroxy-deoxy guanine (Shimura-Miura *et al.*, 1999), and decrease of glutathione (Chinta *et al.*, 2007; Di Monte *et al.*, 1992; Perry *et al.*, 1982) were shown to be involved in neurodegeneration in PD. The metabolism of dopamine itself gives rise to various molecules that can act as endogenous toxins if not handled properly. Dopamine can be enzymatically deaminated by monoamine oxidase (MAO) into its non-toxic metabolite 3,4-dihydroxyphenylacetic acid (DOPAC) and hydrogen peroxide. Alternatively, it can auto-oxidize into toxic dopamine-quinone species, superoxide radicals, and hydrogen peroxide. Superoxide can then be further converted into hydrogen peroxide or reactive peroxinitrite radicals. The normally harmless hydrogen peroxide can also be further metabolized into cytotoxic hydroxyl radicals in a reaction catalyzed by iron, which is present in the substantia nigra in higher amounts than in other brain regions (Lotharius & Brundin, 2002). Hence, nigral dopaminergic neurons are particularly exposed to oxidative stress. In addition, oxidative

stress was also found to increase oligomer formation of α-synuclein. These oligomers impair membrane structures such as mitochondria or synaptic vesicles, which are normally transported along microtubules to release their cargo only at the synapse (Rochet *et al.*, 2004).

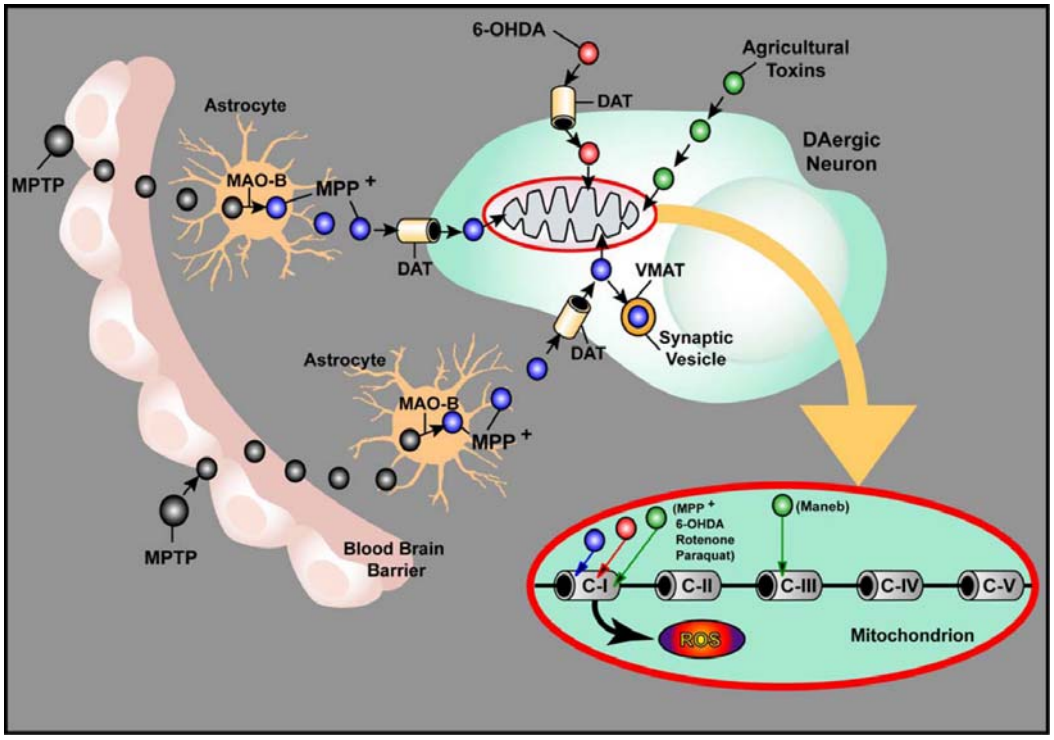

Figure 1: Schematic overview of molecular and intracellular pathways of dopaminergic neurotoxins that cause PD-like features in animal models.
MPTP (black vesicles) easily crosses the blood-brain barrier, is taken up into astrocytes and converted into its active form, MPP^+ (blue vesicles), via catalyzation by MAO-B (monoamine oxidase-B). MPP^+ is released into the extracellular space and specifically uptaken into dopaminergic neurons by the dopamine transporter (DAT). There it is either concentrated in mitochondria, where it irreversibly inhibits complex I activity, or is sequestered into synaptic vesicles (blue vesicle with orange boundary) by VMAT (vesicular monoamine transporter). 6-OHDA (red vesicles), when injected stereotactically into the brain, is selectively taken up by dopaminergic neurons via transport by DAT. There it can also be accumulated in mitochondria and inhibit complex I. Agricultural toxins as e.g. rotenone, maneb (green vesicles), and paraquat, enter dopaminergic neurons and accumulate in mitochondria as well, where they inhibit mitochondrial respiration which leads to generation of reactive oxygen species (ROS) and less ATP synthesis. Adapted from (Schober, 2004). DA; dopamine; MPTP: 1-methyl-4-phenyl-tetrahydropyridine; MPP^+: 1-methyl-4-phenylpyridinium ion; 6-OHDA; 6-hydroxy dopamine; C I – C V: complexes I-V of the mitochondrial respiratory chain.

2.1.1.3 Microtubules and cytoskeletal transport

As mentioned above, long-term, systemic administration of rotenone, a widely used pesticide, leads to selective degeneration of nigral dopaminergic neurons and PD-like locomotor symptoms in animal models (Betarbet *et al.*, 2000). Rotenone functions in two different ways in the cell. In addition to inhibiting complex I of the mitochondrial respiratory chain (Chance *et al.*, 1963), it also depolymerizes microtubules (Brinkley *et al.*, 1974; Marshall & Himes, 1978). MPTP, another complex I inhibitor and PD toxin, also exhibits the ability to depolymerize microtubules (Cappelletti *et al.*, 1999; Cappelletti *et al.*, 2001; Cappelletti *et al.*, 2005). Furthermore it was shown that the PD-linked protein α-synuclein can directly interact with free tubulin. In addition, Lee *et. al*. could show that overexpression of α-synuclein leads to disruption of the microtubule network and microtubule-dependent trafficking, as well as Golgi fragmentation and neuritic degeneration, two commonly known downstream effects of microtubule dysfunction (Lee *et al.*, 2006). Another important discovery with respect to the involvement of microtubule in PD pathogenesis was the finding that parkin, the gene corresponding to *PARK2*-linked parkinsonism, encodes for a protein-ubiquitin E3 ligase that strongly binds to microtubules (Feng, 2006). Moreover, Leucine rich repeat kinase 2 (LRRK2), another gene causing familial PD, was shown to be localized to membraneous and vesicular structures and the microtubule network (Biskup *et al.*, 2006). In 2005, Ren and coworkers found out, that midbrain dopaminergic neurons are selectively more vulnerable than non-dopaminergic neurons to microtubule-depolymerizing agents such as rotenone, colchicine, or nocodazole. One important function of microtubules is the axonal transport of synaptic vesicles via microtubule-based motor proteins. Microtubule depolymerization disrupts vesicular transport which then leads to the accumulation of vesicles in the soma (Ren *et al.*, 2005). Because neurotransmitter-containing vesicles are innately leaky, this increases cytosolic concentrations of the neurotransmitter (Feng, 2006). In dopaminergic neurons these vesicles are loaded with dopamine, whose oxidation produces large quantities of ROS (see 2.1.1.2 Mitochondrial impairment and oxidative stress) and might initiate cell death (Hastings *et al.*, 1996). Like these, various

circumstances might form vicious circles inside nigral neurons that will finally lead to cell death, and hence clinical manifestations of Morbus parkinson. As mentioned above, the disease might result from a combination of environmental exposures and hereditary deficiencies of the following genes.

2.1.2 Familial Parkinson's disease

PD was long considered to be a nongenetic disorder of sporadic origin. But during the last decade linkage analysis and candidate/gene association studies provided findings from different geographical areas, that strengthened the hypothesis that genetic susceptibility plays an important role in PD. Up to the present, 13 genetic loci have been associated with familial PD (Belin & Westerlund, 2008; Mizuno *et al.*, 2008). The corresponding genes of 9 of these loci have been discovered so far, implicating 8 specific genes in PD pathogenesis (see Table 1: Genetic causes of Parkinson's disease).

PARK locus	gene	chromosome	form of PD
PARK1	*α-synuclein*	4q21	AD
PARK2	*Parkin*	6q25.2-q27	AR J
PARK3	unknown	2p13	AD
PARK4	*α-synuclein*	4q21	AD
PARK5	*UCH-L1*	4p14	AD, idiopathic
PARK6	*PINK1*	1p35-p36	AR, EO
PARK7	*DJ-1*	1p36	AR, EO
PARK8	*LRRK2*	12q12	AD, idiopathic
PARK9	*ATP13A2*	1p36	Kufor-Rakeb syndrome, EO PD
PARK10	unknown	1p32	idiopathic
PARK11	unknown	2q36-q37	AD, idiopathic
PARK12	unknown	X	familial
PARK13	*HTRA2/OMI*	2p13	idiopathic

Table 1: Genetic loci associated with Parkinson's disease.
13 genetic loci (PARK1-13) implicated in PD have been discovered so far. UCH-L1: ubiquitin C-terminal hydroxylase 1; PINK1: PTEN induced kinase; LRRK2: leucine rich repeat kinase 2; ATP13A2: ; HTRA2: high temperature requirement A2; AD: autosomal dominant; AR: autosomal recessive; J: juvenile; EO: early onset.

α-synuclein, which corresponds to *PARK1* and *PARK4* induced PD, was the first of the 8 genes discovered (Polymeropoulos *et al.*, 1997). It is abundantly expressed, it can be found in the cytosol, binds to lipids, and is natively unfolded (Vekrellis *et al.*, 2004). In presynaptic nerve terminals, α-synuclein exists in an equilibrium of different states, namely free or plasma membrane/vesicle-bound (McLean *et al.*, 2000). α-synuclein might be involved in synaptic vesicle recycling, storage, and regulation of neurotransmitters (Vekrellis *et al.*, 2004). An important function of α-synuclein is its tendency to form aggregates *in vitro* (Giasson *et al.*, 2000), and mutant α-synuclein protein was shown to form insoluble fibrils (Serpell *et al.*, 2000). These findings imply the misfolding, accumulation and subsequent aggregation of α-synuclein to be important in PD pathogenesis. α-synuclein toxicity is discussed to result from a toxic gain-of-function. Several transgenic mouse lines expressing *α-synuclein* under various different promotors habe been published. Widespread pathology in the central nervous system was reported, however, none of these mutant mouse models were able to replicate the selective cell death of nigral dopaminergic neurons (Maingay *et al.*, 2005). Overexpression of wildtype *α-synuclein* resulted in α-synuclein and ubiquitin-immunoreactive granular inclusions in the cytoplasm and nuclei of cortical and nigral neurons, dopaminergic terminal loss in the basal ganglia, and motor impairments (Masliah *et al.*, 2000). Three different mouse lines used catecholaminergic neuronal expression of transgenic *α-synuclein*, however, none of them showed PD-specific nigral pathology (Matsuoka *et al.*, 2001; Rathke-Hartlieb *et al.*, 2001; Richfield *et al.*, 2002). But the mice showed increased striatal levels of the dopamine transporter (DAT), and enhanced neurotoxicity upon MPTP treatment (Richfield *et al.*, 2002). Furthermore, several mouse models overexpressing *α-synuclein* with point mutations (A30P and/or A53T) were reported. Their symptoms included age-dependent dopamine decrease and motor impairments (Richfield *et al.*, 2002), age-dependent motor impairment and intracytoplasmic neuronal accumulation of α-synuclein and pathological neuronal accumulation of ubiquitin in several areas including striatum and dorsal midbrain. But as in the other overexpressor mouse models, no dopaminergic cell death could be seen (Giasson *et al.*, 2002; Lee *et al.*, 2002). Furthermore an α-synuclein knockout mouse line was published as well. These

mice are viable and fertile. They showed a reduction in the synaptic vesicle reserve pool in the hippocampus, but just a slight decline in striatal dopamine levels (Abeliovich *et al.*, 2000).

Parkin was found to be the gene corresponding to the *PARK2* locus (Abbas *et al.*, 1999). In contrast to common sporadic PD, were Parkin was found to be a component of classical Lewy bodies, analysis of post mortem brains with *PARK2* PD did not show any Lewy bodies in affected brain regions (Farrer *et al.*, 2001). Parkin functions as a ubiquitin E3 ligase, which is another indication for dysfunctions in the ubiquitin-proteasome system in PD. Mammalian Parkin protein is localized in the cytoplasm of postmitotic cells, as well as associated to the outer mitochondrial membrane (see Figure 3), although only a low percentage of Parkin showed this association under normal conditions (Darios *et al.*, 2003). Furthermore Parkin was shown to localize to mitochondria, and it improves mitochondrial biogenesis by regulation of mtDNA transcription and replication in proliferating tumor cell lines (Kuroda *et al.*, 2006). Parkin seems to have a neuroprotective role, which could also be confirmed in different rodent models (Casarejos *et al.*, 2006; Klein *et al.*, 2006; Vercammen *et al.*, 2006). Loss-of-function mutations of the *Parkin* gene are the most frequent cause of early onset autosomal recessive parkinsonism. Several mouse models with loss of Parkin function or protein have been published so far (Goldberg *et al.*, 2003; Itier *et al.*, 2003; Palacino *et al.*, 2004; Von Coelln *et al.*, 2004). Parkin deficient mice showed motor and cognitive deficits, and inhibition of amphetamine-induced dopamine release (Itier *et al.*, 2003). Another mouse model lacking Parkin displayed grossly normal brain morphology, increased striatal extracellular concentrations of dopamine, but no alterations in the latencies for remaining on the rotating rod (Goldberg *et al.*, 2003). Furthermore these animals showed decreased abundance of a number of proteins involved in mitochondrial function or oxidative stress, and decreased levels of proteins involved in protection from oxidative stress, lower serum antioxidant capacity, increased protein and lipid peroxidation revealing an essential role for Parkin in the regulation of mitochondrial function. But electron microscopic analysis of these mice did not reveal any gross morphological abnormalities of striatal

mitochondria (Palacino *et al.*, 2004). Von Coelln *et al.* found that their Parkin null mice showed a loss of catecholaminergic neurons in the locus coeruleus, an accompanying loss of norepinephrine in discrete regions of the central nervous system, and a reduced startle response. Striatal levels of dopamine, and its metabolites DOPAC and HVA, however, were unaffected in these mice (Von Coelln *et al.*, 2004). Although some of these Parkin deficient mouse models even showed changes in or impairment of the dopaminergic system, neither of them displayed a loss of nigral dopaminergic neurons in different stages of age. This suggests that Parkin is not essential for the survival of nigral neurons in mice.

Mutations in the *PARK3* locus correspond the *ubiquitin C-terminal hydroxylase 1* (*UCH-L1*), and were only detected in one German family. Affected family members display clinical signs of idiopathic PD, including early olfactory dysfunction and late cognitive impairment (Leroy *et al.*, 1998). UCH-L1 is one of the most abundant proteins in the brain, solely localized to neurons, and can in addition to its role as a ubiquitin hydroxylase also function as an E3 ligase (Wilson *et al.*, 1988). These functions of UCH-L1 further validate a role of distraction in protein degradation via the UPS in the pathogenesis of Morbus parkinson. Knockout mice for the gene *UCH-L1* were first published as gracile axonal dystrophy (*gad*) mice (Yamazaki *et al.*, 1988). These animals exhibited progressive symptoms such as ataxia beginning at about 80 days of age, followed by tremor, difficulty in moving, and muscular atrophy of the hind limbs. Pathologically, they showed neuroaxonal dystrophy and degeneration in the gracile nucleus of the medulla oblongata and the gracile fascicules of the spinal cord, and they died around 5 to 6 months of age (Yamazaki *et al.*, 1988). In 1999, *UCH-L1* was discovered as the mutated gene in the *gad* mouse model. But since clinical and pathological symptoms of the mice were not consistent with PD pathology, it was suggested that these discrepancies might result from the different mutations which may cause different phenotypes (Saigoh *et al.*, 1999). In 2007, transgenic mice carrying the humanized point mutation in the *UCH-L1* gene were reported to exhibit age-

dependent loss of nigral dopaminergic neurons and accumulation of insoluble UCH-L1 protein in the midbrain (Setsuie *et al.*, 2007).

Pink1 (*PARK6*) linked parkinsonism is characterized by an early onset of recessively inherited disease. Heterozygous *Pink1* mutations are more frequent in sporadic PD patients than in controls, hence Pink1 might be a risk-factor for development of the disorder (Abou-Sleiman *et al.*, 2006a). Pink1 was also seen in the characteristic protein inclusions of PD patients and patients with DLB (dementia with Lewy bodies) (Murakami *et al.*, 2007). Pink1 protein consists of a serine-threonine kinase domain and a mitochondrial targeting motif, it was shown to localize to mitochondria (see Figure 3), and it was the first gene directly implicating mitochondrial function in the pathogenesis of PD. For more detailed information, see 2.2 PTEN induced kinase 1 (Pink1).

Patients carrying mutations in *DJ-1* (*PARK7*) display early-onset parkinsonism due to a loss of function of DJ-1 protein, which is comparable with *Parkin*- and *Pink1*-linked forms of the disease. DJ-1 was just occasionally found in the haloes of Lewy bodies, but it is an essential component of neuronal protein inclusions in diseases typically characterized by tau aggregation (Neumann *et al.*, 2004). DJ-1 is involved in oncogenic mechanisms, control of gene transcription, regulation of mRNA stability, fertilization, and it can function as an antioxidant (Bonifati *et al.*, 2003; Mitsumoto & Nakagawa, 2001). In humans it is expressed ubiquitously, and its expression in the brain is mainly astrocytic. DJ-1 physiologically forms homodimers, and is partially localized to the mitochondrial matrix and inter membrane space (Vila & Przedborski, 2004; Zhang *et al.*, 2005). It was shown that DJ-1 has a protective role and is involved in sustaining the function of the mitochondrial complex I under oxidative stress conditions *in vitro* (Taira *et al.*, 2004), which is another hint that interconnects mitochondria with PD (Figure 3). In the case of *DJ-1*-linked parkinsonism, the disease is also caused by loss-of-function mutations (Goldberg *et al.*, 2005). Several DJ-1 deficient mouse models were reported since 2005. *DJ-1*$^{-/-}$ mice showed reduced evoked dopamine overflow in the striatum, absence of corticostriatal

long-term depression, and hypoactivity in the open field (Goldberg *et al.*, 2005). Another knockout mouse model of *DJ-1* displayed normal levels of striatal dopamine, hypolocomotion when subjected to amphetamine challenge, and increased striatal denervation and dopaminergic neuron loss induced by MPTP (Kim *et al.*, 2005). Chen *et al.* reported that DJ-1 deficiency in mice led to age-dependent and task-dependent motoric behavioral deficits, increased dopamine reuptake rates, and elevated tissue dopamine content (Chen *et al.*, 2005). Further symptoms of DJ-1 deficient mice included subtle locomotor deficits (Manning-Bog *et al.*, 2007), a deficit in scavenging mitochondrial H_2O_2 (Andres-Mateos *et al.*, 2007), hypoactivity and mild gait abnormalities (Chandran *et al.*, 2008). But none of these mouse models lacking functional DJ-1 protein was able to recapitulate the parkinsonian symptom of dopaminergic neuron loss in the substantia nigra (Andres-Mateos *et al.*, 2007; Chandran *et al.*, 2008; Chen *et al.*, 2005; Goldberg *et al.*, 2005; Kim *et al.*, 2005; Yamaguchi & Shen, 2007).

LRRK2 (*leucine rich repeat kinase 2*), the gene corresponding to *PARK8*-linked PD, was discovered in 2004 (Zimprich *et al.*, 2004). Mutations in *LRRK2* are the most abundant genetic cause in familial as well as sporadic PD. *LRRK2* mutations are discussed to result in a toxic gain of function. LRRK2 can be localized to the halo of Lewy bodies, but it is not a major component of these. It is expressed in the brain with highest levels of expression in the striatum (Galter *et al.*, 2006; Higashi *et al.*, 2007). LRRK2 protein was assumed to play a role in cytoskeletal process regulation and seems to be associated with intracellular membraneous structures like golgi, endoplasmic reticulum, lysosomes, and mitochondria (Schiesling *et al.*, 2008). In the case of *LRRK2* mutant mice have not been reported so far.

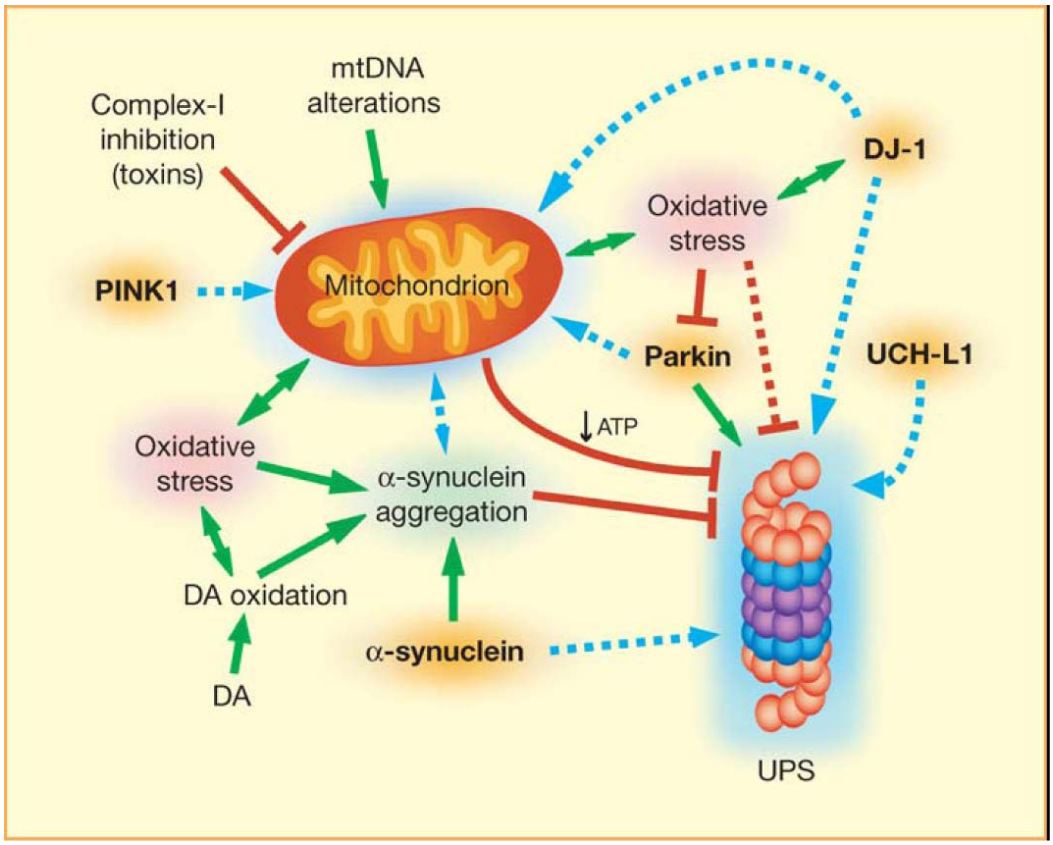

Figure 2: Connections of common pathways underlying PD pathogenesis.
Mutations in *α-synuclein*, *Parkin*, *UCH-L1*, *Pink1*, and *DJ-1* are associated with familial forms of PD through pathogenic pathways that may commonly lead to deficits in mitochondrial and UPS function. PINK1, parkin, and DJ-1 may play a role in normal mitochondrial function, whereas parkin, UCH-L1, and DJ-1 may be involved in normal UPS function. α-synuclein fibrillization and aggregation is promoted by pathogenic mutations, oxidative stress, and oxidation of cytosolic dopamine (DA), leading to impaired UPS function and possibly mitochondrial damage. α-synuclein may normally be degraded by the UPS. Some environmental toxins and pesticides can inhibit complex-I and lead to mitochondrial dysfunction, whereas alterations in mitochondrial DNA (mtDNA) may influence mitochondrial function. Impaired mitochondrial function leads to oxidative stress, deficits in ATP synthesis, and α-synuclein aggregation, which may contribute to UPS dysfunction. Oxidative and nitrosative stress may also influence the antioxidant function of DJ-1, can impair parkin function through S-nitrosylation, and may promote dopamine oxidation. Excess dopamine metabolism may further promote oxidative stress. Mitochondrial and UPS dysfunction, oxidative stress, and α-synuclein aggregation ultimately contribute to the demise of DA neurons in PD. Red lines indicate inhibitory effects, green arrows depict defined relationships between components or systems, and blue dashed arrows indicate proposed or putative relationships. Adapted from (Moore *et al.*, 2005). UPS: ubiquitin proteasome system.

ATP13A2 corresponds to the *PARK9* locus and was initially described as cause of the Kufor-Rakeb syndrome (Ramirez *et al.*, 2006). It displays an early onset of symptoms and rapid disease progression. ATP13A2 in its wildtype form is located in lysosomes, whereas mutant protein is found in the endoplasmic

reticulum and degraded via the ubiquitin-proteasome pathway. These findings further strengthen the hypothesis that protein degradation is involved in PD pathogenesis. No *ATP13A2* mutant mice have been reported up to now.

Omi/ HtrA2 (high temperature requirement A2) is a serine protease of the HtrA family of oligomeric proteases. It is expressed as a 49 kDa proenzyme, that is targeted to the mitochondrial inter membrane space (IMS) where it undergoes proteolytic cleavage, thereby losing its N-terminal mitochondrial localization signal (Vande Walle *et al.*, 2008). However, a fraction of endogenous Omi/HtrA2 was detected in the nucleus of resting cells (Martins *et al.*, 2002), and after apoptotic stimulation, Omi/HtrA2 is released into the cytosol, where it is able to induce caspace-dependent apoptosis (Hegde *et al.*, 2002). Under non-apoptotic conditions it is involved in maintaining mitochondrial homeostasis. The mouse mutant mnd2 (motor neuron degeneration 2), which corresponds to a missense mutation in the protease domain of the mitochondrial serine protease Omi/HtrA2, exhibits muscle wasting, neurodegeneration, involution of the spleen and thymus, and premature lethality. Degeneration of striatal neurons, with astrogliosis and microglia activation begins at around 3 weeks of age, and other neurons are affected at later stages (Jones *et al.*, 2003). Another mouse line carrying mutations in the *Omi/HtrA2* gene displays loss of striatal neurons and premature lethality. Because of the parkinsonian phenotype of these mice, Strauss *et al.* tested *Omi/HtrA2* for linkage to PD. They performed a mutation screening for the *Omi/HtrA2* gene in German PD patients and were able to confirm the link by identifying a novel heterozygous missense mutation and a novel polymorphism that was associated with PD (Strauss *et al.*, 2005). Concerning Omi/HtrA2, another mouse model, completely lacking expression of the gene, was reported in 2004. These animals show no evidence of reduced rates of cell death. On the contrary they display loss of a population of neurons in the striatum, which results in a neurodegenerative disorder with a parkinsonian phenotype and premature death of the mice around 30 days after birth (Martins *et al.*, 2004). Liu *et al.* established a transgenic mouse model with neuron-specific

overexpression of Omi/HtrA2. These mice showed normal development without any sign of apoptotic cell death (Liu *et al.*, 2007).

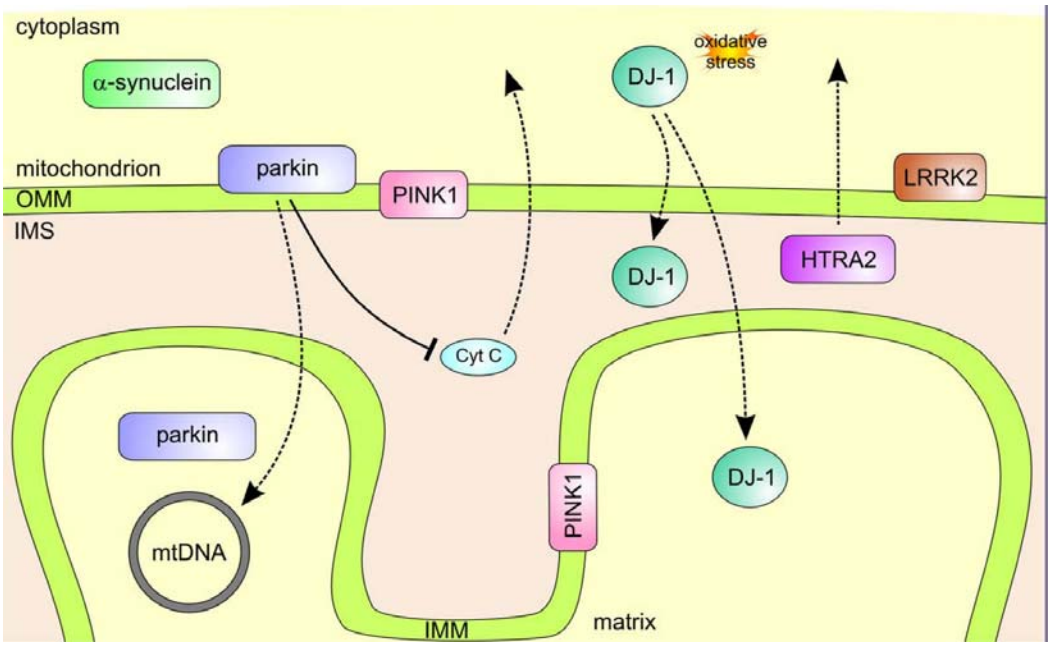

Figure 3: PD genes and their involvement in mitochondria.
Aggregation of α-synuclein might be an upstream actor of mitochondrial alterations. Parkins associates with the outer mitochondrial membrane (OMM) and was shown to be involved in mitochondrial biogenesis by regulation transcription and translation of mtDNA. Pink1 has an N-terminal mitochondrial targeting motif and is localized to mitochondrial membranes, whereas oxidation of a key Cys-residue in DJ-1 leads to its relocalization to mitochondria. LRRK2 resides diffusely throughout the cytosol, but is partly associated with the OMM. HtrA2/Omi is localized in the IMS, from where it is released upon apoptotic stimuli. Adapted from (Bogaerts *et al.*, 2008). IMM: inner mitochondrial membrane.

2.2 PTEN induced kinase 1 (Pink1)

Pink1 was first discovered in 2001 as a gene being transcriptionally activated in PTEN overexpressing cancer cell lines (Unoki & Nakamura, 2001). In 2004, Valente and colleagus identified *Pink1* as the gene responsible for *PARK6*-linked parkinsonism (Valente *et al.*, 2004a). Pink1 exhibits high homology throughout different species. Human Pink1 protein consists of 8 exons spanning 1.8 kb, resulting in a 581 amino acid protein. The N-terminal region of Pink1 contains a predicted cleavable mitochondrial targeting motif for driving interaction with the mitochondrial protein import machinery (Figure 4). Early

studies in mammalian cell lines propose this motif sufficient to drive mitochondrial import (Muqit *et al.*, 2006; Silvestri *et al.*, 2005). For proteolytic cleavage of the mitochondrial targeting motif, there are several possibilities discussed to date, as cleavage occurs within the first 100 amino acids (Beilina *et al.*, 2005; Muqit *et al.*, 2006), and protein fragments containing the N-terminal 34 or 77 amino acids were shown to be sufficient for mitochondrial targeting (Muqit *et al.*, 2006; Silvestri *et al.*, 2005). Overexpression of Pink1 protein *in vitro* revealed two different proteolytically processed forms (~45 kDa and ~55 kDa) in addition to the full length protein (about 66 kDa) of Pink1. These findings support the possibility that processing occurs at multiple cleavage sites. Cellular localization studies of recombinant and endogenous Pink1 protein in mammalian cells showed that Pink1 exists in both the mitochondria and cytosol (Beilina *et al.*, 2005; Gandhi *et al.*, 2006; Haque *et al.*, 2008; Plun-Favreau *et al.*, 2007; Pridgeon *et al.*, 2007; Silvestri *et al.*, 2005), and it was also observed in Lewy bodies and in aggresomes (Gandhi *et al.*, 2006; Muqit *et al.*, 2006). However, by what mechnism Pink1 gets imported into the mitochondria and where it is localized submitochondrially, is still unclear and discussed controversial. Outer membrane removal and protease sensitivity assays, as well as immuno-gold electron microscopy of recombinant Pink1 in cell lines detected the protein on the inner mitochondrial membrane (IMM) (Muqit *et al.*, 2006; Silvestri *et al.*, 2005). Another group could verify localization of recombinant Pink1 in the mitochondrial intermembrane space (IMS) of human embryonic kidney 293 cells (Pridgeon *et al.*, 2007). But in rat brain, Pink1 seems to be localized in the mitochondrial outer and inner membranes (Gandhi *et al.*, 2006). Secondly, Pink1 contains a serine-threonine kinase domain, that spans the biggest part of the protein (Figure 4). It was shown to be capable of *in vitro* autophosphorylation (Beilina *et al.*, 2005; Silvestri *et al.*, 2005), and the kinase activity of Pink1 is essential for protective Pink1 effects (Haque *et al.*, 2008; Petit *et al.*, 2005). However, Pink1 mutations are distributed all over the protein, not just inside the kinase domain (Figure 4). It is possible that they all affect kinase activity, but they might also alter Pink1 function in other ways.

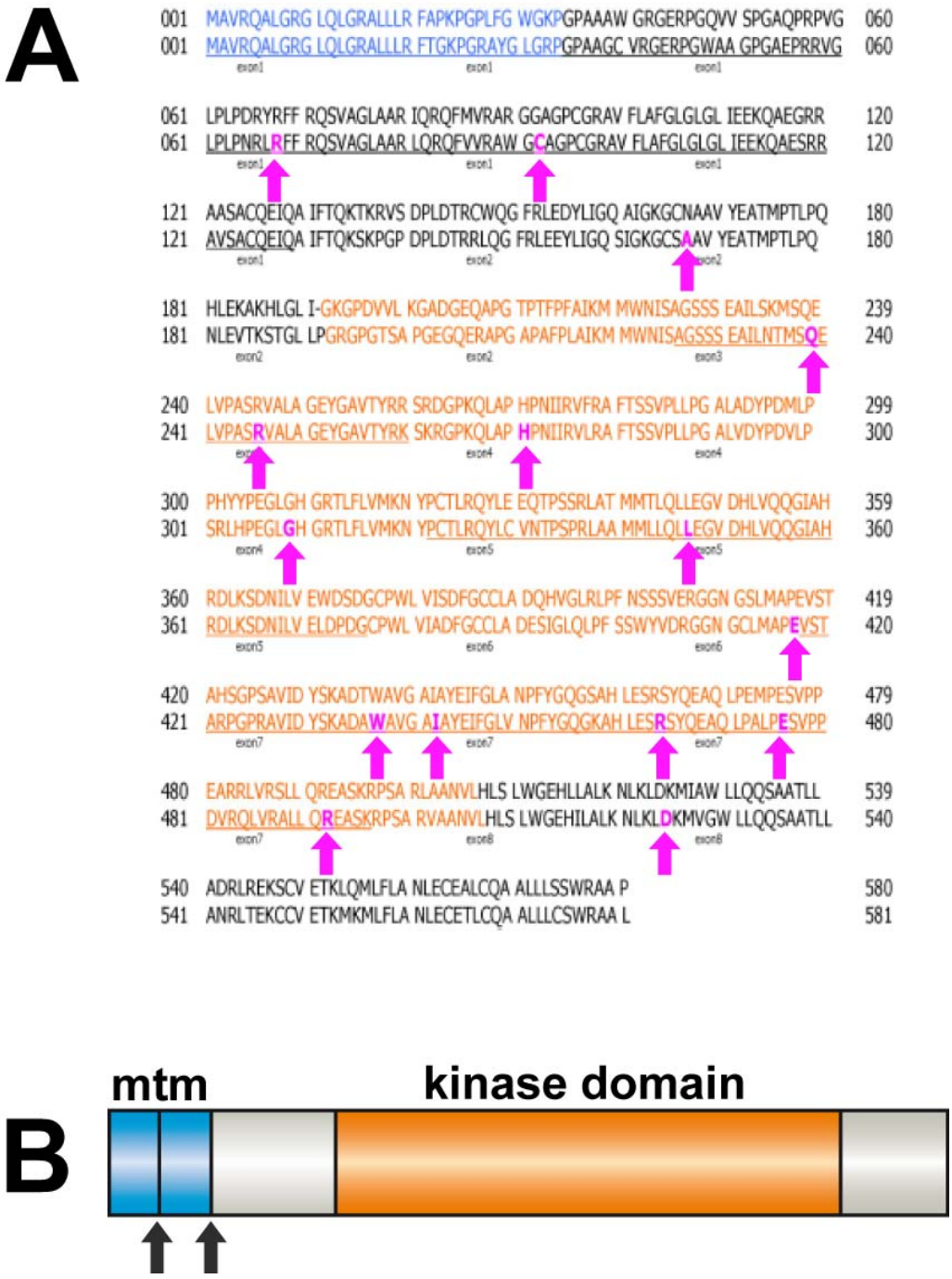

Figure 4: Schematic drawing of Pink1 protein strucure with functional domains.
(**A**) Pink1 mouse (upper row) and human (lower row) amino acid sequence with corresponding exons (alternating underlined and non-underlined) and mutation sites found in *PARK6*-linked PD patients (pink). (**B**) Schematic drawing of Pink1 protein structure. Light blue: Mitochondrial targeting motif; orange; kinase domain; Pink arrows accentuate PD mutations; black arrows show the two putative proteolytic cleavage sites.

2.2.1 Pink1 and apoptosis

A major part of both, the extrinsic and intrinsic apoptosis pathways, is regulated via mitochondria (Zhivotovsky & Kroemer, 2004). Adult neurons are usually programmed to survive throughout lifespan, and premature death of neurons is the cause of several neurodegenerative diseases. Under normal conditions, adult neurons are protected from undergoing cell death by intrinsic antiapoptotic mechnisms, which become activated in response to cellular stress (Mills *et al.*, 2008). Hence it was suggested that Pink1 might play a critical role in mitochondria-triggered apoptosis. In 2005, Petit and colleagues discovered that recombinant Pink1 prevents basal and induced apoptosis in neuronal cell lines, an effect which was abolished by PD-related mutations (Petit *et al.*, 2005). Furthermore, expression of recombinant wildtype but not PD-associated mutant forms of Pink1 blocks mitochondrial cytochrome c release and subsequent apoptotic cell death triggered by proteasomal inhibition or opening of the mitochondrial permeability transition pore (mPTP) in mammalian cells. An N-terminal deletion mutant lacking the mitochondrial targeting motif also failed to block cytochrome c release initiated by UPS inhibition (Wang *et al.*, 2007).

2.2.2 Pink1 deficient *Drosophila* models

Removal of Pink1 in *Drosophila* leads to male sterility, energy depletion, apoptotic flight muscle degeneration, defects in mitochondrial morphology, and increased sensitivity to oxidative stress (Clark *et al.*, 2006; Park *et al.*, 2006; Wang *et al.*, 2006; Yang *et al.*, 2006). Some of the Drosophila models also showed selective degeneration of dopaminergic neurons accompanied by locomotive disturbances, or even embryonic lethality (Park *et al.*, 2006; Wang *et al.*, 2006; Yang *et al.*, 2006). Furthermore lack of Pink1 in the *drosophila* eye resulted in ommatidial degeneration of the compound eye (Wang *et al.*, 2006). Parkin deficient *Drosophila* exhibit a strikingly similar phenotype. Several of the described phenotypes of Pink1 deficiency, including mitochondrial defects, could be rescued by overexpression of Parkin. But Pink1 expression in *Drosophila* lacking Parkin was not sufficient to ameliorate

the symptoms (Clark *et al.*, 2006; Park *et al.*, 2006; Yang *et al.*, 2006). This suggests that Pink1 and Parkin function, at least in part, in a common pathway, with Parkin acting downstream of Pink1. In addition, Bcl2 was sufficient to ameliorate part of the phenotypes (Park *et al.*, 2006), and antioxidants could protect against dopaminergic neuron loss (Wang *et al.*, 2006). This suggests that Pink1 plays a key role in maintaining neuronal survival via an oxidative stress pathway, which needs to be confirmed in other models, as e.g. murine animal models.

2.2.3 Pink1 mouse models

In 2007, Zhou and colleagues reported the generation of an RNAi mediated knockdown of Pink1 in the mouse. However they could not observe degeneration of dopaminergic neurons in the substantia nigra pars compacta. Neither did they find significant differences in the concentrations of dopamine and its metabolites (DOPAC and homovanillic acid) in the striatum (Zhou *et al.*, 2007). Another Pink1 deficient mouse model was published in 2007. In this Pink1 knockout model exons 4-7 are deleted. Likewise, these Pink1 mutant mice showed normal numbers of substantia nigra dopaminergic neurons and levels of striatal dopamine. But the mutant mice exhibited a marked decrease in presynaptic evoked dopamine release and impaired synaptic plasticity of striatal medium-sized spiny neurons (Kitada *et al.*, 2007).

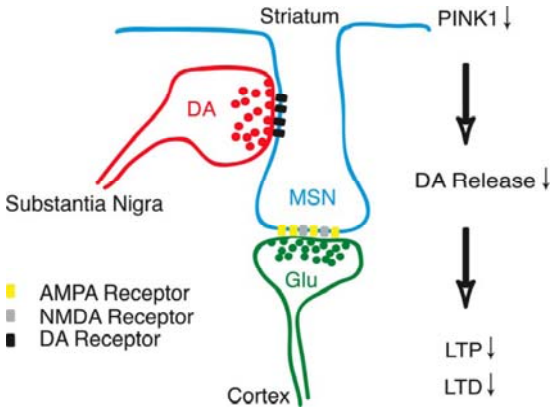

Figure 5: Schematic model for PINK1 function at the nigrostriatal and corticostriatal heterosynapse. The model illustrates the neuromodulatory role of the nigrostriatal input at glutamatergic corticostriatal synapses of striatal medium spiny neurons (MSN). Simultaneous activation of convergent nigrostriatal dopaminergic and corticostriatal glutamergic inputs induces synaptic release of dopamine and glutamate, and activation of postsynaptic D1/D2 and NMDA/AMPA receptors, respectively. Acti-vation of D1 receptors is necessary for the induction of long-term potentiation (LTP) at corticostriatal synapses, whereas activation of both D1 and D2 receptors is necessary for induction of long-term depression (LTD). In the absence of PINK1, impaired dopamine release from nigrostriatal

terminals leads to reduced activation of postsynaptic D1 and D2 receptors, and consequent defects in both LTP and LTD. Adapted from (Kitada *et al.*, 2007).

Furthermore, these mice were examined for impairment of mitochondrial function at the age of 3-4 and 24 months (Gautier *et al.*, 2008). They showed reduced striatal Aconitase activity, no gross changes in the ultrastructure and number of striatal mitochondria, but impaired mitochondrial respiration in the striatum at 3-4 and 24 months of age. In the cerebral cortex, impaired mitochondrial respiration could be detected only at 24 months of age or at 3-4 months of age only upon induction via cellular stress, such as H_2O_2 exposure or heat shock (Gautier *et al.*, 2008).

2.2.4 Pink1 and mitochondrial dynamics

The before mentioned *Pink1* deficient *Drosophila* models (2.2.2 Pink1 deficient *Drosophila* models) showed enlarged mitochondria with disintegrated cristae, which gave the first hints that Pink1 might have a function in mitochondrial dynamics (Clark *et al.*, 2006; Park *et al.*, 2006; Wang *et al.*, 2006; Yang *et al.*, 2006). Mitochondria are ubiquitous cell organelles in eukaryotic cells, where oxidative phosphorylation generates ATP to provide the energy a cell needs. In various cell types they form a network of interconnected mitochondrial tubules that is maintained by an equilibrium of fission and fusion processes (Nunnari *et al.*, 1997; Okamoto & Shaw, 2005). However the dynamic nature of mitochondrial morphology is reflected by differences in their number, size, and positioning in different cell lines, tissues, and organisms. Mitochondria have been intricately linked to the process of apoptosis, and there is growing evidence that this involves the participation of mitochondrial morphology components via regulation of fission/fusion dynamics (Frazier *et al.*, 2006). Several proteins are involved in the process of mitochondrial dynamics. These include for instance Dynamin related protein 1 (Drp1), which promotes mitochondrial fission and was shown to genetically interact with Pink1 (Yang *et al.*, 2008), or Optic Atrophy 1 (OPA1), which is needed for fusion of mitochondria. OPA1 protein is found in the cell in several

constitutions of variable size, which are generated by proteolytic cleavage of the full length protein. These isoforms of OPA1 show different abundance in relation to each other, which changes upon mitochondrial dysfunction. Proteolytic processing of OPA1 was suggested to play a key role in inducing mitochondrial fragmentation and thereby regulating mitochondrial morphology (Duvezin-Caubet *et al.*, 2006). Up to now, the influence of Pink1 on mitochondrial morphology was assessed in different models lacking Pink1. As mentioned above, in *Drosophila* it was shown that Pink1 deficiency leads to swollen mitochondria with fragmented cristae, and this phenomenon could be rescued by overexpression of Parkin, Drp1, or downregulation of OPA1 (Clark *et al.*, 2006; Deng *et al.*, 2008; Park *et al.*, 2006; Park *et al.*, 2009; Poole *et al.*, 2008; Wang *et al.*, 2006; Yang *et al.*, 2006; Yang *et al.*, 2008). In contrast to these results, Gautier and coworkers observed clearly defined, intact cristae and outer membranes in striatal mitochondria of *Pink1*$^{-/-}$mice (Gautier *et al.*, 2008). Furthermore siRNA silencing of Pink1 in human HeLa cells lead to fragmented mitochondria when grown in low-glucose media (Exner *et al.*, 2007). The same effect was seen in fibroblast cells from human PD patients carrying mutations in the *Pink1* gene and in Pink1 deficient SH-SY5Y cell lines (Exner *et al.*, 2007; Lutz *et al.*, 2009), suggesting that Pink1 rather plays a role in mitochondrial fusion.

Taken together, the analysis of toxin induced models and genetically engineered mouse models of PD helped to establish the molecular aetiology of the disease. However, none of the transgenic mouse models completely replicates the symptoms of PD. Therefore, new mouse models are needed to unravel the *in vivo* function of more recently discovered PD genes, to combine them with exposure of environmental risk factors, and to generate mouse models targeting two or more PD genes at once.

2.3 Aim of study

The fundamental aim of this thesis was the generation of a Pink1 knockout mouse model, and the consequential characterization of this mouse model with respect to the involvement of Pink1 in the pathogenesis of Morbus parkinson.

A conditional knockout model of Pink1 in the mouse was thought to be advantagous to avoid possible embryonic lethality of a complete gene knockout. In this project the Cre/loxP system was used. This technique is not only convenient for conditional models, it additionally allows generation of a complete knockout derived from the conditional. *Cre deleter* mice were planned to cross with conditional Pink1 mutants to yield a complete Pink1 knockout mouse line. If Pink1 knockout mice emerged to be viable, as well as capable of reproduction, the use of a conditional model would be obviated and the project would be continued with the analysis of the complete Pink1 knockout mouse line. To allow a quick preliminary investigation of putative Pink1 functions, it was planned to generate mouse embryonic fibroblast (MEF) cell lines from Pink1 knockout mice, the analysis of which would be verified in the mouse model afterwards. In this approach, Pink1 MEF cell lines were planned to be analyzed for their mitochondrial morphology, intending to unravel involvement of mitochondrial function in PD pathogenesis. In order to assess characteristical PD-like symptoms, Pink1 knockout mice were planned to be analyzed in terms of their motoric behavior, quantities of nigral dopaminergic neurons, and the dopaminergic, serotonergic, and noradrenergic system. Furthermore it was planned to analyze some non-motor symptoms of PD as e.g. anxiety and depression-like behavior and cognitive impairment. These analyses aimed to disclose Pink1 function with regard to characteristical clinical symptoms seen in Parkinson’s disease patients.

3 MATERIAL

3.1 Instruments

autoclave	Aigner, type 667-1ST
balances	Sartorius, LC6201S, LC220-S
bottles for hybridization	ThermoHybaid
cassettes for autoradiography	Amersham, Hypercassette
centrifuges	Sorvall, Evolution RC; Eppendorf, 5415D, 5417R; Heraeus, Varifuge 3.0R, Multifuge 3L-R
chambers for electrophoresis (DNA)	MWG Biotech; Peqlab
confocal microscope	Zeiss ISM 510
cryostat	Mikrom, HM560
developing machine	Agfa, Curix 60
digital camera	Zeiss, AxioCam MRc
DNA sequencer	Applied Biotech, DNA Analyzer 3730
freezer (-20°C)	Liebherr
freezer (-80°C)	Heraeus HFU 686 Basic
fridges (4°C)	Liebherr
gel-/blottingsystem “Criterion” (protein)	BioRad
gel-/blottingsystem “Xcell SureLock^{TM} Mini-Cell” (protein / RNA)	Invitrogen
glass pipettes	Hirschmann
glassware	Schott
HPLC machine	Bischoff
HPCL column Bischoff Pronto Sil 120-3C18 AQ (150 x 4 mm)	Bischoff
ice machine	Scotsman, AF 30
incubators (for bacteria)	New Brunswick Scientific, innova 4230
incubators (for cells)	Heraeus
laminar flow	Nunc Microflow 2
light source for microscopy	Leica KL 1500
liquid szintillation counter	Hidex, Triathler

luminometer	Berthold, Orion I
magnetic stirrer / heater	Heidolph, MR3001
microscope	Zeiss Axioplan 2
microwave oven	Sharp R-937 IN
Neubauer counting chamber	Brand
oven for hybridization	Memmert, UM 400; MWG-Biotech, Mini 10; ThermoElectron, Shake'n'Stack
paraffin embedding machine	Leica, EG1160
PCR machine	Eppendorf, MasterCycler Gradient
pH-meter	InoLab, pH Level 1
photometer	Eppendorf, Biophotometer 6131
pipetteboy	Eppendorf, Easypet; Hirschmann, Pipettus akku
pipettes	Gilson; Eppendorf
power supplies for electrophoresis	Consort, E443; Pharmacia Biotech, EPS200; Thermo, EC250-90, EC3000-90
radiation monitor	Berthold, LB122
rotating rod apparatus	Bioseb, Letica LE 8200
shaker	Heidolph, Promax 2020
slide warmer	Adamas instrument, BV SW 85
sonifier	Branson sonifier, cell disrupter B15
stereo microscope	Zeiss, Stemi SV6
thermomixer	Eppendorf, comfort
ultramicrotom	Microm, HM 355S
UV-DNA/RNA-crosslinker	Scotlab, Crosslinker SL-8042; Stratagene, UV-Stratalinker 1800
UV-lamp	Benda, N-36
vortex	Scientific Industries, Vortex Genie 2
water bath	Lauda, ecoline RE 112; Leica, HI1210; Memmert, WB7
water conditioning system	Millipore, Milli-Q biocel

3.2 Chemicals

α-^{32}P-dCTP	Amersham
β-Mercaptoethanol	Sigma, Gibco
[α-thio^{35}S]-UTP	Amersham
1 kb + DNA Ladder	Invitrogen
3,3'-diaminobenzidine (DAB)	Sigma
acetic acid	Merck
acetic anhydride	Sigma
agarose (for gel electrophoresis)	Gibco Life Technologies, Biozym
ammonium acetate	Merck
ampicillin	Sigma
Ampuwa	Fresenius
antifade solution, Aqua Poly/Mount	Polysciences Inc.
ascorbic acid	Sigma
bacto agar	Difco
bacto peptone	BD Biosciences
bicine	Fluka
boric acid	Merck
bovine serum albumin (BSA, 20 mg/ml)	NEB, Sigma
bromphenol blue	Sigma
calcium chloride	Sigma
carrier DNA	Sigma
chicken serum	Perbio
chlorobutanol	Sigma
Complete® Mini (protease inhibitors)	Roche
cresyl violet acetate	Sigma
Criterion™ XT Bis-Tris-gels, 10% (protein)	BioRad
dextran sulphate	Sigma
3,4-Dihydroxybenzylamine (DHBA)	Merck
dithiotreitol (DTT)	Roche
DMEM	Gibco
DMSO	Sigma
dNTP (100 mM dATP, dTTP, dCTP, dGTP)	MBI

EDTA	Sigma
EGTA	Sigma
Eosin Y	Sigma
ethanol absolute	Merck
ethidiumbromide	Fluka
ethylene glycol	Sigma
fetal calf serum (FCS)	PAN, Hybond
Ficoll 400	Sigma
formamide	Sigma
gelatine	Sigma
glucose	Sigma
glycerol	Sigma
HEPES	Gibco
human chorion gonadotropin (hCG/Ovogest)	Intervet
hydrochloric acid (HCl)	Merck
hydrogen peroxide, 30%	Sigma
isopropanol	Merck
kanamycin	Sigma
Lipofectamin™ 2000	Invitrogen
magnesium chloride ($MgCl_2$•$4H_2O$)	Merck
Mannitol	Sigma
MEM nonessential aminoacids	Gibco
MES hydrate	Sigma
methanol	Merck
mineral oil	Sigma
MOPS	Sigma
Nonidet P40 (NP-40)	Fluka
NuPAGE® Novex Bis-Tris gels, 10% (protein)	Invitrogen
1-octanesulfonic acid sodium salt	Sigma
Opti-MEM® I Reduced-Serum medium (1x)	Invitrogen
orange G	Sigma
PBS (for cell culture)	Gibco
perchloric acid	Merck

PIPES	Sigma
polyvinylpyrrolidone 40 (PVP 40)	Sigma
potassium chloride (KCl)	Merck, Sigma
potassium ferricyanide ($K_3Fe(CN)_6$)	Sigma
potassium ferrocyanide ($K_4Fe(CN)_6 \bullet 3H_2O$)	Sigma
potassium hydroxide (KOH)	Sigma
potassium phosphate ($KH_2PO_4 \bullet H_2O$, K_2HPO_4)	Roth
protease inhibitor	Roche
pregnant mare's serum gonadotropin (PMSG)	Intervet
Quick Start Bradford Protein Assay	Bio-Rad
RapidHyb buffer	Amersham
RNaseZAP®	Sigma
Roti-HistoKit® II	Roth
Roti-Histol®	Roth
saccharose	Sigma
salmon sperm DNA	Fluka
SeeBlue® Plus2 Prestained protein ladder	Invitrogen
skim milk powder	BD Biosciences
SmartLadder DNA marker	Eurogentec
sodium acetate (NaOAc)	Merck, Sigma
sodium chloride (NaCl)	Merck
sodium citrate	Sigma
sodium desoxycholate	Sigma
sodium dodecylsulfate (SDS)	Merck
sodium hydroxide (NaOH)	Roth
sodium phosphate ($NaH_2PO_4 \bullet H_2O$, Na_2HPO_4)	Sigma
spermidin	Sigma
sucrose	Sigma
triethanolamine	Merck
TriReagent	Sigma
Tris (Trizma-Base)	Sigma

Triton-X 100	Biorad
Trizol	Invitrogen
tRNA	Roche
trypsin	Gibco
tryptone	BD Biosciences
Tween 20	Sigma
yeast extract	Difco

3.3 Common and stock solutions

loading buffer for agarose gels	15%	Ficoll 400
	200 mM	EDTA
	1 - 2%	orange G
paraformaldehyde solution (PFA, 4%)	4% PFA w/v in PBS	
PBS (1x)	171 mM	NaCl
	3.4 mM	KCl
	10 mM	Na_2HPO_4
	1.8 mM	KH_2PO_4
		pH 7.4
SSC (saline sodium citrate, 20x)	3 M	NaCl
	0.3 M	sodium citrate
		pH 7.0
sucrose solution (20%)	20%	sucrose w/v in PBS
TAE (10x)	0.4 M	Tris base
	0.1 M	acetate
	0.01 M	EDTA
TBE (10x)	0.89 M	Tris base
	0.89 M	boric acid
	0.02 M	EDTA
TBS (10x)	0.25 M	Tris-HCl pH 7.6
	1.37 M	NaCl
TBS-T (1x)	1 x	TBS
	0.05%	Tween 20
TE (Tris-EDTA)	10 mM	Tris-HCl pH 7.4
	1 mM	EDTA
Tris-HCl	1 M	Tris base
		pH 7.5

3.4 Consumables and others

cell culture dishes	Nunc
centrifuge tubes 15 ml, 50 ml	Falcon
cleaning columns	Amersham, MicroSpin S-300 Roche
coverslips for sections on slides	Menzel Gläser, 24 mm x 50 mm; 24 mm x 60 mm
coverslips for MEF cell culture	Menzel Gläser, 12 mm #1
cuvettes for electroporation	Biorad, 0.4 cm cuvettes
developer (*in situ* hybridization)	Kodak D19
embedding pots	Polysciences, Peel-A-Way
films for autoradiography	Kodak, Biomax MS, Biomax XAR, Biomax MR
films for chemiluminescence detection	Amersham, Hyperfilm
filter paper	Whatman 3MM (Kat.-Nr.:3030 917)
filter tips 10 µl, 20 µl, 200 µl, 1 ml	Art, Starlab
fixer (*in situ* hybridization)	Kodak fixer (Kat.-Nr.: 197 1720)
gloves	Kimberley-Clark, Safeskin PFE Safeskin, Nitrile
nylon membrane for DNA transfers	Amersham, Hybond N Plus
one-way needles	Terumo, Neolus 20G, 27G
one-way syringes	Terumo, 1ml, 10ml, 20ml, 50ml
Pasteur pipettes	Brand
PCR reaction tubes 0,2 ml	Biozym
Phase Lock Gel™, heavy	Eppendorf
pipette tips	Gilson
plastic pipettes	Greiner, 1 ml, 5 ml, 10 ml, 25 ml, 50ml
PVDF membrane for Western blotting	Pall Biosciences
reaction tubes (0.5 ml, 1.5 ml, 2 ml)	Eppendorf
slides	Menzel Gläser, Superfrost Plus
tissue cassettes	Merck
tissue embedding molds	Polysciences, Inc.

3.5 Molecular biology

3.5.1 Kits for molecular biology

DNA Highspeed Maxi Prep Kit	Qiagen, Sigma
DNA Mini Prep Kit	Qiagen, Sigma
ECL Detection Kit	Amersham/GE
PCR Purification Kit	Qiagen
QIAquick Gel Extraction Kit	Qiagen
RediPrime™ II DNA Labeling Kit	Amersham/GE
RNeasy Mini Kit	Qiagen
SuperScript™ II First-Strand Synthesis System for RT-PCR	Invitrogen
Vectastain Elite ABC Kit	Vector Labs
Wizard Genomic DNA Purification Kit	Promega

3.5.2 Work with bacteria

3.5.2.1 *E.coli* bacteria strain

DH5α	Gibco Life Technologies

3.5.2.2 Solutions

Ampicillin selection agar	LB agar with 100 µg/ml ampicillin
Ampicillin selection medium	LB medium with 50 µg/ml ampicillin
$CaCl_2$ solution	60 mM $CaCl_2$ 15% glycerol 10 mM PIPES pH 7.0 autoclave or filter sterile
Kanamycin selection agar	LB agar with 50 µg/ml kanamycin
Kanamycin selection medium	LB medium with 50 µg/ml kanamycin
LB (lysogeny broth, (Bertani, 2004)) agar	98,5% LB medium 1,5% Bacto agar
LB (lysogeny broth, (Bertani, 2004)) medium	10 g Bacto peptone 5 g yeast extract 5 g NaCl

	ad 1 l	H_2O

3.5.3 Solutions for Southern blot analysis

Lysis buffer for genomic DNA extraction	0.1 M	Tris pH 8.5
	5 mM	EDTA
	0.2%	SDS
	0.2 M	NaCl
	0.1 mg/ml	Proteinase K
Church buffer	0.5 M	Na_2HPO_4
	0.5 M	NaH_2PO_4
	1%	BSA
	7%	SDS
	1 mM	EDTA pH 8,0
	0.1 mg/ml	salmon sperm DNA
Hybridization Buffer	Rapid Hyb Buffer, Amersham/GE; Church Buffer	
Denaturation solution	0.5 M	NaOH
	1.5 M	NaCl
Neutralization solution	0.1 M	Tris - HCl pH 7.5
	0.5 M	NaCl
Stripping solution	0.4 M	NaOH
Wash solution I	2 x	SSC
	0.1%	SDS
Wash solution II	0.5 x	SSC
	0.5%	SDS
Wash solution III	0.5 x	SSC
	1%	SDS

3.5.4 Western blot analysis

3.5.4.1 Solutions

Blocking solution	4%	skim milk powder in TBS-T
Laemmli buffer (5x)	313 mM	Tris-HCl pH 6.8
	50%	glycerol
	10%	SDS

	0,05%	bromphenolblue
	25%	ß-mercaptoethanol
MES running buffer (10x, for NuPAGE gels)	500 mM	MES
	500 mM	Tris
	1%	SDS
	10 mM	EDTA
		pH 7.2
MOPS running buffer (10x, for Criterion gels)	500 mM	MOPS
	500 mM	Tris
	1%	SDS
	10 mM	EDTA
		pH 7.7
NuPAGE transfer buffer (10x, for NuPAGE gels)	250 mM	bicine
	250 mM	bis-tris
	10 mM	EDTA
	0.05 mM	chlorobutanol
NuPAGE transfer buffer (1x, for NuPAGE gels)	10%	10x transfer buffer
	10%	Methanol
RIPA buffer	50 mM	Tris-HCl pH 7.4
	1%	NP-40
	0,25%	sodium desoxycholate
	150 mM	NaCl
	1 mM	EDTA
Tris glycine blotting buffer (10x)	0.25 M	Tris
	1.92 M	glycine
Tris glycine blotting buffer (1x)	10%	10x blotting buffer
	10%	methanol

3.5.4.2 Antibodies

antibodies	organism	dilution	company
anti-Pink1, polyclonal	rabbit	1:1.000	Abcam
anti-Pink1, polyclonal	rabbit	1:1.000	Novus Biologicals
anti-Omi/HtrA2, monoclonal	rabbit	1:2.000	Abcam
anti-OPA1, polyclonal (Duvezin-Caubet *et al.*, 2006)	rabbit	1:1.000	Kind gift of W. Neupert (LMU München)
anti-β-Actin, monoclonal	mouse	1:10.000	Abcam

anti-ShcA, polyclonal	rabbit	1:1.000	Abcam
anti-mouse, polyclonal, peroxidase-conjugated	goat	1:10.000	Dianova
anti-rabbit, polyclonal, peroxidase-conjugated	goat	1:5.000	Dianova

3.5.5 HPLC analysis

extraction buffer	100 µl	0,5 M EDTA pH 8,0
	1,43 ml	70% perchloric acid
	100 µl	0,1 mM ascorbic acid
	250 µl	0,02 mg/ml DHBA (internal standard)
	ad 0,1 l	H_2O
probe run buffer	7.54 g/l	NaOAc
	7.28 g/l	citric acid
	57 mg/l	EDTA
	114 mg/l	1-octanesulfonic acid sodium salt
	2 mM	KCl
	pH	4.3

3.5.6 Mitochondria extraction

RSB buffer	10 mM	HEPES
	1 mM	EDTA pH 8,0
	210 mM	Mannitol
	70 mM	Saccharose
	1 tablet	protease inhibitor

3.5.7 Enzymes

DNase I (RNase-free)	Roche
PCR-Mastermix 5x	Eppendorf, 5 PRIME
proteinase K	Roche
restriction enzymes	Roche, MBI, NEB, Promega

RNA polymerases (T7, SP6)	Roche
RNase A	Serva
RNasin RNAse inhibitor	Roche
T4 DNA ligase	NEB

3.5.8 Vectors and plasmids

name of plasmid	construct from	description
Pink1 cl 7.13	Barbara di Benedetto	Contains complete targeting construct for conditional Pink1 knockout with all three homologous arms
P1-Pink1 ISH	Barbara di Benedetto	*In situ* probe for Pink1; contains part of Pink1 exon 8 and 3'-UTR; Genebank accession: Pink1-3'UTR/BC607066-1649-2332 bp
P2-Pink1 SB	Barbara di Benedetto	contains Pink1 3'-Southern blot probe which is 680 bp long, starting 97 bp upstream of the end of exon 7, ending 583 bp downstream the end of exon 7 in intron 7 (digested with EcoRI)
pMSSVLT	(Schuermann, 1990)	contains SV40 largeT antigen, used for immortalization of MEF cell lines
pKJ-1 Neo	(Adra *et al.*, 1987)	contains neo resistance cassette, used for Southern blot probe (digested with PstI)
lenti-GFP mDsRed	kind gift of Ravi Jagasia and Chichung Lie	contains cytosolic GFP and mitochondrial DsRed for production of lentiviruses
pMDL	Chichung Lie	structural lentiviral packaging system; contains gag, coding for virion main structural proteins; pol, responsible for

		retrovirus specific enzymes; and rev, which encodes a post-transcriptional regulator for efficient gag and pol expression
pVSVG	Chichung Lie	envelope construct for production of lentiviruses
pRSV-Rev	Chichung Lie	transfer vector for production of lentiviruses; contains Rev cDNA

3.5.9 Oligonucleotides

3.5.9.1 Oligonucleotides for PCR amplification

name	sequence	conditions	size of product
Cre forw	5'-GAT CGC TGC CAG GAT ATA CG -3'	95°C 30 sec 60°C 30 sec 35 x 72°C 30 sec	450 bp (genotyping Cre deleter, mutant allele)
Cre rev	5'-CAT CGC CAT CTT CCA GCA G-3'		
expgk3	5'-CAC GCT TCA AAA GCG CAC GTC TG-3'	94°C 60 sec 65°C 60 sec 30 x 72°C 60 sec	280 bp (alternative genotyping Pink1 conditional knockout mice, mutant allele)
exneo2	5'-GTT GTG CCC AGT CAT AGC CGA ATA G-3'		
Dat Cre up	5'-TCC ATA GCC AAT CTC TCC AGT-3'	95°C 30 sec 58°C 45 sec 35 x 72°C 60 sec	400 bp (genotyping Dat Cre mice, wildtype allele)
Dat Cre low	5'-GTT GAT GAG GGT GGA GTT GGT C-3'		
Dat Cre down	5'-GCC GCA TAA CCA GTG AAA CAG C-3'	95°C 30 sec 58°C 45 sec 35 x 72°C 60 sec	600 bp, with Dat Cre up (genotyping Dat Cre mice, mutant allele)
ex1 f	5'-ATC CAG AGG CAG TTC ATG GT-3'	94°C 30 sec 60°C 60 sec 35 x 72°C 120 sec	580 bp wildtype, 206 bp knockout (for RT-PCR)
ex4 r	5'-GGA AAA CCC GGA TGA TGT TA-3'		
ex8 f	5'-CAG CCA CTC TGC TGG CTG ACA G-3'	94°C 30 sec 60°C 60 sec 35 x 72°C 120 sec	671 bp (wildtype and mutant allele) (for RT-PCR and P1-Pink1 ISH)
3'-UTR r	5'-GGC ATG GAG ACT GTC TTT AAT GCT C-3'		

3.6 Histological methods

3.6.1 Solutions for RNA *in situ* hybridization on paraffin sections

ammonium acetate stock solution (10x)	3 M	NH_4OAc
chamber fluid	50%	formamide
	2x	SSC
hybridization mix	50%	formamide
	20 mM	Tris-HCl, pH 8.0
	300 mM	NaCl
	5 mM	EDTA, pH 8.0
	10%	dextrane sulphate
	0.02%	Ficoll 400
	0.02%	PVP40
	0.02%	BSA
	0.5 mg/ml	tRNA
	0.2 mg/ml	carrier DNA, acid cleaved
	20 mM	DTT
NTE buffer (5x)	0.5 M	NaCl
	10 mM	Tris-HCl (pH 8.0)
	5 mM	EDTA (pH 8.0)
		autoclave
proteinase K buffer (PK buffer)	50 mM	Tris-HCl (pH 7.6)
	5 mM	EDTA (pH 8.0)
		autoclave
triethanolamine solution	0.1 M	triethanolamine pH 8.0 (with HCl)

3.6.2 Antibodies for Immunohistochemistry

antibodies	organism	dilution	company
Anti-Tyrosin Hydroxylase	rabbit	1:10.000	Pel-Freeze® biologicals
Anti-NeuN	mouse	1:500	Millipore
Anti-mouse, polyclonal, peroxidase-conjugated	goat	1:300	Dianova

Anti-rabbit, polyclonal, peroxidase-conjugated	goat	1:300	Dianova

3.6.3 Antibodies for Immunocytochemistry

antibodies	organism	dilution	company
Anti-GFP, polyclonal	chicken	1:200	Aves
Anti-DsRed/RFP, polyclonal	rabbit	1:200	Chemicon
Anti-chicken, Cy™2-conjugated	donkey	1:250	Dianova
Anti-rabbit, Cy™3-conjugated	donkey	1:250	Dianova

3.6.4 LacZ staining solutions

LacZ fix	4%	PFA
	5mM	EGTA
	10mM	$MgCl_2$
	in	PBS
LacZ staining solution	0.1%	X-gal
prepare fresh, protect from light	5mM	potassium ferricyanid
	5mM	potassium ferrocyanid
	in	LacZ wash buffer
LacZ storage solution	5mM	EGTA
	1mM	$MgCl_2$
	in	PBS
LacZ wash buffer	0.02%	NP-40
	0.01%	sodium desoxycholate
	5mM	EGTA
	2mM	$MgCl_2$
	in	PBS

3.6.5 Counterstaining solutions

cresyl violet staining solution	0.5%	cresyl violet acetate
	2.5 mM	sodium acetate

	0.31%	acetic acid
	ad 500 ml	H_2O
	filter	before use

3.7 Cell culture

3.7.1 Embryonic stem cell lines

TBV2	wild type, originates from the mouse strain 129/S2

3.7.2 Mouse embryonic fibroblast cell lines

All mouse embryonic fibroblast cell lines were self-generated from E12-15 embryos of Pink1 ko and Pink1 cko mouse lines. See 7.1 Overview of generated MEF cell lines for complete list of all cell lines.

3.7.3 Solutions

feeder medium	10%	FCS
	in	DMEM
ES cell medium	90%	DMEM
	10%	FCS (PAN)
	$9x10^8$ U	Lif
MEF cell medium	90%	DMEM
	10%	FCS
	1%	Penicillin/Streptomycin
freezing medium (1x)	50%	FCS (PAN for ES cells)
	40%	DMEM
	10%	DMSO
freezing medium (2x)	50%	FCS (PAN for ES cells)
	30%	DMEM
	20%	DMSO
gelatine solution	1%	gelatine
	in	H_2O

3.8 Mouse lines

3.8.1 Wild type mice

C57Bl/6J	wild type mice
CD1	wild type

3.8.2 Cre recombinase expressing mice

Cre deleter	Cre deleter mouse line, Cre expression is X-linked and occurs during early embryogenesis before implantation

3.8.3 Transgenic mice

Pink1 cko	*Pink1* conditional knockout, mouse line with floxed *Pink1* exons 2 and 3, and neo resistance cassette flanked by FRT sites lying between the first loxP site and exon 2 of the Pink1 locus (5.2.1 The conditional Pink1 knockout construct)
Pink1 ko	*Pink1* knockout mouse line, *Pink1 cko* after breeding with Cre deleter line, exons 2 and 3 of the *Pink1* locus are missing throughout the whole body

4 METHODS

4.1 Molecular biology

4.1.1 Cloning and work with plasmid DNA

4.1.1.1 Preparation of plasmid DNA

For the extraction of plasmid DNA the following kits were used: Qiagen DNA Highspeed Maxi Prep Kit, Qiagen DNA Mini Prep Kit and Sigma GenElute HP Plasmid Maxiprep Kit.

For mini-prep one colony was inoculated in 6 ml LB medium containing the appropriate selection marker and incubated over night. 4 ml of the culture was used for preparation of plasmid DNA following the manufacturer's instructions.

In case of maxi-prep one colony was inoculated over day in 5 ml LB medium containing the corresponding selection marker. 200 ml of LB medium with selection marker were inoculated with 1 ml preculture and incubated overnight. The whole culture was used for plasmid preparation following the manufacturer's instructions.

The concentration of DNA was determined by measuring the optical density (OD) at a wavelength of 260 nm in a photometer with one OD_{260} corresponding to 50 µg double stranded DNA per ml.

4.1.1.2 Restriction digestion of plasmid DNA

The amount of restriction enzyme used was usually 2-10 U of enzyme per µg of supercoiled DNA. Exact enzyme concentrations were determined depending on to the amount of plasmid DNA, and the restriction digestion efficiency of the enzyme used. Reaction conditions were adequately adjusted to the chosen enzyme's requirements and manufacturer's instructions. Restriction digestions were incubated from 2 hours to overnight at the appropriate temperature of the chosen enzyme.

4.1.1.3 Separation and isolation of DNA fragments

For separation of vector fragments gel electrophoresis was used. In general 0.8% agarose in 1x TAE gels were used, containing ethidium bromide to visualize the DNA via UV light. The gels were run using 1x TAE buffer. Restriction digestions were supported with 5x loading buffer and applied to gels. In general, smart ladder was used as length standard. Needed fragments were cut out of the gel with a clean scalpel after separation by gel electrophoresis. To avoid DNA damage, gels were visualized just short-time using long wave UV radiation (366 nm) while cutting out the needed fragment, pictures of gels were taken afterwards at short wave UV radiation (254 nm).

Qiagen Gel Extraction Kit was used for DNA extraction from agarose following manufacturer's instructions. Concentration of DNA fragments was determined by measuring the optical density (4.1.1.1 Preparation of plasmid DNA).

4.1.2 Analysis of genomic DNA

4.1.2.1 Isolation of genomic DNA

Mouse tail tips were incubated in lysis buffer for 3-5 hours at 55°C, until they were termed as digested by eye. In case of DNA preparation from mouse embryos, the tissue was put into lysis buffer and cut in pieces as small as possible using scissors, before incubation over night. Genomic DNA from ES cells and mouse tissue was isolated using Promega's Wizard genomic DNA purification kit following the manufacturer's instructions.

4.1.2.2 Southern Blot analysis

10-20 µg of genomic DNA were digested with the appropriate restriction digestion enzyme (20-50 U depending on the digestion ability of the enyzme) in a total volume of 30 µl digestion mix. Restriction digestion mix consisted of the adequate enzyme with its appropriate digestion buffer, 3.3 mM spermidine

for better digestion accuracy, and RNase A to remove all residual RNA. Restriction digestion mix was added to the DNA probes and incubated for 2 hours up to overnight (depending on the digestion ability of the used enzyme) at 37°C. Digested DNA probes were separated by gel electrophoresis using 0.8% agarose in 1x TBE for 14 to 20 hours at 40-65 V. Duration of gel runs and amount of voltage were adjusted depending on the length of the expected bands. Run gels were photographed to control the restriction digestion efficiency. Gels were rinsed in water to wash off removing TBE buffer, and then incubated in 0.25 M HCl for 15-30 min at RT on a shaker, to gain a better blotting efficiency of large-sized DNA fragments. Afterwards, gels were rinsed in water again. To denature and in the next step neutralize the DNA fragments, gels were agitated 2x 15-20 min in denaturation solution, rinsed in water again, and agitated again for 2x 15-20 min in neutralization solution. Single stranded DNA was then blotted overnight via capillary transfer on a nylon membrane using 20x SSC. After DNA transfer the membrane was briefly rinsed with 2x SSC and UV cross-linked. If not used for immediate hybridization, the membrane was dried, put between whatman papers, enclosed in plastic foil, and stored at 4°C.

After crosslinking the membrane was prehybridized at 65°C for at least one hour in a hybridization bottle containing 10 ml Rapid Hyb Buffer or Church Buffer to reduce unspecific binding of radioactive probe. For radioactive DNA labeling with α-^{32}P-dCTP, 50-80 ng of DNA probe was labeled via the Rediprime II kit following manufacturer's instructions. Radioactively labeled reaction mix was centrifugated through a Microspin S-300 column to remove left over nucleotides and radioactively labeled DNA fragments $\leq$ 100 bp. To determine the labeling efficiency, the activity of 1 µl of cleaned up probe was measured in a liquid scintillation counter. After prehybridization, hybridization buffer was poured out of the hybridization bottle, and filled up with fresh buffer to a total of 10 ml again. radioactively labeled probe was denatured at 95°C for 5 min, chilled on ice, and 500.000-1.000.000 cpm probe/ml hybridization buffer were added to the buffer, mixed thoroughly, and poured back into the hybridization bottle. The membrane with the single stranded DNA probes was hybridized either 5-6 hours or over night at 65°C. Residual probe was frozen

at -20°C for up to three weeks. Probes were thawn at RT and the amount of radioactivity was measured again before reuse.

To eliminate unspecifically hybridized probe, the membrane was washed with wash solution II for 40 min at 65°C. The following washing steps were carried out at 65°C for 30 min each, using either wash solution II or III. Number of washing steps and appropriate use of the different washing buffers were adjusted by determining the amount of radiation left on the membrane after each washing step. In case of very resistant background signal the washing temperature was adjusted to 70 or 75°C. The washed membrane was wrapped in plastic foil and exposed to an autoradiography film for 1-3 days at -80°C. In case of weak signals the Biomax MS film was used together with a Biomax screen to intensify the signal six times compared to a conventional film without enhancer screen. After exposition the film was developed in a developing machine. If signals were too weak or too strong, another film was exposed again for 2 hours to 5 days depending on the intended signal intensity.

For additional hybridization with another probe, the signal of the former hybridization was removed by a 20 min incubation at RT in stripping solution. Thereafter the membrane was rinsed with 2x SSC, prehybridization and hybridization were performed as described above.

4.1.2.3 Polymerase Chain Reaction

For amplification of DNA fragments from either genomic DNA or vector DNA, polymerase chain reaction (PCR) was performed. About 20-400 ng of DNA template were used with the appropriate primers and a 5x PCR mastermix in 30 µl total reaction volume.

After initial denaturation of the template DNA into single strands at 95°C, the PCR was performed for 25 to 35 cycles, each consisting of the following steps:

- 30-60 s of DNA denaturation at 95°C
- 30-60 s of annealing at the primer pair specific temperature

- 60-90 s of primer elongation at 72°C, depending on product size

After a final elongation phase for 10 min at 72°C, the samples were chilled at 4°C until processing. For optimal results the cycle times and the annealing temperature were adjusted for each primer pair (sequences can be found under 3.5.9.1 Oligonucleotides for PCR amplification).

PCR products were separated in a 0.8% agarose in 1x TAE gel (4.1.1.3 Separation and isolation of DNA fragments), visualized on a UV desk with short wave UV radiation (254 nm), and photographed for documentation.

4.1.3 Analysis of RNA

Only RNase free solutions, chemicals, and tubes were used for work with RNA to avoid RNA degradation by RNases. For pipetting cleaned pipettes and separate filter tips were used. The equipment used was either commercially purchased RNase-free plastic ware treated with RNaseZAP®. Glass equipment was baked at 180°C for at least 4 hours before use. The working space was cleaned with RNaseZAP® or 100% ethanol and fresh MilliQ water before use. Samples were kept on ice, handled with clean gloves and exposed to air as short as possible to prevent RNA degradation or RNase contamination.

4.1.3.1 Sample preparation and isolation of RNA

For sample preparation from mouse tissue, the animal was asphyxiated with CO_2, decapitated, and the tissue of interest was rapidly dissected. The tissue or further dissected parts were immediately frozen on dry ice or liquid nitrogen to prevent the degradation of RNA. Samples were either stored at -80°C or homogenized with TriReagent or Trizol in a glass homogenizer.

ES or MEF cell samples were trypsinized, detached from their cell culture dishes, washed with 1x PBS, and cells pellets were homogenized with TriReagent or Trizol immediately. After homogenization the samples were either stored at -80°C or further processed right away.

Total RNA was extracted from homogenized samples following manufacturer's instructions. For higher purity, Phase Lock Gel™ heavy was applied following manufacturer's instructions for separation of aqueous and organic phases. Total RNA was resuspended in RNA storage solution and probe concentrations were determined using a photometer, where an OD_{260} of 1 corresponds to 40 µg RNA per ml. If not processed immediately, isolated RNA was stored at -80°C.

4.1.3.2 Reverse transcription of mRNA into cDNA

cDNA was generated by reverse transcription (RT-PCR) of mRNA by the reverse transcriptase SuperScriptII™. 5 µg of RNA were incubated with oligo(dt) primer, dNTPs, SuperScriptII™, and corresponding buffers at 42°C following manufacturer's instructions. Afterwards the RNA template was removed by RNase H digestion, and cDNA samples were run on an agarose gel.

4.1.4 Analysis of protein

4.1.4.1 Western blot analysis

For detection of proteins with specific antibodies, Western blot analysis was carried out. Protein samples were applied to an SDS polyacrylamide gel for electrophoretical separation (SDS-PAGE) according to their size (Laemmli, 1970). Commercially available gel systems from Invitrogen (NuPAGE® Novex) and Biorad (Criterion™ XT) were used. Amounts of protein used varied between 5 and 20 µg of total protein. Protein samples were mixed 1:5 with 5x Laemmli buffer, denatured at 95°C for 3-5 min, chilled on ice and an equal amount of protein was loaded into the pockets of the gel, together with an adequate molecular weight marker depending on the expected protein band size. Gel electrophoresis was performed at 200 V for 1-1.5 hours. Afterwards the gel was blotted on a PVDF membrane, which had been soaked in 100% methanol for activation. Gels were blotted either 1 hour at 30 V with the Invitrogen module, or 2 hours to overnight at 50 V using the Biorad apparatus.

In case of blotting times of more than 2 hours, it was performed at 4°C, instead of RT.

To prevent unspecific binding of the antibodies, membranes were blocked with 4% skim milk or BSA in TBS-T for 1 hour (RT) to overnight (4°C). Afterwards membranes were incubated with the first antibody in TBS-T for 1 hour. To remove unbound antibody membranes were washed three times in TBS-T for 10 min. Thereafter membranes were incubated with the second horseradish-peroxidase-conjugated antibody in TBS-T for 45 to 60 min and washed again three times in TBS-T for 10 min. The detection reaction was initiated with ECL detection reagent following manufacturer's instructions. Then membranes were exposed on chemiluminescent films for 5 s to 10 min depending on the signal intensity. Films were developed using a developing machine.

4.1.4.2 Sample preparation for HPLC analysis

Dissected tissue samples (see 4.6.1 Dissection of cortex, hippocampus, striatum, and ventral midbrain) were thawn on ice, weighed, and the weight of each sample was calculated and recorded. 500 µl extraction buffer was added per sample and they were homogenized using a pestle with mini motor. Additional 500 µl of extraction buffer were added, samples were mixed via pipetting, and centrifuged at 14.000 rpm and 4°C for 15-20 min. Supernatants were sterile filtered using a 0,2 µm filter and stored at -80°C.

For measurements of protein content cell pellets were washed with 500 µl water (MiliQ) and centrifuged at 14.000 rpm and 4°C for 10-15 min. Pellets were suspended in 200 µl 0,1M Tris HCl, pH 8,0 and thoroughly homogenized via a pestle with mini motor. 50 µl protein suspension were mixed with 50 µl 6N NaOH and further diluted 1:5 to 1:20 with water depending on the intensity of reaction color in bradford reagent. 10 µl per sample were mixed with 1 ml bradford reagent, incubated for 5 min at RT, and optical densities were measured in a photometer at 595 nm.

4.1.4.3 Quantification of neurotransmitters via HPLC analysis

For the quantification of catecholamines an HPLC machine with an electrochemical detector was used. It contained an automatic probe supplier and the column oven was used at a temperature of 32°C. A sample run was carried out with a flow rate of 0,7 ml/min.

4.2 Embryonic stem (ES) cell culture

Embryonic stem cells are pluripotent cells. Thus they are able to differentiate into all different cell types *in vitro* as well as *in vivo*. They can be obtained from blastocysts because the inner cell mass of a blastocyst consists of ES cells which will form the embryo, while the outer cells contribute to extraembryonic tissue. This ability of ES cells enables them for various experiments, which is why they are used very diversely in scientific research. One important possibility is the genetic modification of organisms as e.g. the mouse. Genetically modified mouse ES cells can be injected into wildtype blastocysts. When these are then implanted into pseudo-pregnant foster mother mice, they will give birth to chimeras consisting partly of wildtype cells (originating from the inner cell mass of the wildtype blastocyst) and genetically modified cells (originating from the ES cell which were injected into the wildtype blastocyst). If the genetically modified ES cells develop into germ cells of the chimeras, these can be crossed to wildtype mice to pass on their genetic modification to the next generation. These animals now exhibit the genetic modification in all of their cells. With this technique new, genetically modified mouse lines can be created.

Unless you want to generate a specific celltype out of ES cells, it is particularly important to keep them in a pluripotent and consequentially undifferentiated state, which means ES cells need to be cultured under special conditions (Smith *et al.*, 1988; Williams *et al.*, 1988). Therefore the cultivating medium was supplemented with leukemia inhibiting factor (LIF) and specially tested fetal calf serum (FCS), and ES cells were grown on mitotically inhibited fibroblast cells (see 4.2.1 Preparation of feeder cells). Furthermore, their

growth and condition was watched every day, and they were splitted every 1-3 days. The exact time intervals between splitting were estimated depending on their confluency to avoid either extinction of a cell line by too high dilution, or confluent growing resulting in cell differentiation. In general culture dishes with ES cells were kept in an incubator under a 5% CO_2 atmosphere at 37°C. For passaging, picking, and any other experiments, cells were worked at under a sterile cell culture hood, trying to keep them out of the incubator as short as possible.

TBV2, the mouse ES cell line used, was created at the Institute of Developmental Genetics of the Helmholz Zentrum München by Veronique Blanquet and originates from the mouse strain 129/S2.

4.2.1 Preparation of feeder cells

Feeder cells are mitotically inactivated primary mouse fibroblast cells. They need to be resistant for the chosen selection marker used in later transfections. Primary neomycin resistant fibroblasts were obtained from embryos of the transgenic mouse strain C57Bl/6J-Tg(pPGKneobpA)3Ems/J at the age of E14.5 to E16.5 under sterile conditions. Cultivated primary fibroblasts were expanded for two passages and grown on 10 cm cell culture dishes until confluence. For mitotical inactivation, cells were incubated with medium containing 10 µg/ml mitomycin c for 2 hours at 37°C. After intensive washing with PBS, feeder cells were trypsinized and plated on a fresh cell culture dish or frozen in 1x freezing medium at -80°C for further use. Feeder cells were plated at a density of 2-2.5 x 10^4 cells/cm^2 at least one day before plating of ES cells to be able to see any feeder cell contamination prior to use.

4.2.2 Splitting of ES cells

For expansion, ES cell densitiy was controlled every day and ES cells were splitted regularly every 1-3 days before they started growing confluent. At this stage the cells should form round, distinct, light breaking colonies. After visual

control of the cells via microscope, medium was removed and the cells were washed with PBS. To detach them from the surface they were treated with trypsin 5 min at 37°C. The reaction was stopped by adding at least an equal amount of medium to the cells and the suspension was resuspended carefully by pipetting up and down several times. The cell suspension was splitted on fresh culture dishes in a dilution depending on the desired amount of cells per dish. Since this procedure is very stressing for ES cells and can harm them, it was always performed as carefully and quickly as possible. In case of specifically vulnerable ES cell lines, the cell supsension was centrifuged 4 min at 1200 rpm, the trypsin containing medium was sucked of carefully without touching the cell pellet, cells were resuspensed in fresh medium, and distributed on fresh feeder coated cell culture dishes.

For determination of cell number, 10 µl of cell suspension were pipetted in a Neubauer counting chamber. ES cells were counted in each of the four quadrants, and for averaging, numbers were added and divided by four. The averaged counted cell number multiplied by 10^4 corresponds to the number of cells per ml cell suspension.

4.2.3 Freezing and thawing of ES cells

ES cells can be conserved for later use by freezing at very low temperatures. Cells were trypsinized (4.2.2 Splitting of ES cells), and the reaction was stopped by adding medium. 10 µl of cell suspension were counted while the remaining suspension was centrifuged 4 min at 1200 rpm. The cell pellet was carefully resuspended in precooled 1x freezing medium, and splitted to an appropriate number of cryovials (usually 10^6 cells in 1 ml freezing medium per vial). ES cells survive the freezing process best when the temperature decreases very slowly. Therefore the vials were frozen in an isopropanol containing freezing container, which when frozen takes several hours until it reaches the final temperature of -80°C. During the next 1-3 days the vials were transferred into liquid nitrogen for long term storage or remained at -80°C for storage of 3 to 6 months at the most. Cells on a 96-well plate were trypsinized with 30 µl trypsin and resuspended in 70 µl medium to stop the

reaction. An equal amount (100 µl) 2x freezing medium was added to achieve a final contrencation of 1x freezing medium. For slow temperature decrease during the freezing process, 96-well plates were wrapped in cellulose and put in paperback boxes at -80°C.

For thawing, either cryovials or multi-well plates were wrapped in a plastic bag and put into a 37°C water bath. After thawing cells in cryo vials were resuspended in at least 5 ml of prewarmed medium. To remove the cell-toxic DMSO from the medium they were centrifuged, resuspended in fresh medium and plated on an appropriate amount of cell culture dishes. Cells in multi well dishes were centrifuged after thawing. Very carefully the freezing medium was sucked off. Fresh, prewarmed medium was added to the wells and cells were pipetted carefully to resuspend them. In both cases the medium of freshly thawed cells was changed early the next day to eliminate all residual traces of DMSO.

4.2.4 Electroporation of ES cells

When cells are electroporated at a certain voltage, their cell membranes become permeable for a short time. During this time, foreign DNA can enter the cells. This method can be used to plant DNA into the ES cells. Circular plasmids stay transiently in the cells, while linearized DNA can be stably integrated into the genomic DNA of a cell. For genomic manipulation in a certain locus, vector constructs are cloned with long (several kb) homologous arms surrounding the genetically modified part of the gene of interest. If homologous recombination takes place, the genetically manipulated gene is then stably inserted into the genome.

For each single electroporation 5×10^6 - 10^7 ES cells were electroporated. Cells were trypsinized, centrifuged 4 min at 1200 rpm, washed with PBS, centrifuged again and resuspended in 800 µl PBS containing up to 50 µg of the appropriate DNA for electroporation. The cell-DNA suspension was transferred into a precooled electroporation cuvette and electroporated with

300 V and 500 µF for 2 ms. After electroporation cells were incubated on ice for 5 min, then diluted with 1000 µl medium, and plated on an appropriate number of feeder cell culture dishes (10^7 cells on 3 10 cm-dishes). The medium was changed the next day, selection was started on the second day after electroporation.

4.2.5 Selection and picking of recombined clones

To select ES cell clones with stably integrated modified DNA, the appropriate antibiotic was added to the medium. When a neomycin resistance cassette was cloned into the vector, Geneticin (G418, a neomycin analog) can be used for selection at a concentration of 100 – 150 µg/µl. Only cell clones with the neomycin resistance cassette are able to produce the neomycin resistance gene and therefore survive and form colonies, while all cells without resistance should die during selection. Selection medium was used for 7 days. Many vector constructs are cloned with a diphteria toxin A gene downstream (3') to the end of the 3'-homologous arm. Gancyclovir was added to the medium 4 days after electroporation. This drives the expression of the toxic substance in all cell clones that have integrated any 3'-part of the vector backbone, and leads to cell death of clones with unspecific integration anywhere in the genome. During selection ES cells do not need to be splitted since a lot of cells are expected to die. So the surviving colonies should be so few that there is no likeliness for them to grow confluent and differentiate. But it is very important to keep a steady concentration of antibiotic, therefore cells were supplied with fresh medium every day.

After 7 days of selection and 3 days of gancyclovir treatment, the remaining ES cell clones formed round, light breaking, conspicuous colonies. To pick these colonies, medium was removed from the cell culture dishes, and colonies were picked with a 20 µl pipette into a pointed shape 96-well plate. After a maximum time of 45 minutes the clones were trypsinized with 30 µl trypsin, 70 µl was added to stop the enzymatic reaction, cells were carefully pipetted up and down several times to detach and dispense them, and the suspension was pipetted on a fresh feeder-coated 96-well plate. Medium was

changed early the next day to remove trypsin from the medium. The clones were carefully observated the next days, and they were splitted either 1:2 or 1:3 depending on their density on two feeder coated 96-well plates two days after picking. Cell densities were controlled every day and over the next days there were synchronized and expanded to two copies on feeder-coated 96-well plates for later use of cells and two copies on gelatine coated 96-well plates to avoid any feeder cell contamination for DNA extraction. ES cells on feeders were frozen in 1x freezing medium at -80°C (4.2.3 Freezing and thawing of ES cells), while cells on gelatine were allowed to grow 100% confluent, washed with PBS and frozen at -20°C for genomic DNA extraction.

4.2.6 Screening for positive homologous recombination

Gelatine coated cell plates were either used directly or thawn for 30 min at RT for genomic DNA extraction (see 4.1.2.1 Isolation of genomic DNA). Genomic DNA was screened by southern blot (4.1.2.2 Southern Blot analysis) for confirmation of homologous recombination.

4.3 Mouse embryonic fibroblast (MEF) cell culture

Mouse embryonic fibroblast (MEF) cells are less vulnerable than ES cells. Since they are already differentiated, they do not need specific culture conditions or media additives. For MEF cell survival it is important that the cells have physical contact to each other. They grow in very flat, blotch-like shapes and can form long processes which reach their neighboring cells. When MEF cells are confluent, they start growing on top of each other, but at a certain density they start dying.

In general MEFs were grown on plain cell culture dishes in a 37°C incubator under a 5% CO_2 atmosphere. In general, medium was supplied with 10% FCS and 1% penicillin/streptomycin. Cell density and condition was controlled regularly and cells were splitted every 1-7 days depending on their density. For best conditions cells were kept at 40-90% confluency.

4.3.1 Generation of MEF cell lines

For the generation of MEF cell lines, mouse breedings pairs were set up and vaginal plugs of the females were controlled and recorded. 12-15 days after fertilization, female mice were asphyxiated with CO_2. Uteri were taken out, put in 1x PBS and cooled on ice. Since dissection has to be done under the microscope, all instruments and surroudings were cleaned thoroughly with 100% ethanol, dissection was performed in comercially available, sterile petridishes filled with sterile 1x PBS. Embryos were dissected out of the uteri. Heads were excised from the rest of the bodies, collected for genomic DNA extraction and genotyping, and either straightly processed or frozen at -20°C. Torsos were opened ventrally, and all inner organs and large blood vessels were removed under the microscope. Residual tissue was immediately transferred under a sterile cell culture hood and collected in 6-well cell culture plates. The tissue was minced with scalpels, while using a fresh, sterile scalpel for every embryo. During mincing the scalpel causes a lot of scratches on the bottom of the cell cultures dishes. The irregular surface of the wells is not only harmless, but even wanted, because in this condition fibroblasts attach better to the bottom of the culture dish. 1 ml of medium, containing 50% FCS, was added to every well, and cell culture dishes were put in a 37°C incubator with a 5% CO_2 atmosphere. On the next day, medium was carefully sucked out of the wells via pipettes with 1 ml tips and replaced by fresh medium. On the second day, large, unattached parts of tissue were removed from the cultures and medium was changed. Over the next 7 days, the FCS content of the medium was gradually reduced from 50% to 10%. The scratches on the bottom of the cell culture dishes create several different compartments, in which fibroblasts grow differently all over the well. In case of highly diverse distribution of cell densities, cells were tryplated by trypsination and seeding on fresh 6-well dishes without dilution. Cell confluency was controlled every day and as soon as the fibroblasts were grown dense enough, cells were splitted on 10 cm dishes. The exact time point of splitting was chosen independantly for every single cell line in regard to its cell density.

4.3.2 Splitting of MEF cells

MEF cells density and condition was controlled every 1-2 days. They were splitted every 1-7 days depending on the cell density, trying to keep them always between 40% and 90% confluency. When MEFs were highly confluent or starting to grow on top of each other, they were splitted to a desired amount of fresh cell culture plates. Splitting procedure was performed as in 4.2.2 Splitting of ES cells.

4.3.3 Freezing and thawing of MEF cells

Preservation at very low temperatures is also possible for MEF cells, as for ES cells. MEF cell freezing and thawing was performed as in 4.2.3 Freezing and thawing of ES cells. MEF cells were kept at -80°C for up to 12 months for working stocks, and frozen in liquid nitrogen for conservation.

4.3.4 Immortalization of MEF cell lines

Primary MEF cell cultures grow nicely and with a high growth rate until about 5-15 passages after MEF cell preparation from the embryo. Soon their growth rate slows down dramatically until cell densities are very low and all cells die. To work with established cell lines, which can be passaged over a very long period time without extinction, primary MEF cells can be immortalized.

4.3.4.1 3T3 cells

For immortalization of primary MEF cell lines, two different methods were used. The first method was modified from the 3T3 method (Todaro & Green, 1963). Primary fibroblast cultures were controlled every day and splitted every 3-10 days according to their cell density. Usually 5-15 passages after MEF cell generation, the growth rate of fibroblasts slows down very fast, until they die. To prevent cell death and to high dilution of cells, MEFs were either splitted or

tryplated every 3-10 days for a time period of at least 6 months. During this time, spontaneous mutation can occur, leading to cancerous growth behavior of the cells and thus immortalization. A negative effect of this method is, that one cannot be sure what kind of spontaneous mutation might have occured in the cells genome, and cell lines might show a great variety. Hence different cell lines, can prove not be genetically equal, although they underwent the same protocoll. It is therefore not always convenient to compare e.g. knockout and control cell lines which were immortalized by this method. Therefore we decided to use another immortalization method in parallel.

4.3.4.2 SV40 largeT antigen transfection

For this kind of immortalization, MEFs were transfected with SV40 largeT antigen (Jensen *et al.*, 1963; Koprowski *et al.*, 1963) via Lipofectamin™ 2000. For this purpose, MEFs were splitted on 6 cm cell culture dishes and grown until they reached 70-90% confluency. 5 µg of sterile DNA (SV40 largeT antigen, unlinearized plasmid) was added to 500 µl of Opti-MEM® I Reduced-Serum medium (1x), 12,5 µl Lipofectamin™ 2000 were added to another 500 µl of Opti-MEM® I Reduced-Serum medium (1x), and both were incubated for 5 min at RT. The two solution were pipetted together, mixed gently and incubated for 20 min at RT so that Lipofectamin™ 2000 can form complexes with the DNA. Medium was removed from cell culture dishes, they were washed with 1x PBS and supplied with 4 ml fresh, prewarmed medium and 1 ml of the transfection mix, and put back into a 37°C incubator under 5% CO_2 atmosphere. Medium was changed the next day.

Established MEF cell lines of both methods of immortalization were passaged for at least 6 months until they were at passages between 40 and 55, before they were used for any kinds of experiments.

4.3.5 Isolation of mitochondria from MEF cells

MEF cells were cultured in big cell culture flasks (175 cm^2) or cell culture dishes until they reached 70-80% confluency. Cells were trypsinized (4.3.2 Splitting of MEF cells), washed with 1x PBS, collected in eppendorf tubes, and either frozen at -80°C or further processed immediately. An equal amount of 5 mM EDTA in 1x PBS was added to the cell pellet, and the suspension was centrifuged at 750 g for 10 min at 4°C. Cells were kept on ice during all following steps. The cell pellet was resuspended in 1 ml RSB buffer, centrifuged at 750 g for 10 min at 4°C, and resuspended again in 1 ml RSB buffer. Now cells were homogenized by passaging them carefully, through a 25G needle fitted to a 5 ml syringe, while trying to avoid any bubbles. The homogenate was centrifuged at 2.000 g for 10 min at 4°C. The remaining pellet, consisting of nuclei and whole cells, was resuspended again in RSB buffer for further homogenization steps. After centrifugation the post-nuclear supernatant (PNS) was centrifuged at 16.500 g for 10 min at 4°C. The post-mitochondrial supernatant (PMS) was removed by pipetting into another eppendorf cup, and the remaining crude mitochondria pellet was resuspended in 40-80 µl RSB buffer and stored on ice. The leftover nuclei-cell pellet from the first homogenization step was homogenized again and the whole procedure from homogenization to resuspension of crude mitochondria pellets was performed again for 3-4 times until almost no crude mitochondrial pellet was left. Crude mitochondria resuspensions of the same cell lines were pooled and protein concentrations were determined via Quick Start Bradford Protein Assay following manufacturer's instructions.

4.4 Lentiviruses

4.4.1 Generation of lentiviruses

HEK 293 cells were were cultured on twelve 10 cm culture dishes until confluency. 12 ml Opti-MEM® I Reduced-Serum medium (1x) was mixed with 600 µl Lipofectamin™ 2000 and incubated for 5 min at RT. Another 12 ml Opti-MEM® I Reduced-Serum medium (1x) were mixed with 90 µg of GFP

mDsRed, 60 µg pMDL, 22,8 µg pRSV-Rev, and 30 µg pVSVG DNA (see 3.5.8 Vectors and plasmids). Lipofectamin solution and DNA-Opti-MEM® solution were pipetted into a 15 ml tubes, each tube containing 3 ml of both solutions. Tubes were gently inverted 3-4 times and incubated 20 min at RT. After inbucation 2 ml of the mix was added dropwise to each of the twelve 10 cm culture dishes. Dishes were gently shaken and put in a 37°C incubator under 5% CO_2 atmosphere. 5 hours after infection cells were supplied with fresh medium, and incubated for another 2 days. After the 2 day incubation media containing virus particles were transfered into 50 ml conical tubes, centrifuged 3 min at 2000 rpm, supernatants were filtered through a 0,22 µm pore filter, and centrifuged at 4°C and 19.400 rpm for 2 h. Pellets containing the viruses were dissolved in 700 µl PBS per tube and incubated over night for better resolution. On the next day solutions in all tubes were mixed by pipetting up and down 30 times, transfered to one ultracentrifugation tube, and centrifuged again at 4°C and 19.400 rpm for 2 h. The pellet was resuspended in 50 µl cold PBS by pipetting up and down several times. The suspension was transfered to a fresh tube, 50 µl of PBS was used to wash the previous tube and added to the fresh one. After a quick spin the left over supernatant was portioned into 5 ml aliquotes and the solution containing virus particles was frozen at -80°C.

4.4.2 Viral infection of MEF cell lines

For infecting MEF cells with lentivirus, cells were cultured until they reached 60-80% confluency. Coverslips were baked at 180-20°C for at least 4 hours to prevent any contamination. Under a cell culture hood, coverslips were carefully put into 24-well cell culture dishes with sterile tweezers, putting a single coverslip into every well. MEF cells were trypsinated (4.3.2 Splitting of MEF cells), 10 µl of cell suspension was counted while the rest was centrifuged, trypsin containing medium was sucked off, and cells were resuspended in fresh, prewarmed medium. 5×10^3 cells were seeded into each well in a total volume of 1 ml medium, the dish was moved carefully to distribute cells equally over the coverslips, and was put back into an incubator for over night. Usually 3 to 6 wells were seeded with cells of the same MEF

cell line. On the following day 400 µl fresh medium were mixed with 2 µl of virus solution, and 1-10 µl of this mixture was added to each well depending on the virus titer (using always 1 virus particle per cell). After two days of incubation cells were washed with PBS and coverslips were either mounted on slides directly or further processed performing immunohistochemistry for GCP and DsRed (4.6.8 Immunocytochemistry on MEF cells).

4.4.3 Determination of virus titer

For titer determination 5 x 10^4 HEK 293 cells were plated on coverslips, the procedure being the same as in 4.4.2 Viral infection of MEF cell lines. When infecting the cells with virus, a concentration series was done, and the following volumes of virus-medium mixture were pipetted into one well: 200 µl, 100 µl, 20 µl, 10 µl, 1 µl, 0,5 µl, 0,1 µl, 0,05 µl, 0,005 µl, and 0,0005 µl. After two days in the incubator, cells were washed with PBS, coverslips were either mounted on slides directly or further processed performing immunohistochemistry depending on fluorescence signal intensity of the infected cells. Infected cells of different virus concentrations were counted under a fluorescence microscope and the titer was calculated and recorded.

4.5 Animal husbandry

4.5.1 Animal facilities

All mice were kept and bred in the Helmholtz Zentrum München animal facility in accordance with national and institutional guidelines. Mice were group housed in open cages with a maximum of five mice per cage. They were maintained with food and water ad libitum on a 12 hours light/dark cycle with a temperature of 22 ± 2°C and relative humidity of 55 ± 5%.

Mice were bred in single or double matings and pups were weaned and separated by gender at the age of three to four weeks. They were numbered by earmarks for identification. Tail clips were taken for genotyping and stored

at -20°C or processed right away for DNA extraction (4.1.2.1 Isolation of genomic DNA).

4.5.2 Blastocyst injection and embryo transfer

For mouse blastocysts (E3.5) production female C57BL/6 mice were superovulated to increase the number of ovulated oocytes. Superovulation was performed with analoga of the gonadotropins follicle-stimulating hormone and luteinizing hormone. The hormones were injected intraperitoneally between noon and 1 pm, starting with 7.5 I.E. of pregnant mare's serum gonadotropin (PMSG) to induce follicle maturation. 48 hours later 7.5 I.E. of the ovulation initiation hormone human chorion gonadotropin (hCG/Ovogest), were injected. After hCG injection, female mice were mated with one C57BL/6J male for one day. The uteri of pregnant females were dissected 3 days post coitum and blastocysts were flushed with M2 medium. Isolated blastocysts were fixed with one capillary of a micromanipulator, while 10-20 mutant ES cells were injected into the blastocoel with a second capillary, to contribute to the inner cell mass.

Pseudo-pregnant CD1 females were used as foster mothers for the modified E3.5 embryos. To achieve pseudo-pregnancy, CD1 females were mated to sterile, vasectomized males. Foster mothers were put under anesthetic (dosage dependent on body weight, normally 0.25 ml of 1% ketamine and 0.1% rompun in isotonic saline solution), their retroperitoneal cavity was opened, and ovaries and uteri were dissected for embryo transfer. The proximal sides of the uterus were perforated with a thin cannula and up to 10 manipulated blastocysts per side were transferred to the uterus through this opening. The surgery field was closed again with clips and the foster mothers were kept on warming plates until awakening. To prevent blindness of the mice and avoid dehydration of their cornea, eyes were kept wet with 0.9% NaCl during surgery.

4.5.3 Establishment of new mouse lines

Chimeric mice were born 14-16 days after embryo transfer. C57BL/6J cells from the blastocyst code for black fur color, while the modified TBV2 ES cells give rise to mice with agouti fur color. With this technique chimeric mice show a mixture of black and agouti fur, and the percentage of agouti fur color gives information of the amount of contribution of mutant ES cells to the chimera.

High-percentage brown fur chimeras were mated to wild type C57Bl/6J mice to obtain offspring with germline transmission of the modified allele. The first indication for positive germline transmission is the presence of brown pups in the offspring of the chimera, indicating that mutant ES cells have populated the gonads. But nevertheless offspring has to be controlled for germline transmission of the modified gene, therefore offspring was screened by southern blot for confirmation.

4.6 Histological methods

4.6.1 Dissection of cortex, hippocampus, striatum, and ventral midbrain

Mice were asphyxiated with CO_2 and brains were dissected removing bones and meninges. Afterwards dissections of different brain regsion was carried out under the microscope using very sharp, thin-tipped tweezers. Tissue of cortex, hippocampus, striatum, and ventral midbrain was carefully dissected, trying to avoid any contamination with tissue from surrounding brain regions. Tissue was collected in preweighed eppendorf cups and fast frozen in liquid nitrogen and stored at -80°C or further processed immediately.

4.6.2 Perfusion

Mice were asphyxiated with CO_2 and the thoracic cavity was opened via scissors to dissect the heart. A blunt needle was inserted through the left

ventricle into the ascending aorta and the right atrium was opened by a small cut. Vessels were rinsed with PBS using a pump, until the liver was observed to become pale. For perfusion 4% precooled, fresh diluted PFA/PBS was pumped through the animal for 4-6 min until its body was stiff. The mouse was decapitated and the brain was carefully dissected removing bones and meninges. Brains were postfixed in 4% PFA/PBS for 1 hour to overnight at 4°C, depending on the subsequent procedure.

4.6.3 Paraffin sections

For paraffin sections brains were postfixed overnight at 4°C after perfusion, then dehydrated in an ascending ethanol scale, equilibrated and embedded in paraffin. Using an automated embedding machine, the following program was used:

step	reagent	temp. [°C]	time [min]	remarks
dehydration	30% EtOH	RT	90	
dehydration	50% EtOH	RT	90	
dehydration	75% EtOH	RT	90	
dehydration	85% EtOH	RT	90	
dehydration	95% EtOH	RT	90	
dehydration	100% EtOH	RT	90	
dehydration	100% EtOH	RT	60	under vacuum
clarification	Roti-Histol	RT	60	under vacuum
clarification	Roti-Histol	RT	60	under vacuum
paraffination	50% Roti-Histol / 50% paraffin	65	60	under vacuum
paraffination	paraffin	65	60	under vacuum
paraffination	paraffin	65	480	under vacuum
embedding	paraffin	65 to RT		

Paraffin embedded tissue was stored at 4°C until cutting with the microtome. Paraffin blocks with embedded brain tissue were mounted on a tissue cassette with paraffin and cooled at 4°C for at least 30 min. Afterwards they were fixed on the microtome. 8 µm thick sections were cut and put into a

water bath (37-42°C) for flattening. Usually sections were mounted on slides in series of 8 and dried first on a heating plate for 1-3 hours and afterwards at 37°C over night. Dry slides were directly used for experiments or stored in object slide boxes at 4°C.

4.6.4 Frozen sections

For frozen sections, brains were postfixed for 1-4 hours at 4°C after perfusion and equilibrated in 20% sucrose in 1x PBS at 4°C overnight. For longer storage 0.01% sodium azide in 20% sucrose/PBS was used.

To generate frozen sections on the cryostat the tissue was fast frozen at -50°C on an object holder with freezing medium. Horizontal sections of 40 µm thickness were cut with an object temperature of -14°C to -16°C, and a blade temperture 2°C below the temperature of the object. Series of 12 were collected free-floating in cryoprotection solution and stored at -20°C.

4.6.5 Radioactive *in situ* hybridization on paraffin sections

For the detection of mRNA expression in embryos and in the brain, radioactive *in situ* hybridizations (ISH) were performed on paraffin sections. During the whole procedure RNase free solutions and materials were used to avoid degradation of mRNA and the RNA probe.

To detect the mRNA of a desired gene, a probe containing cDNA information of the gene of interest is labeled with radioactive sulfurus (^{35}S). Radioactively labeled RNA probes were generated by *in vitro* transcription with an appropriate RNA polymerase in the presence of [α-thio^{35}S]-UTPs. As templates, plasmids containing part of the cDNA of the gene to analyze and promoters for the RNA polymerases T7 and SP6 were linearized shortly behind the end of the cDNA sequence with an appropriate restriction enzyme.

One 1x transcription reaction consisted of the following ingredients:

3 µl 10x transcription buffer

3 µl	dNTP mix (rATP/rCTP/rGTP 10mM each)
1 µl	0.5 M DTT
1 µl	RNasin (RNase inhibitor; 40 U/µl)
1,5 µg	linearized plasmid DNA template
3 µl	[α-thio-^{35}S]-UTP (12.5 mCi/mM)
ad 30 µl	H_2O
1 µl	RNA polymerase (T7 or SP6; 20 U/µl)

The reaction was incubated at 37°C for 3 hours in total. After one hour additional 0.5 µl of RNA polymerase was added. The DNA template was destroyed by adding 2 µl of RNase-free DNase I and incubation at 37°C for 15 min after transcription. Probes were purified via the RNeasy Mini Kit following manufacturer's instructions and activity was measured in a liquid scintillation counter.

Before hybridization paraffin sections were dewaxed and pretreated with the following treatment:

step	time	solution	remarks
dewaxing	2 x 15 min	Roti-Histol	
rehydration	2 x 5 min	100% Ethanol	
rehydration	5 min	70% Ethanol	
rehydration	3 min	H_2O	
fixation	20 min	4% PFA in PBS	on ice
wash	2 x 5 min	1x PBS	
permeabilization	7 min	20 µg/ml proteinase K in proteinase K buffer	
wash	5 min	1x PBS	
fixation	20 min	4% PFA in PBS	on ice
wash	5 min	1x PBS	
acetylation / denaturing of ribosomes	10 min	0.1 M triethanolamine-HCl	add 600 µl acetic anhydride; rapidly stirring
wash	2 x 5 min	2x SSC	
dehydration	1 min	60% Ethanol	
dehydration	1 min	70% Ethanol	

dehydration	1 min	95% Ethanol	
dehydration	1 min	100% Ethanol	

Slides were air dried dust free. To each slide 100 µl hybridization mix were added and cover slips were put on top to prevent evaporation. Slides were prehybridized for at least 1 hour at 57°C.

For hybridization, the labeled probe was diluted to a concentration of 35,000 - 45,000 cpm/µl in hybridization mix. The radioactive hybridization mix was denatured for 2 min at 90°C and cooled on ice for 2 min. Prehybridized slides were dispensed from their cover slips and 90 µl radioactive solution were added to each slide. Slides were covered with fresh coverslips again and kept at 57°C in a humid chamber with chamber fluid overnight.

The following day cover slips were removed and slides underwent the following treatment:

step	time	solution	temp.
wash, low stringency	4 x 5 min	4x SSC (radioactive waste)	RT
RNA digestion	20 min	20 µg/ml RNase A in 1x NTE buffer	37°C
wash	2 x 5 min	2x SSC / 1mM DTT	RT
wash	10 min	1x SSC / 1mM DTT	RT
wash	10 min	0.5x SSC / 1mM DTT	RT
wash	2 x 30 min	0.1x SSC / 1mM DTT	64°C
wash	2 x 10 min	0.1x SSC / 1mM DTT	RT
dehydration	1 min	30% Ethanol in NH_4OAc solution (1x)	RT
dehydration	1 min	50% Ethanol in NH_4OAc solution (1x)	RT
dehydration	1 min	70% Ethanol in NH_4OAc solution (1x)	RT
dehydration	1 min	95% Ethanol in NH_4OAc solution (1x)	RT
dehydration	2 x 1 min	100% Ethanol in NH_4OAc solution (1x)	RT

Slides were air dried for at least 30 min and exposed to an autoradiography film (BioMax MR) at RT for 2-3 days. After developing the film slides were dipped in a prewarmed photo emulsion (diluted 1:1 with H_2O) and stored at 4°C in the dark room to avoid light exposure of either photo emulsion or emulsion coated slides. The storage time was between 3 and 6 weeks, depending on the signal intensities on the film. For development slides were

equilibrated to RT for at least one hour, incubated in developer for 5 min, rinsed with tap water and incubated in fixer for 7 min. Afterwards they were rinsed again for 20 – 30 min in cold, running tap water. Remaining photo emulsion on the backside of the slides was scratched away with a razor blade and slides were air dried.

4.6.6 Nissl staining (cresyl violet)

After development dried slides were Nissl stained with cresyl violet according to the following protocol:

step	time	solution	remarks
staining	1 - 5 min	cresyl violet staining solution	
wash		H_2O	
clearing	1 min	70% Ethanol	until slide is clear
clearing	10 – 60 sec	96% Ethanol + 0.5% acetic acid	
dehydration	2 x 1 min	96% Ethanol	
dehydration	2 x 2 min	100% Ethanol	
embedding	2 x 10 min	Roti-Histol	

Slides were embedded in Roti-Histokitt II, covered carefully with cover slips to avoid air bubbles, and dried over night under the hood.

4.6.7 Immunohistochemistry (DAB-staining) on free floating sections

Frozen free floating sections were taken out of their cryo protection solution and best washed overnight in 1x PBS at RT. On the next day they were treated according to the following protocol:

step	time	solution	remarks
wash	3 x 10 min	1x PBS	
incubate	10 min	0.1% H_2O_2 1x PBS	
wash	2 x 10 min	0.1% Triton-X/PBS (1x)	

blocking	2 h	2% fetal calf serum in 0.1% Triton-X/PBS	RT
1st antibody	over night	1st antibody in 0,1% Triton-X/PBS	4°C
wash	6 x 10 min	0.1% Triton-X/PBS	
2nd antibody	45 min	2nd antibody (1:300), 0.1% Triton-X/PBS	RT
wash	6 x 10 min	0.1% Triton-X/PBS	
intensifying with ABC-solution	45 min	ABC (1:300) in 0.1% Triton-X/PBS; prepare 30 min before use	RT, keep dark
wash	4 x 10 min	0.1% Triton-X/PBS	
wash	2 x 10 min	0.1M Tris-HCl	
DAB-staining	2-20 min	0.05% DAB, 0.02% H_2O_2 in Tris-HCl; prepare fresh and put on sections immediately	keep dark
wash	10 min	Tris-HCl	
wash	10 min	1x PBS	

After the immunohistochemistry staining, sections were mounted on slides out of 1x PBS and air dried. Then they were embedded in Roti-Histokitt II, covered carefully with cover slips to avoid air bubbles, and dried over night under the hood.

4.6.8 Immunocytochemistry on MEF cells

In general, MEF cells are not specifically vulnerable compared to other cell lines. But in this case, we wanted to observe the mitochondrial morphology of the fibroblasts. Mitochondria are very sensitive and react very fast on changing conditions. Therefore only prewarmed (37°C) medium and solutions were used, and the cells were kept out of the incubator as short as possible. Coverslips were baked at 180-20°C for at least 4 hours. Under a cell culture hood, coverslips were carefully put into 24-well cell culture dishes with sterile tweezers, putting a single coverslip into every well. MEF cells were trypsinated (4.3.2 Splitting of MEF cells), 10 µl of cell suspension was counted while the rest was centrifuged, trypsin containing medium was sucked off, and cells were resuspended in fresh, prewarmed medium. 5 x 10^3 cells were seeded into each well in a total volume of 1 ml medium. Usually 3 to 6 wells were

seeded with cells of the same MEF cell line. After infection with lentivirus (4.4.2 Viral infection of MEF cell lines), cells were tried to keep in the dark to circumvent reduction of fluorescence, and were either mounted directly or underwent the following protocol:

step	time	solution	remarks
fixation	10-15 min	4% PFA in medium	RT
wash	3 x 5 min	1x PBS	
permeablize	5 min	ice cold acetone	at 4°C
wash	3 x 5 min	1x TBS	
blocking	30 min	3% BSA, 0.2% tritonX100 in 1x TBS	RT
primary antibody	1 hour or over night	1st antibody in 3% BSA, 0.2% tritonX100 in 1x TBS	RT (1 h) or 4°C (o.n.)
wash	3 x 5 min	1x TBS	
secondary antibody/ies with fluorecent tag	2 hours	1: 333 in 1x TBS	RT
wash	3 x 5 min	1x TBS	
DAPI	5 min	1:2000 in 1x TBS	
wash	3 x 5 min	1x TBS	

To mount the cover slips, TBS was removed carefully, 1 drop of antifade was added directly on the slide, and cover slips were put upside down on the slide. After 1-3 minutes they were sealed with colorless nail polish, dried in the dark at RT over night, and stored in a box at 4°C.

4.6.9 LacZ staining of mouse tissue

A common reporter in various applications is the lacZ gene which encodes the enzyme β-galactosidase (LacZ). This enzyme converts X-gal to galactose and a blue water-insoluble indigo dye. For the detection of lacZ expression in mice it is important to maintain the activity of LacZ in the tissue. Therefore all solutions used for LacZ staining were substituted with $MgCl_2$ and EGTA and staining was performed as soon as possible. Brains were fixed via perfusion of the mice with LacZ fix. Brains were stored overnight at 4°C in 20% sucrose.

Then they were immediately sectioned and collected free-floating in LacZ storage solution. Free floating sections were washed for 15 min with LacZ wash buffer and transferred to freshly prepared LacZ staining solution. Sections were kept light shielded and were incubated overnight at 37°C. The staining reaction was stopped by washing the sections in 1x PBS. Slides were used immediately to take pictures.

4.6.9.1 Stereological quantification of dopaminergic neurons in the substantia nigra

After immunohistochemistry on free floating sections, the mounted sections were observed under the stereo microscope for cell countings. Out of the twelve series originating from one mouse brain, two series with an interval of six were chosen randomly for every brain. Stained cells of the substantia nigra were counted blind using the Stereo Investigator software, descending from dorsal to ventral. The following settings were used:

Serial section manager

block advance	40 µm
mounted sections thickness	25 µm
evaluation interval	6
Z axis value	0

Optical fractionator

x-value	150 µm
y-value	150 µm
desired sampling sites	10 (or lower value as given by the program for most dorsal sections with small substantia nigra area)
fixed distance	3 µm
optical disector height	20 µm
mounted section height	25 µm

Numbers of cells per brain were calculated by Stereo Investigator software and recorded.

4.6.9.2 Quantification of mitochondrial morphology

MEF cells conserved on slides were observated under a confocal microscope. For quantification, cells were divided into three different subtypes, namely cells with *tubular*, *intermediate*, and *fragmented* mitochondria:

defined mitochondrial morphology	longest mitochondrial tubule per cell
tubular	mitochondrion ≥ 5 µm
intermediate	5 µm > mitochondrion ≤ 0,5 µm
fragmented	0,5 µm > mitochondrion

For each experiment and cell line 65-100 cells were counted blind. The longest mitochondrial tubule in each counted cell was determined by eye and its length was measured using LSM Image Browser 510 software.

4.7 Behavioral testing

At the age of three to four months mice were transferred to a seperate room. After a minimum of one week of habituation, the animals went through the following tests:

- open field
- accelerating rotarod
- forced swimming
- tail suspension
- social discrimination
- object recognition
- odor preference

- odor sensitivity
- odor discrimination

For each test, 10 to 12 mice for each sex and genotype (males and females, wildtypes and Pink1 ko) were tested. All animals were generated by crossings of F_2/F_3 Pink1$^{+/-}$ mice with a mixed C57BL/6J / 129S2 background and their maximum difference of age was 2 weeks. Mice were housed in groups with mixed genotypes. Behavioral testing occured during the light cycle and was performed by the same investigator without knowledge of genotypes.

Data were statistically analyzed using SPSS and GraphPad Prism software. The chosen level of significance was $p < 0.05$.

All test were carried out under light conditions of 200 lux unless mentioned else.

4.7.1 Open field test

For the open field a 50x50 cm hard plastic arena with 50 cm high walls was used. The test animal was put in one corner of the area, and its movement in the open field was recorded by a camera for 10 min. For evalutation the time the mouse spent in the 16% and 45% center, and the time it stayed close to the walls was considered. The open field was disinfected after each animal was tested.

4.7.2 Accelerated rotarod

Motor coordination and balance was assessed using a rotating rod apparatus. The rod was made of hard plastic material covered by soft black rubber foam, with a diameter of approximately 4.5 cm, and lane widths of 5 cm. Each animal was tested three times with intertrial intervals of 15 min. Per each trial, three mice were placed on the rod leaving an empty lane between two mice. In the beginning of each test trial the rod was rotating at a constant speed of 4 rpm, to allow positioning of each mouse in its respective lane. After

positioning all mice the trial was started, and the rod accelerated from 4 rpm to 40 rpm over a time period of 5 min. Fall off latency and speed were observed and recorded. Passive rotations were counted as a fall off and the respective mouse was carefully removed from the rod. The rotarod was disinfected and dried after each trial.

4.7.3 Forced swim test

In the forced swimming test, mice were put into a glass beaker filled with water (25 ± 1°C) to a depth of 21 cm (Ebner *et al.*, 2002). The beaker had a 24.5 cm diameter and a volume of 10 l, and light conditions were adjusted to 30 lux. Inside the cylinder, the mice are not able to climb or jump out, thus they are forced to swim. A trained observer registered the behavior of each mouse for 6 min with a hand-held computer. Behavior of the test animals was recorded according to three different indicators. One indication of behavior was struggling, defined as movement of the forelegs and thereby braking the water's surface. Second, swimming was monitored, defined as movement in the cylinder caused by motion of forelegs and hindlegs without breaking the water surface. Third, floating of the animals was recorded, defined as minimal limb movement of the animal without changing its position inside the cylinder, just to keep its equilibrium. Furthermore spraying of toes was used as another indication of floating, which makes it easier for the observer to recognize. For every mouse fresh water was used, and the animals were dried and put into a fresh cage after each test trial.

4.7.4 Tail suspension test

For the tail suspension test, the animals tail was fixed with a clothespin on top of a slit of a hard plastic cube so that the mouse was hanging head down underneath the slit. For 6 min the animal was watched by a trained observer using a hand held computer. Behavior of the mice was recorded and analyzed considering frequency and duration of periods of activity and immobility,

latency to the first period of immobility, and total, mean, and maximum durations of activity and immobility.

4.7.5 Social discrimination test

In the social discrimination test the mice have to discriminate between a known and an unknown mouse. Each animal was put into an empty, cleaned cage 2 hours prior to testing. During a test phase of 4 min the test animal and an ovarectomated mouse were placed into a clean, disinfected test cage. 2 hours later the same, now for the test animal known mouse, and another ovarectomated, unknown mouse were placed into the test cage again for 4 min. The time the test animal spent with exploring each of the two mice was recorded. Exploration of another mouse was defined as sniffing, grooming, physical contact of the two animals without any movement, and crawling over and under the other animal.

4.7.6 Object recognition test

To assess the animals memory they went through an object recognition test. The test area consisted of a disinfected, empty cage. During three 5 min sample phases with intervals of 15 min, the mice were presented with two equal metal cubes. 3 hours after the end of the third sample phase the test animal was put again into the test area for a test phase of 5 min. This time the two objects were one of the now known metal cubes from the sample phases and an unknown plastic cube. 24 hours after the end of the last sample phase the animal was tested again for 5 min. In the second test phase one of the two objects in the cage was again the metal cube, the second one was a counter of blue color. The time the animal spent exploring each of the two different objects was documented during each of the two test phases.

4.7.7 Odor preference test

To find out whether the mice were able to discriminate between two different odors, an odor preference test was performed. The test environment consistet of an empty, disinfected cage with two holes in the bottom. In one of the holes an eppendorf cup with clean cage wood shavings was put, the second hole contained an eppendorf cup with cage wood shavings from a cage of mice who were unfamiliar to the test animal. The test animal was put into the cage for 10 min, and the time it spent olfactorily exploring each of the two eppendorf cups was recorded.

4.7.8 Odor sensitivity test

To get a more detailed analysis of the mice' smelling abilities, an odor sensitivity test was carried out. First of all, each mouse was trained to recognize and pick a specific odorant. For the Pink1 mouse line two different odorants, apple and strawberry, were used. The odorant was applied to cage wood shavings. For training and test sessions mice were put in an empty, disinfected cage. Mice were seperated by a synthetic, see-through plate from two small bowls each containing cage wood shaving. For the training sessions, one alternating of the two bowls contained cage wood shavings with the specific odorant the respective mouse was supposed to be trained to, and a piece of chocolate underneath the cage wood shavings, while the other bowl did not contain chocolate or odorous shavings. At the beginning of each session the seperating plate was taken away to let the mouse start to dig. Mice were trained to recognize their specific odorant and dig in the corresponding bowl to receive the chocolate. During the test sessions, one bowl contained plain chage wood shavings while the shavings in the other contained either apple or strawberry odorant, respectively. To circumvent that the mice just orient towards the smell of chocolate, both bowls contained a piece of chocolate during test sessions. Starting from the same concentration of odorant for every test animal, concentrations were lowered in binary steps and the maximum number of steps where the test animal was still able to pick the bowl containing odorous cage wood shavings was recorded.

4.7.9 Odor discrimination test

In the odor discrimination test mice have to discriminate between binary mixtures of odorants. The same odorants as in the odor sensitivity test were used, apple and strawberry. As explained above, every mouse was trained to one of the two odors. The test was carried out like the aforementioned odor sensitivity test, but in this test mice had to choose between binary mixtures of the two odorants. Starting at 100% of apple in one bowl and 100% of strawberry in the other, concentrations of binary mixtures were lowered. This means the concentration of the odorant in both bowls was decreased, while the concentration of the respective other odorant was increased in both bowls. From 100% meaning single odorants in both bowls concentrations were decreased to 70% (meaning 70% apple with 30% strawberry in one bowl and 70% strawberry with 30% apple in the other), 55%, 53%, 51%, and 50%. At the concentrations of 100%, 70%, 55%, and 53% mice had 12 trials, at the concentrations of 51% and 50% they had 20 trials. The number of trials the test animals made the correct choice were recorded, and the percentage of correct choices was calculated.

5 RESULTS

5.1 *Pink1* expression in the wild type mouse

At the beginning of this project very few things were known about Pink1. In 2004 it was discovered to be the gene responsible for *PARK6* linked familial parkinson's disease (Valente *et al.*, 2004a). At that time it was still called *PTEN induced* ***putative*** *kinase 1* because its phosphorylation capability was not proven yet. Furthermore it was predicted to have an N-terminal mitochondrial targeting motif. I wanted to know more about the areas of high importance for Pink1 function. Therefore I carried out a detailed expression analysis of *Pink1* mRNA during mouse embryonic development and in the adult mouse brain. To visualize *Pink1* mRNA expression on mouse tissue I used radioactive *in situ* hybridization (4.6.5 Radioactive *in situ* hybridization on paraffin sections) with a *Pink1*-specific probe (P1-Pink1 ISH) on 8 µm thick paraffin sections of CD-1 mouse brain and embryos.

5.1.1 *Pink1* expression during embryonic development

At the earliest stage examined, E7.5, *Pink1* expression could not be observed (data not shown). From E9.0 onwards, *Pink1* is ubiquitously expressed throughout the whole embryo. At this early stage, the overall expression intensity is lower than in later stages (Figure 6 A). Actually it is near to the detection limit by in situ hybridization method. From E10.0 onwards, *Pink1* is differentially expressed in the developing embryo (Figure 6 B'), however it can be observed in all organ systems. At this stage, strong *in situ* hybridization signals can be observed in the developing neural structures and the developing heart. Particularly the mantel layer of the neural tube shows a strong signal (Figure 6 C'). Furthermore, intense expression is observed in the dorsal root ganglia and the ventral horns of the spinal cord (Figure 6 B'). This differential expression can still be seen during later stages like E13.0 (Figure 6 D') and E14.0 (Figure 6 E'). Here Pink1 expression is observed throughout the whole developing brain. In the forebrain it is especially strongly expressed

in dorsal layers of the cortex and the strongest expression domain can be found in the developing hypothalamus (Figure 6 F'). The dorsal midbrain shows moderate expression whereas in the hindbrain the cranial nerve nuclei, the pontine nuclei and the developing raphe nuclei show high expression. Apart from the brain, *Pink1* is found in the olfactory epithelium, gonads (data not shown), the tongue, heart, lung, kidney, liver and mesenchyme of the developing limbs. In the P1 mouse brain *Pink1* mRNA is mainly found in the outer layers of the developing olfactory bulb, the uppermost layers of the cortex, hippocampus, ventral midbrain and hindbrain (Figure 6 G', H'). Furthermore high levels of expression are found in the centromedial and dorsomedial thalamic nuclei, while the anterior ventromedial thalamic nuclei show even more intense signals (Figure 6 H'). A particularly strong expression in the midbrain can now be seen in the red nucleus (Figure 6 H') whereas in the hindbrain the nucleus trochlearis is conspicuously strongly labelled (data not shown). Additionally, in the hindbrain the granular layer of the cerebellum exhibits striking *Pink1* expression (Figure 6 H' and data not shown).

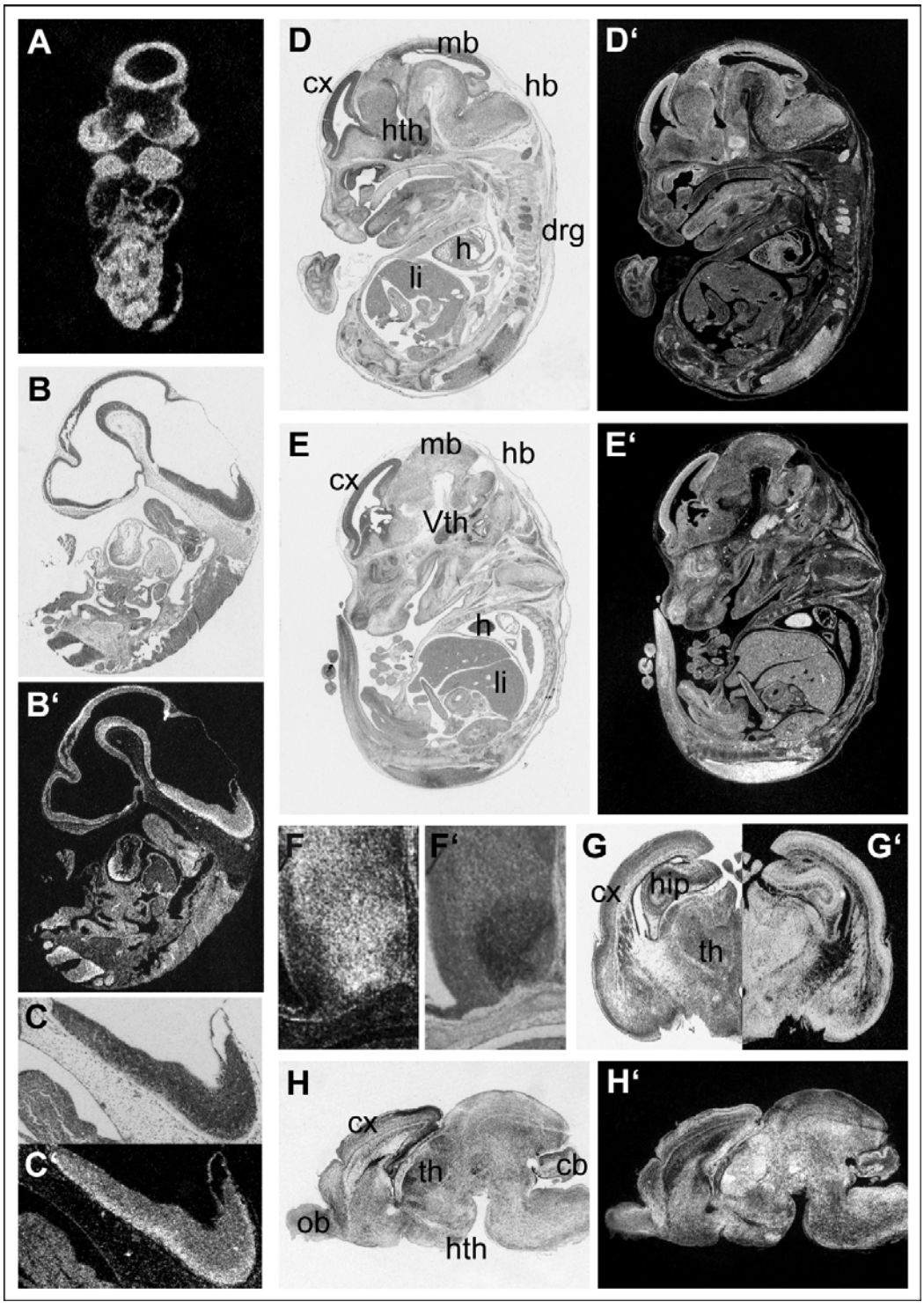

Figure 6: Pink1 expression during mouse embryonic development.
Radioactive *in situ* hybridization with *Pink1*-specific probe on CD-1 wildtype sections. (**A**) Coronal section of a E9.0 embryo. Pink1 is ubiquitously expressed throughout the whole embryo. (**B, B'**) Sagittal section of an E10.5 embryo, (**C, C'**) Higher magnification of B, B' shows ubiquitous expression of *Pink1*. Specifically strong expression can be seen in the mantelzone of the developing mouse brain, dorsal root ganglia and ventral horns of the spinal cord. (**D, D'**) sagittal section of an E13.0 embryo. Areas of strong *Pink1* mRNA signals are the developing brain, especially the developing hypothalamus, and the dorsal root ganglia. (**E,**

E') Sagittal section of an E14.0 embryo. Specifically the dorsal layers of the cortex show high levels of *Pink1* expression. (**F, F'**) High magnification of the developing hypothalamus of an E13.0 embryo. (**G, G',** and **H, H'**) Coronal and sagittal section of P1 mouse brain, respectively. *Pink1* shows ubiquitous expression throughout the whole mouse brain. In the centromedial and dorsomedial thalamic nuclei very high levels of *Pink1* can be seen, in the anterior ventromedial thalamic nuclei they are even higher. Further areas of strong expression are the uppermost layers of the cortex, the hippocampus, ventral midbrain, specifically the red nucleus, and the hindbrain, in particular the granular cells of the cerebellum. (**B, C, D, E, F, G,** and **H**) are corresponding brightfield images of Nissl stained sections to darkfield images of (**B', C', D', E', F', G',** and **H'**), respectively.

5.1.2 *Pink1* expression in the adult mouse brain

In the adult mouse brain *Pink1* is ubiquitously expressed but with remarkable distinct expression levels differing regionally. In the forebrain the olfactory bulbs are generally weakly labeled, however, the mitral cell layer exhibits strikingly strong staining (Figure 7 F'). *Pink1* mRNA is particularly found throughout the cortex with high levels in the piriform cortex. In the hippocampus strong expression is confined to the pyramidal layers of regions CA1-3 and the granular layer of the dentate gyrus. In addition, the differential and strong expression of *Pink1* observed in the perinatal thalamus continues in the adult brain (Figure 7 B'). The nuclei showing strongest expression are the latero-dorsal and ventrolateral thalamic nuclei; the anterodorsal thalamic nucleus to an even higher extend (Figure 7 B' and data not shown). The amygdala and, remarkably with regard to PD the striatum, exhibit only moderate levels of Pink1 expression (Figure 7 A', F').

In the midbrain region, superior and inferior colliculi, the parabrachial nucleus, the nuclei of the cranial nerves III and IV, and the dorsal raphe exhibit intense *Pink1* expression (Figure 7 B', C'). Interestingly there is strong expression in the substantia nigra pars compacta, while it is remarkably weaker in the adjacent substantia nigra pars reticulata (Figure 7 G').

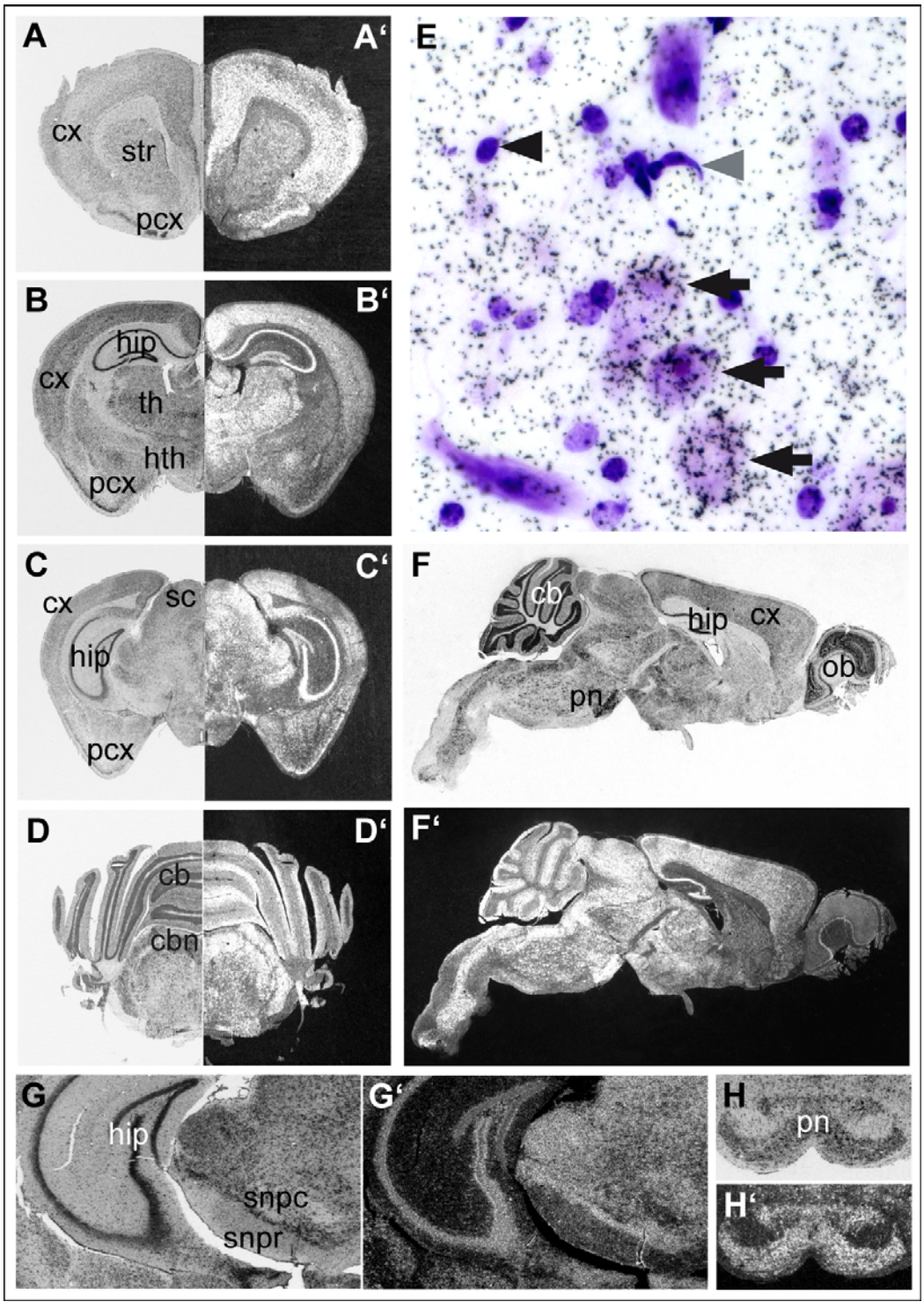

Figure 7: Expression of Pink1 in the adult mouse brain.
Radioactive *in situ* hybridization with *Pink1*-specific probe on CD-1 wildtype sections. (**A, A', B, B', C, C', D, D'**) Coronal sections through the adult mouse brain, going from anterior (**A, A'**) to posterior (**D, D'**). Ubiquitous *Pink1* signal can be seen. High levels of expression are displayed in the cortex, hippocampus, thalamus, the molecular layer of the cerebellum and the cerebellar nuclei.The midbrain shows specifically strong signal intensities in superior and inferior colliculi, parabrachial nucleus, the nuclei of the cranial nerves III and IV, and the dorsal raphe. (**F, F'**) Sagittal section through the adult mouse brain. As can be seen on the coronal

sections, the cortex, hippocampus, thalamus, molecular layer of cerebellum, and cerebellar nuclei show strong expression of *Pink1*. Furthermore high levels of expression can be seen in the mitral cell layer of the olfactory bulb and in the trigeminal nucleus. (**G, G'**) Higher magnification image of coronal section through substantia nigra. High levels of *Pink1* expression are displayed in the substantia nigra pars compacta while the adjacently lying substantia nigra pars reticulata shows only moderate signal intensity. (**H, H'**) Higher magnification image of coronal section through the midbrain. The pontine nuclei exhibit high levels of *Pink1* expression. (**E**) High magnification image of the cortex. On the cellular level can be seen, that *Pink1* is specifically strongly expressed in neurons (black arrows). But no specific expression could be seen in glial cells (black arrowhead). Furthermore it seems to be restricted to certain specific neuronal populations and is absent from endothelial cells (gray arrowhead). (**A, B, C, D, F, G,** and **H**) are brightfield images of Nissl stained sections corresponding to darkfield images of (**A', B', C', D', F', G',** and **H'**), respectively.

The hindbrain displays remarkable levels of expression in the pontine nuclei (Figure 7 H'), tegmental nuclei, the cochlear nucleus, the trigeminal nucleus, the molecular layer of the cerebellum and the cerebellar nuclei (Figure 7 D', F' and data not shown). On the cellular level, Pink1 shows a strongly neuronal expression (see black arrows in Figure 7 E). It could only be seen very weakly in glia (black arrowheads in Figure 7 E) and it is absent from endothelial cells (see gray arrowhead in Figure 7 E, respectively). However, only a subset of neurons seems to express Pink1 at high levels (Figure 7 E, black arrows). In sum this adult expression pattern is highly similar to the one observed perinatally, indicating that there are no striking developmental changes occurring postnatally.

5.2 The Pink1 conditional knockout mouse line

5.2.1 The conditional Pink1 knockout construct

The targeting construct for the conditional Pink1 knockout was planned to remove exons 2 and 3 of the *Pink1* locus. On RNA levels this leads to a shift of the open reading frame and thereby forms a stop codon. On the protein level only a truncated form of Pink1 will be left, which simply consists of the aminoacids encoded by the first of the eight exons.

Deletion of a gene in the whole mouse organism can lead to lethality when the gene of interest has a basic function in cellular biology or development, which cannot be substituted by another enzyme. To circumvent such happening,

conditional knockouts can be generated by using e.g. the Cre/loxP system. This provides the possibility of a controlled knockout in a chosen area or cell type of the organism and at specific developmental stages, depending on the promotor of the Cre recombinase. Hence the targeting strategy of the *Pink1* locus was planned and generated as a conditional knockout.

To generate the targeting vector construct 129/Ola genomic DNA fragments were amplified by PCR. To ensure that the frequency of homologous recombination is as high as possible, the construct was planned in three parts with long homologous arms (Figure 8). For the 5' homologous arm a 3 kb fragment starting 1366 base pairs downstream of the end of exon 1 containing part of intron 1 was inserted. 4369 base pairs downstream of exon 1 a 2 kb floxed arm was inserted. The floxed arm is flanked by two loxP sites. Furthermore it consists of a phosphoglycerat kinase promotor (pgk) driven neomycin resistance cassette flanked by two FRT sites, and exons 2 and 3. The neomycin resistance cassette was cloned in front of exon 2 to screen for positive integration of the construct in the *Pink1* locus. In case of creating a genetically mutated mouse, a leftover neomycin resistance cassette might influence the surrounding genes. Therefore two FRT sites were cloned into the construct surrouding the neo-cassette. Thereby it can be removed via flp-mediated recombination. Furthermore two loxP sites were cloned in the same orientation into the construct. In between the two loxP sites lies the neomycin resistance, the FRT sites and exons 2 and 3 of the Pink1 locus. If Cre recombinase is present in cells, it binds to loxP targets on the chromosome and deletes the interjacent DNA containing exons 2 and 3 via recombination. For the 3' homologous arm a 3.9 kb fragment containing exons 4, 5, 6, and part of exon 7 was added to the end of the homologous arm, 504 base pairs downstream the end of exon 3. The three arms were cloned together in one vector for homologous recombination. This vector contains a diphteria toxin A gene at the 3'-end of the insertion site, for negative selection against random integration after homologous recombination. When gancyclovir is applied to cells containing this domain they will express the toxic substance and die. Thereby ES cell clones containing an insertion of vector backbone on the 3'-end of the homologous arms will be eliminated.

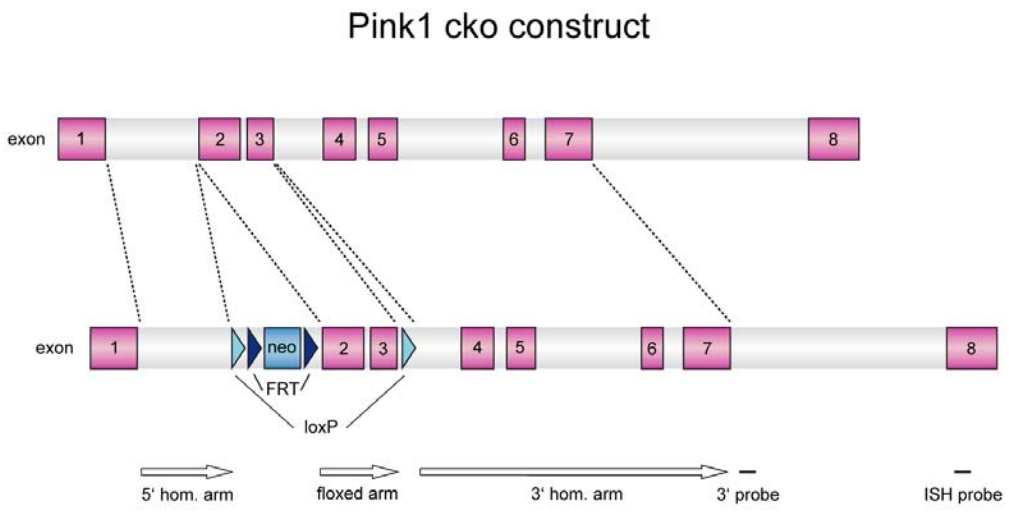

Figure 8: Schematic drawing of *Pink1* targeting strategy.
5' homologous arm, floxed homologous arm, and 3' homologous arm are shown as white arrows. An FRT-flanked neomycin resistance cassette was inserted before exon 2. LoxP sites flank the FRT-flanked neo cassette and exons 2 and 3. A 3' probe for Southern blot verification lies at the beginning of intron 7, outside the homologous arms. An ISH probe lies in exon 8.

5.2.2 Generation of the conditional Pink1 knockout mouse

The linearized DNA was electroporated into ES cells (ES cell line TBV2) (4.2.4 Electroporation of ES cells). After selection with G418, 600 surviving clones were picked (4.2.5 Selection and picking of recombined clones). The 600 clones were synchronized and expanded to have two copies seeded on feeder cells and two copies on gelatine. The copies on feeder cells were frozen in freezing medium at -80°C, the copies on gelatine were frozen without any medium at -20°C for preparation of genomic DNA (4.2.3 Freezing and thawing of ES cells). The clones were screened by Southern blot (4.1.2.2 Southern Blot analysis) for homologous recombination. Genomic DNA was digested by the restriction enzyme ScaI and hybridized with radioactively labelled probe P2 (Pink1-3'-probe). This should result in a band of 6,8 kb corresponding to *Pink1* wildtype allele and a band of 8,7 kb corresponding to floxed *Pink1* (see schematic drawings in Figure 9). Seven clones were found to be possibly genetically modified by homologous recombination, and called

Pink1 3.1-3.7. The feeder-cell-plate copies of these seven clones were thawn and expanded. After expansion they were screened again by Southern blot. One aliquot of genomic DNA was digested with ScaI and hybridized with P2-Pink1 SB probe for verification. Another aliquot was digested with BsmI, hybridized once with a neo probe, and once with P2-Pink1 SB probe to further confirm the 3' integration. Clones Pink1 3.4, 3.5, and 3.7 showed a band of 8,6 kb for the targeted allele with either probe. A third aliquot was digested with MfeI (also called MunI) and hybridized with neo probe as well to confirm the 5' integration. In this case the the floxed allele showed a band of 7,3 kb (see Southern blot in Figure 10 B). From the originally seven clones, only clones Pink1 3.4, 3.5, and 3.7 showed the expected bands for the floxed allele in all different Southern blots and were thus suggested to be positive for 3' and 5' integration of the targeting construct into the *Pink1* locus.

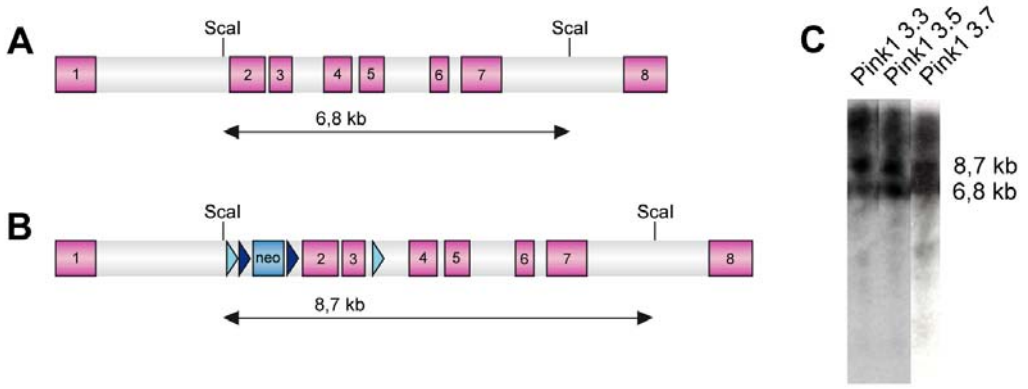

Figure 9: Schematic drawings of *Pink1* wildtype (A) and floxed alleles (B), and Southern blots confirmations of clones Pink1 3.3, 3.5, and 3.7 (C).
Schematic drawings include restriction sites for ScaI, which was used for genomic DNA digestion. Southern blots examples of clones Pink1 3.3, 3.5, and 3.7 shown in this figure exhibit the Pink1 *wildtype* band of 6,8 kb as well as the *Pink1* floxed band of 8,7 kb.

The floxed arm of the construct contains the information for the parts to be ectopically inserted into the *Pink1* locus, namely the neomycin resistance, the frt sites, and the loxP sites. Since the 2nd loxP site lies 2 kb further 3' than the rest of the inserted DNA, it can happen that this loxP site is not inserted into the locus while homologous recombination of the rest of the construct takes

place. The insertion of the 2nd loxP site creates a HindIII digestion site. Thus to confirm the insertion of the 2nd loxP site, HindIII was chosen as enzyme to digest genomic DNA for southern blotting. When using the neo probe for hybridization, this would only lead to a band of 4 kb in case of complete homologous recombination, while without the loxP site, a band of 7 kb can be seen on the film. In several experiments clones 3.4 and 3.7 showed a band of 7 kb, while only clone 3.5 exhibited the specific band of 4 kb, and could therefore be validated as positive for homologous recombination of the complete targeting construct (Figure 10 C).

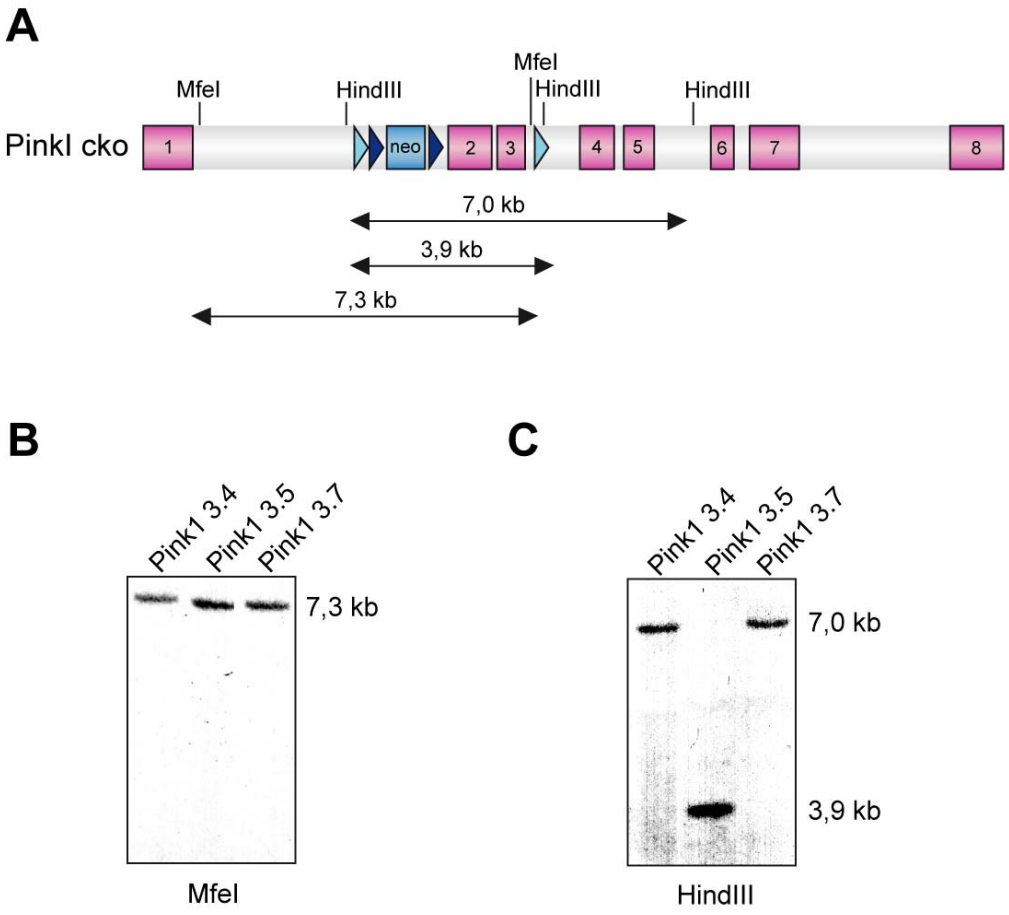

Figure 10: Verification of ES cell clones Pink1 3.4, 3.5, and 3.7 via Southern blot.
(**A**) Schematic drawing of targeted *Pink1* with restriction sites of enzymes used for genomic DNA digestion. (**B**) Southern blot of clones 3.4, 3.5, and 3.7. Genomic DNA was digested with MfeI, for hybridization the neo-probe was used. (**C**) Southern blot of clones 3.4, 3.5, and 3.7. HindIII was used for restriction digestion of genomic DNA, and P2-Pink1 SB probe was used for hybridization.

Clone 3.5 was injected into blastocysts from C57BL/6J mice and these were implantated into the uteri of pseudo-pregnant foster mothers (4.5.2 Blastocyst injection and embryo transfer). These gave birth to 2 female chimeras with 5% and 85% chimerism, and 8 male mice with 85%-100% chimerism. The male animals were crossed with C57BL/6J females. The offspring was screened for germline transmission of the mutated *Pink1* allele via southern blot analysis using the restriction enzyme ScaI for digestion of genomic DNA and P2 for hybridization. Four of the eight male chimeras showed germline transmission and gave birth to mice with *Pink1*$^{l/+}$ genotype.

5.2.3 The Cre deleter mouse line

In this mouse line the Cre gene is under the transcriptional control of a human cytomegalovirus minimal promotor. Cre expression is X-chromosome-linked and occurs during early embryogenesis before implantation (Schwenk *et al.*, 1995). This mouse line was backcrossed several generations to be in a complete C57BL/6J background. If this mouse line is crossed to a conditional knockout mouse line with a floxed gene of interest, the gene should be irreversibly deleted in all cells of the F1 generation. The Cre deleter mouse line can be used for crossing with conditional knockout mouse lines to receive a complete knockout of the targeted gene. Hence I decided to cross it with the Pink1 conditional mouse line for the generation of a complete knockout mouse line of the *Pink1* gene.

5.3 The Pink1 knockout mouse

When Cre recombination occurs in the Pink1 cko mouse line, the FRT sites, the neomycin resistance cassette and exons 2 and 3 are removed, leaving just one loxP site between exons 1 and 4. This generates a frame shift in the *Pink1* coding sequence, which thereby creates a stop codon shortly after exon 1, and thus leads to a truncated Pink1 protein.

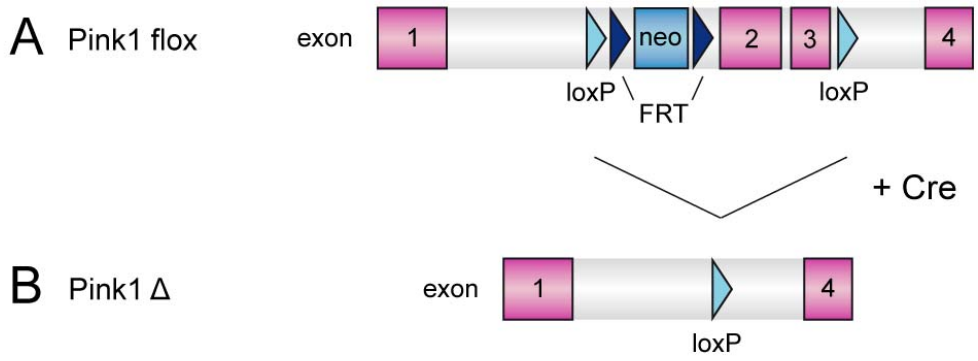

Figure 11: Schematic drawing of floxed *Pink1* allele before (A) and after (B) Cre recombination.

Heterozygous male offspring (*Pink1*$^{l/+}$) of the chimeras was crossed with Cre deleter females for the generation of Pink1 complete knockout animals. Since the *Cre recombinase* gene of the deleter line is located on the X-chromosome, I used mainly homozygous female deleter animals for breeding to get 100% Cre positive offspring. Mice with *Pink1*$^{+/-}$ genotype were intercrossed with each other to generate the first mice with a complete Pink1 knockout (*Pink1*$^{-/-}$), and later *Pink1*$^{+/+}$ animals were crossed with *Pink1*$^{-/-}$ animals over a total time period of 1.5 years to generate a breeding cohort of 30 breeding pairs with *Pink1*$^{+/-}$ genotype. For best conditions in behavioral phenotyping a cohort of 60 animals is needed: 15 wildtype male mice, 15 wildtype female mice, 15 knockout male mice, and 15 knockout female mice. For accurate results I chose to intercross only heterozygous *Pink1*$^{+/-}$ mice so that wildtype controls and Pink1 mutant animals are littermates.

Expression of Cre recombinase can have several different, unwanted secondary effects influencing an organism (Schmidt-Supprian & Rajewsky, 2007). Therefore during these breedings I tried to breed out the Cre to generate a Pink1 knockout mouse line without any Cre left in its genome. Because of time restrictions, in some offspring of the first breeding cohorts the Cre gene was still present. Genotypes were screened for Cre, recorded and taken into account for experimental results.

Pink1$^{-/-}$ mice manifested to be viable and fertile. I therefore chose to concentrate on the analysis of the complete Pink1 knockout mouse line.

5.4 Analysis of the Pink1 knockout mouse line

5.4.1 Verification of Pink1 inactivation

To prove the knockout of the *Pink1* gene on the RNA level, an RT-PCR was carried out (4.1.3.2 Reverse transcription of mRNA into cDNA). The primers were constructed to lie in exon 1 and exon 4 to screen for missing exons 2 and 3 (for primers see 3.5.9.1 Oligonucleotides for PCR amplification). The following PCR program was used:

3 min	94°C	
30 sec	94°C	} 35 cycles
1 min	60°C	
2 min	72°C	
10 min	72°C	
∞	4°C	

In the wildtype the expected band of 590 bp could be seen and the mutant band of 206 bp confirmed the missing exons 2 and 3 on the RNA level (Figure 12 B). Although the amount of tissue used and the RNA probe preparations did not differ from each other, the exhibited mutant band was conspicuously weaker than the wildtype band.

To find out more about this effect and its cause, additional RT-PCRs with primers in exon 8 and in the 3'-UTR (Figure 12 C), and primer pairs spanning exon 6, and exon 7 (data not shown) were performed (for primers see 3.5.9.1 Oligonucleotides for PCR amplification). Both knockout and controls showed the same band height, as expected. Again, in case of the knockout samples were the band intensities strikingly weaker than those from the wildtype samples. This suggests a very low abundance of *Pink1* mutant mRNA, which might result from instability and/or rapid degradation of the truncated *Pink1* RNA. Thus, it seems that *Pink1* mRNA deficient of exons 2 and 3 is very unstable and/or rapidly degraded in the cell.

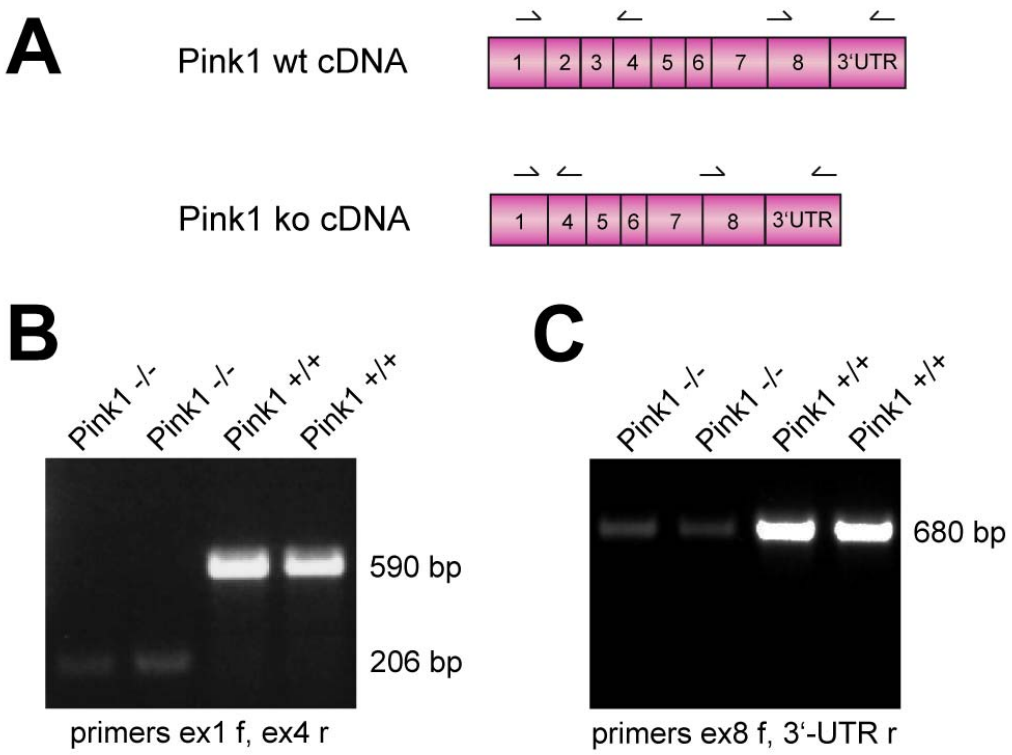

Figure 12: Confirmation of Pink1 knockout via RT-PCR on *Pink1* wildtype and knockout.
(**A**) Schematic drawing of *Pink1* wildtype (wt) and knockout (ko) cDNA with primers used. (**B**) RT-PCR on *Pink1* ko and wt with primers in exons 1 (RT ex1f) and exon 4 (RT ex4r). A band of 590 bp can be seen in the wildtype samples, while the knockout samples show the excised band of 206 bp, which is very weak. (**C**) RT-PCR on *Pink1* ko and wt with primer in exon 8 and the 3'-UTR. All samples show the expected band of 671kb, but again the knockout band is strikingly weak in comparison to the wildtype.

5.4.2 Analysis of Pink1 function in cell biology

5.4.2.1 Generation of mouse embryonic fibroblast (MEF) cell lines

In vivo investigations of animal models are very important, as they give a variety of opportunities for research purposes in a natural environment. Such experiments can be rather time consuming, and restrictions occur because of the amount of animals and tissue needed. Thus, in addition to the analysis of the Pink1 knockout mouse, I decided to find out more about the function of

Pink1 by performing cell culture experiments, the results of which would then be confirmed in the mouse model afterwards.

Heterozygous breeding pairs (*Pink1*$^{+/-}$ genotype in case of the Pink1 knockout line and *Pink1*$^{l/+}$ genotype for Pink1 conditional knockouts) were set up, and a total of 56 mutant and wildtype cell lines, originating from the same offspring, were generated out of E12-15 embryos (for exact description of all cell lines generated see 7.1 Overview of generated MEF cell lines, for method of generation see 4.3.1 Generation of MEF cell lines). Heads of embryos were used for genotyping as fast as possible. As soon as the genotypes were known and there were pairs of homozygous mutant and wildtype cell lines originating from one female, one to four lines per genotype were chosen for immortalization (4.3.4 Immortalization of MEF cell lines). Primary cells were frozen in cryovials (4.3.3 Freezing and thawing of MEF cells) and stored in liquid nitrogen. The following MEF cell lines were successfully immortalized:

cell line	genotype of cell line	method of immortalization	genotype of breeding pair
AR170/7	*Pink1*$^{+/+}$	3T3	*Pink1*$^{+/-}$
AR170/9	*Pink1*$^{-/-}$	3T3	*Pink1*$^{+/-}$
AR170/6T	*Pink1*$^{-/-}$	SV40 large T antigen	*Pink1*$^{+/-}$
AR170/7T	*Pink1*$^{+/+}$	SV40 large T antigen	*Pink1*$^{+/-}$
AR367/5T	*Pink1*$^{-/-}$	SV40 large T antigen	*Pink1*$^{+/-}$
AR367/6T	*Pink1*$^{+/+}$	SV40 large T antigen	*Pink1*$^{+/-}$
AR 2.3T	*Pink1*$^{+/+}$	SV40 large T antigen	*Pink1*$^{l/+}$
AR 2.4T	*Pink1*$^{+/+}$	SV40 large T antigen	*Pink1*$^{l/+}$
AR 2.6T	*Pink1*$^{+/+}$	SV40 large T antigen	*Pink1*$^{l/+}$
AR 2.8T	*Pink1*$^{l/l}$	SV40 large T antigen	*Pink1*$^{l/+}$

Table 2: Overview of successfully immortalized Pink1 MEF cell lines.
Pink scripture stands for a *Pink1*$^{l/+}$ genotype, purple scripture for *Pink1*$^{l/l}$, light blue for *Pink1*$^{+/-}$, dark blue indicates a *Pink1*$^{-/-}$ genotype, and black scripture confers to *Pink1*$^{+/+}$ genotype.

In the case of cell lines transfected with SV40 largeT antigen, a ‘T’ was added at the end of the cell line name for discrimination. Furthermore all cell lines were labeled and recorded with their passage number.

5.4.2.2 Pink1 deficiency does not lead to changes in mitochondrial morphology

Mitochondria are indespensable for cell survival and omnipresent in eukaryotic cells. Their primary function is oxidative phosphorylation to generate ATP and thereby provide the cell with energy for intracellular metabolic pathways. Previous studies have associated mitochondrial disorders and impaired mitochondrial fission and fusion with several neurodegenerative diseases (Chan, 2006). Since Pink1 was shown to localize to mitochondria and was implicated in mitochondrial dysfunction (Clark *et al.*, 2006; Gandhi *et al.*, 2006; Pridgeon *et al.*, 2007), Pink1 MEF cells were analyzed for mitochondrial morphology.

For the analysis of mitochondrial morphology, a lentivirus carrying the lenti-GFP mDsRed plasmid was used, which carries different fluoresceing proteins (see Figure 13). The virus contains two long terminal repeat domains (LTR), which flank the other domains and are responsible for the regulation of transcription and binding of transcription factors. The first LTR domain is followed by a cytomegalovirus promotor (CMV), which drives the expression of the following genes. Downstream of the CMV lies a cytosolically targeted green fluorescence protein (GFP), an internal ribosomal entry site (IRES) and a mitochondrially targeted DsRed (mDsRed). The IRES mediates binding of mRNA to the ribosomes, and the expression of the mDsRed leads to red fluorescing mitochondria. Downstream of this the virus contains a woodchuck hepatitis virus posttranscriptional regulatory element (wPRE) to facilitate RNA transport from the nucleus to the cytosol. At the 3’ end lies the second LTR domain.

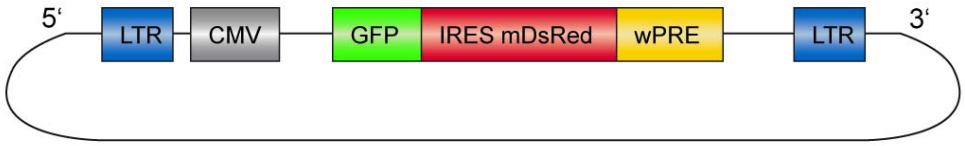

Figure 13: Schematic drawing of lentiviral construct.
The vector contains two long terminal repeat domains (LTR), and a cytomegalovirus promotor (CMV). After the CMV lies a cytosolic green fluorescence protein gene (GFP), an internal ribosome entry site (IRES), and a mitochondrially targeted red fluorescence drFP583 (mDsRed). This is followed by a woodchuck hepatitis virus posttranscriptional regulatory element (wPRE), and the second LTR domain.

After viral infection with GFP mDsRed lentiviruses (see 4.4.2 Viral infection of MEF cell lines) and immunohistochemistry for GFP and DsRed 2 days after infection (4.6.8 Immunocytochemistry on MEF cells) mitochondrial morphology of Pink1 knockout and control MEF cells was quantified. Cells were divided into three different subtypes according to the length of their mitochondrial tubules, which were termed fragmented, intermediate, and tubular (for exact definition see 4.6.9.2 Quantification of mitochondrial morphology). Figure 14 shows the results of two different experiments in which MEF cells were counted blind. 94% of counted *Pink1*$^{+/+}$ MEF cells and 95% of counted *Pink1*$^{-/-}$ MEF cells exhibited mitochondria with intermediate morphology, while tubular mitochondrial morphology was seen in 6% and 5% of counted cells, respectively. Fragmented mitochondrial morphology was not detected in cell lines with either genotype. Thus, the lack of Pink1 does not lead to major morphological defects of mitochondria in MEFs.

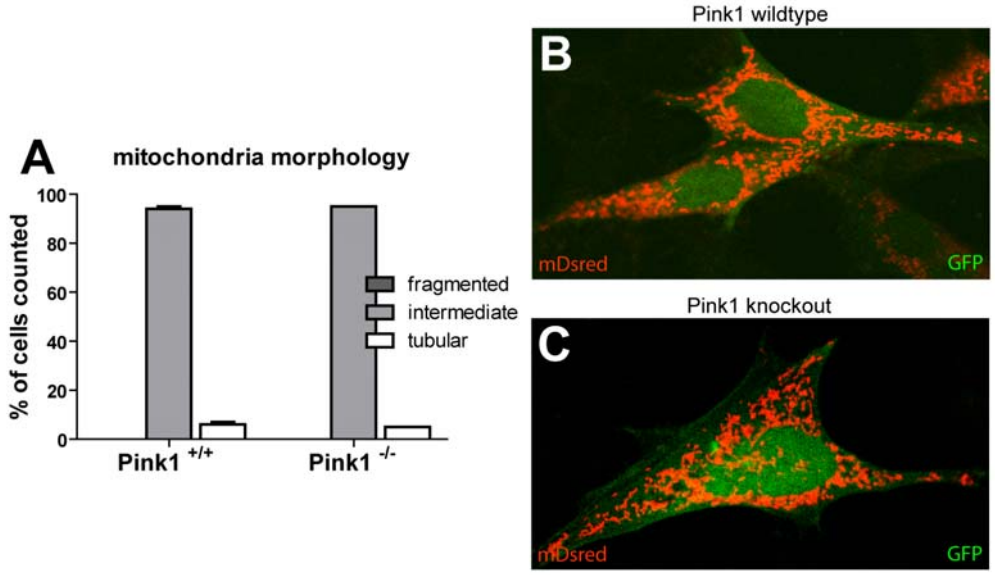

Figure 14: Pink1 deficiency does not lead to dramatic alterations in mitochondrial morphology in MEF cells.
(**A**) Bars show the percentage of cells counted of different mitochondrial morphology: *Intermediate* at least one mitochondrial tubule between 0,5 µm and 5 µm, but none more than 5 µm (white); *tubular* at least one mitochondrial tubule of 5 µm or more (grey). *Fragmented* no mitochondrial tubule longer than 0.5 µm. Cells with fragmented morphology could not be detected. Error bars represent standard error of means (not significant, p = 0.935, student's t-test) (**B**) Representative wildtype MEF cell infected with GFP mDsRed lentivirus. (**C**) Representative example of Pink1 knockout MEF cell infected with GFP mDsRed lentivirus. Cytosolic GFP can be seen in green, red signals visualize mitochondria.

5.4.2.3 Ablation of Pink1 does not change OPA 1 (Optic Atrophy 1) processing

The dynamics of mitochondrial fusion and fission are maintained by the help of various proteins. OPA1 is one these proteins, which was shown to be mandatory for mitochondrial fusion. Distraction of mitochondrial membrane potential yields rapid proteolytic processing of large OPA1 isoforms followed by mitochondrial fragmentation, and OPA1 processing was shown to connect changes of mitochondrial morphology with mitochondrial dysfunction (Duvezin-Caubet *et al.*, 2006). Thus I decided to investigate, whether a lack of Pink1 has an influence on the processing of OPA1. Cell lysates of Pink1 MEF cells were used for Western blot analysis using an antibody against OPA1. The analysis showed that the quantities of occurance of different OPA1

isoforms are not changed in Pink1 knockout cells. Accordingly Pink1 deficiency has no effect on proteolytic processing of OPA1 in MEF cells.

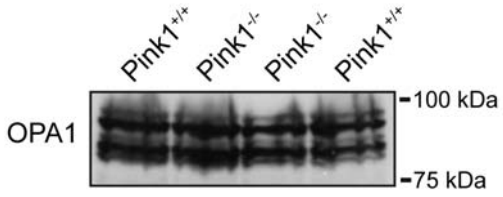

Figure 15: Proteolytic processing of OPA1 is maintained in Pink1 knockout MEF cells.
Cell lysates of Pink1 mutant and control MEF cells were applied to a 10% SDS polyacrylamide gel and detected with an OPA1 specific antibody. No changes can be seen in the ratio of different OPA1 isoforms.

5.4.3 Parkinson's disease mutations in Pink1 affect Complex I activity in mitochondria

The involvement of Pink1 in synaptic and mitochondrial function was analyzed in a collaborative effort with the laboratory of Bart De Strooper MD, PhD, at the KU Leuven, and especially Vanessa A. Morais, PhD. In this approach, corresponding wt and KO pairs of the Pink1 MEF cell lines, and tissue of corresponding wt and KO pairs of the Pink1 KO mouse line were used together with Pink1 *Drosophila* mutants (Morais *et al.*, 2009). It was found that previously characterized $Pink1^{B9}$ null mutant *Drosophila* (Park *et al.*, 2006) show defects in mobilizing the reserve pool (RP) of vesicles which is released upon high frequency stimulation, which is, at least in part, caused by synaptic ATP depletion (Morais *et al.*, 2009). By using a mitochondrially targeted eGFP, no dramatic morphological alterations of mitochondria could be detected in Pink1 deficient MEF cells, $Pink1^{B9}$ mutant neuromuscular junctions (NMJ), Pink1 knockout mouse liver, or brain mitochondria (Morais *et al.*, 2009). Furthermore it was found that the mitochondrial membrane potential (ψ_m) is decreased in Pink1 deficient fly NMJ and MEF cells, and that Pink1 deficient mitochondria have a lowered threshold for opening of the mitochondrial permeability transition pore (PTP). They are more susceptible to Ca^{2+}-dependent apoptotic stimuli, and release more cytochrome c in response to cBID, which induces PTP-dependent mobilization of cytochrome c from the

cristae stores (Morais *et al.*, 2009). When assessing the activities of Complexes I-V of the mitochondrial respiratory chain, a significant reduction in Complex I activity was found in Pink1 deficient fly brain and muscle enriched mitochondrial fractions, and in mouse fibroblasts and brain absent of Pink1. This means that ablation of Pink1 results in a primary defect in the catalytic activity of Complex I. Rescue experiments showed that human Pink1 fully complemented Complex I enzymatic activity, while two PD Pink1 clinical mutations and an artificial kinase inactivated form did not. Thereby the relevance of Complex I deficit in PD was confirmed (Morais *et al.*, 2009).

5.4.4 Analysis of neuronal systems

5.4.4.1 The number of nigral dopaminergic neurons is normal in Pink1 knockout mice

One characterisic of Parkinson's disease is the death of dopaminergic neurons in the substantia nigra pars compacta. In order to determine whether Pink1 knockout mice display these parkinsonian characteristics, numbers of TH-positive neurons in the substantia nigra were quantified.

Brains of 6 months and 19 months old mutants and wildtype littermate controls were perfused (4.6.2 Perfusion), cryosectioned (free floating, 40 µm thick) (see 4.6.4 Frozen sections), and immunohistochemically stained with an anti-TH antibody (4.6.7 Immunohistochemistry (DAB-staining)). No gross differences in tissue and cell structure were observed (Figure 16).

Figure 16: Ventral tegmental area and substantia nigra dopaminergic neurons of Pink1 wildtype and knockout mice.
Immunohistochemistry for tyrosine hydroxylase (TH) was carried out on 40 µm thick horizontal brain cryo sections of 6 months old *Pink1*$^{+/+}$ (**A**) and *Pink1*$^{-/-}$ (**B**) mice. Detail shows magnified image of substantia nigra and ventral tegmental area.

Stereological counting of the TH-positive substantia nigra neurons (4.6.9.1 Stereological quantification of dopaminergic neurons in the substantia nigra) and statistical evalutation did not display significantly reduced numbers of neurons in 6 months (Figure 17 and 7.2 Stereological countings of TH-positive nigral neurons) or 19 months old Pink1 mutant mice (see 7.2 Stereological countings of TH-positive nigral neurons). Thus, Pink1 does not seem to be essential for the survival of nigral dopaminergic neurons.

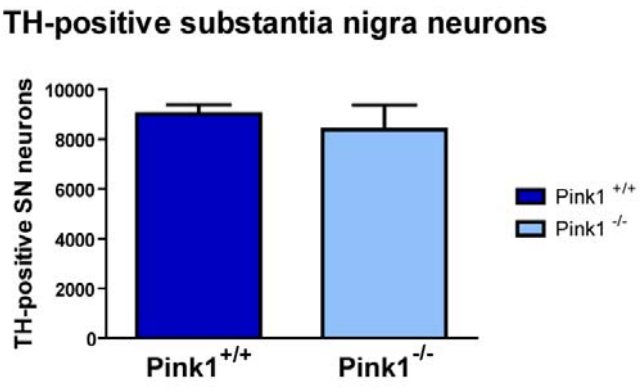

Figure 17: Stereological countings of TH-positive substantia nigra neurons.
6 months old Pink1 knockout mice do not display dopaminergic neuron death in the substantia nigra ($p = 0.316$, unpaired, two-tailed t-test). Columns show means with error bars representing SEM. n = 6.

5.4.4.2 Quantitative analysis of catecholamines in Pink1 knockout brains revealed elevated cortical levels of serotonin (5HT)

Human PD patients show cell death of dopaminergic neurons (mainly those of the substantia nigra pars compacta). Subsequently, this leads to a depletion of dopamine in the regions where those neurons project to (the striatum in case of the substantia nigra pars compacta neurons). This lack of neurotransmitter is a cause of several motor dysfunctions PD patients are suffering from. Furthermore, other cell populations were shown to be affected in PD, as for instance the noradrenergic neurons of the locus coeruleus and the serotonergic neurons of the dorsal raphe nucleus (Shen & Cookson, 2004).

To find out whether the quantities of these neurotransmitters and some of their metabolites are altered in brains of Pink1 mutant mice, HPLC analyses of different brain regions were carried out. Tissue of cortex, hippocampus, striatum, and ventral midbrain was dissected from brains of six months old Pink1 knockout mice and littermate controls (4.6.1 Dissection of cortex, hippocampus, striatum, and ventral midbrain), and further processed for HPLC analysis of serotonin (5HT), 5-hydroxyindole acetic acid (5-HIAA), noradrenaline (NA), dopamine (DA), and 3,4-dihydroxyphenylacetic acid (DOPAC) (see 4.1.4.2 Sample preparation 4.1.4.3 Quantification of neurotransmitters via HPLC analysis).

First I wanted to see whether Pink1 mutants show any changes in the quantities of dopamine. In order to have a closer look into the nigrostriatal system of dopaminergic neurons, quantities of neurotransmitters in ventral midbrain and striati were assessed. (Figure 18 C, D). Additionally, the mesocortical system, which is afferent to cortex and hippocampus, and contains dopaminergic neurons originating from the VTA, was analyzed. Therefore, levels of dopamine and DOPAC in the cortex and hippocampus were quantified. It was found that the amounts of DOPAC in cortex and hippocampus, as well as amounts of dopamine in hippocampus, were below the limit of detection. The quantities of striatal dopamine were found to be

about 10-fold higher than in the other brain regions. Furthermore, compared to controls, Pink1 mutants did not show significant differences in the contents of neurotransmitter in any of the assessed regions of the mouse brain (Figure 18 A, C, D and 7.3 Quantification of neurotransmitter contents via HPLC).

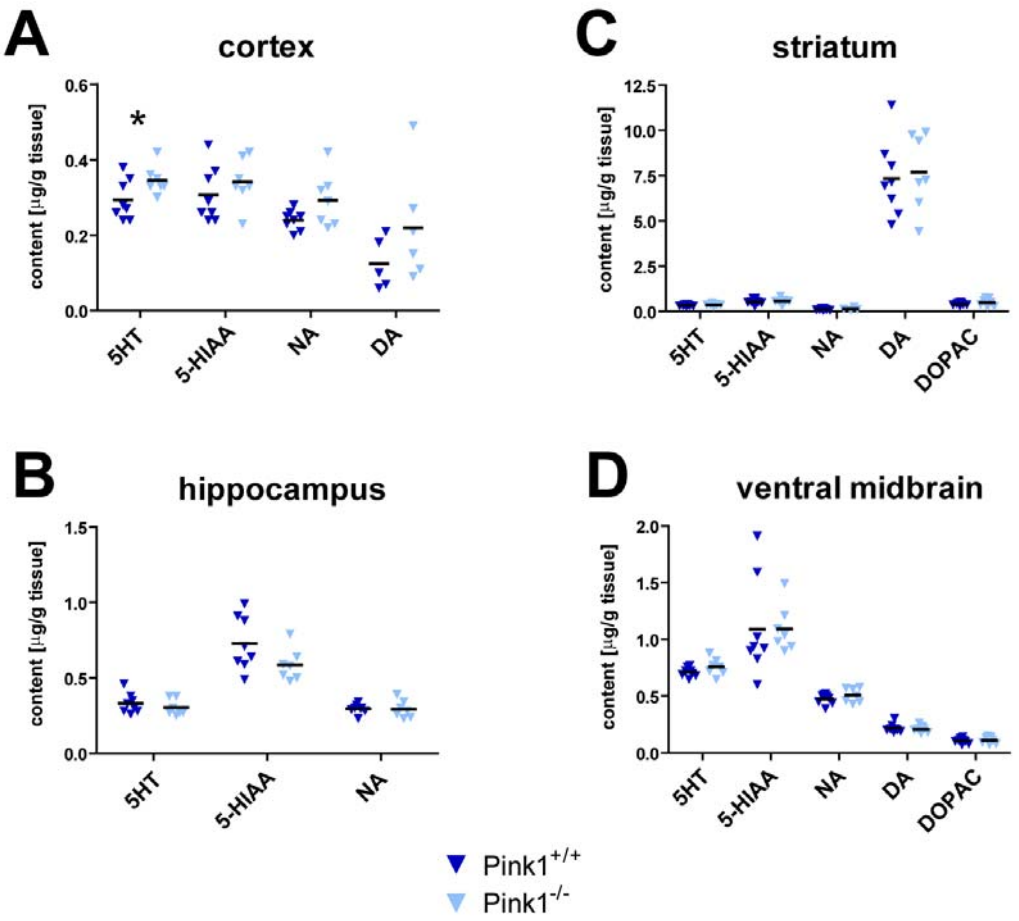

Figure 18: Serotonin, 5-HIAA, noradrenaline, dopamine, and DOPAC quantification via high performance liquid chromatography.
Contents of neurotransmitters and metabolites were determined from cortex (**A**), hippocampus (**B**), striatum (**C**), and ventral midbrain (**D**) of 6 months old Pink1 wildtype and mutant mice. Pink1 mutants showed slightly, but significantly elevated levels of serotonin in the cortex (*p = 0.032, two-tailed t-test). No differences between Pink1 knockout and control mice could be detected in all other areas and neurotransmitters assessed. Black lines show means, n = 7 (ko), 8 (wt).

The loss of noradrenaline occurs constantly in the progress of PD. This can worsen the proceeding of the disease, either by increasing vulnerability of dopamine-containg neurons, or by reducing their recovery after damage.

(Fornai *et al.*, 2007). Hence I wanted to know whether the noradrenergic system is affected in Pink1 knockout mice. The amount of noradrenaline per g tissue were assessed in cortex, hippocampus, striatum, and ventral midbrain of the test animals. Statistical analysis revealed no significant differences between mutants and control mice in the quantities of noradrenaline (Figure 18 and 7.3 Quantification of neurotransmitter contents via HPLC).

In addition, I wanted to analyze levels of serotonin and its metabolite 5-HIAA, especially in the cortex and hippocampus, where many of the serotonergic neurons of the raphe nuclei project to. HPLC analyses for serotonin and 5-HIAA and statistical analysis revealed slightly, but significantly higher levels of cortical serotonin in the mutants compared to controls (Figure 18 A, $p = 0.032$, two-tailed t-test). No significant differences could be observed in any of the other brain regions (Figure 18 A-D, and 7.3 Quantification of neurotransmitter contents via HPLC).

5.4.5 Behavioral analysis of Pink1 knockout mice

To determine whether Pink1 deficiency leads to behavioral obnormalities related to parkinsonism, large cohorts of 10-12 mice per gender and genotype (10 *Pink1*$^{+/+}$ males, 12 *Pink1*$^{-/-}$ males, 11 *Pink1*$^{+/+}$ females, 12 *Pink1*$^{-/-}$ females) went through nine behavioral tasks to evaluate motor ability, anxiety- and depression-like behavior, memory, and smelling. If not stated differently, behavioral testing of Pink1 knockout mice and corresponding wildtype littermates was carried out at the age of 3-9 months.

5.4.5.1 Pink1 mutants show no sign of motor dysfunction or anxiety-like behavior in the open field

Human Parkinson's disease patients usually exhibit a variety of motor disturbances as e.g. impaired balance, rigidity, bradykinesia, or tremor at rest. To test for dysfunctions in their motoric behavior, Pink1 animals were tested in the open field test. In addition to locomotor deficits, the open field test can give

hints about anxiety-related behavior. Adult Pink1 wildtype and mutant animals were analyzed for 30 min in respect to the total distance they travelled, their mean velocity and the time they spent in different areas of the open field (4.7.1 Open field test). The amount of travelling in the area of the open field, which can give hints about the animals' motor function, did not differ significantly between Pink1 knockout animals and their wildtype littermates. (Figure 19 A). Mutant animals of both genders seem to show a tendency to spend more time in the 16% center (see Figure 19 B and 7.4.1 Overview open field test) and 45% center of the open field (7.4.1 Overview open field test), which would define them less anxious than their wildtype littermates. But statistical analysis via 2-factorial ANOVA revealed p-values above 0.05 for interaction, gender or genotype in all parameters investigated. Hence I could not detect an anxiety-like behavior of Pink1 mutants in the open field. Furthermore they did not travel significantly less than the controls in this test.

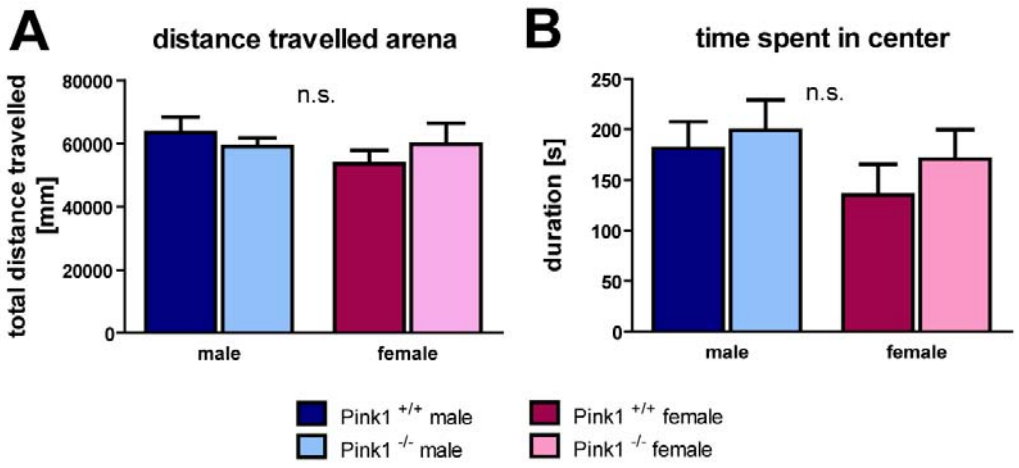

Figure 19: Pink1 knockout mice did not show anxiety-like behavior or motor dysfunctions in the open field test.
Depicted parameters are the total distance travelled by the animals (**A**), and the time they spent in the 16% center (**B**) of the open field. 2-factorial ANOVA could not show any significant differences between mutant and wildtype animals in the total distance travelled the arena of the open field. There seem to be a tendency for the mutant animals to spent more time in the 16% center of the arena than their wildtype littermates, but 2-factorial ANOVA revealed no statistically significant difference. Columns show means, error bars represent SEM, n = 10-12.

To further assess the motoric behavior of Pink1 ko animals in more detail, they were tested on the accelerated rotarod, which examines motor coordination and balance. Pink1 mice were tested how long they are able to stay on a rotarod accelerating from 4 rpm to 40 rpm over a period of 300 s. To exclude extrinsic influences on motor coordination, body weight of the test animals was measured prior to the accelerated rotarod and revealed no significant differences between genotypes (data not shown).

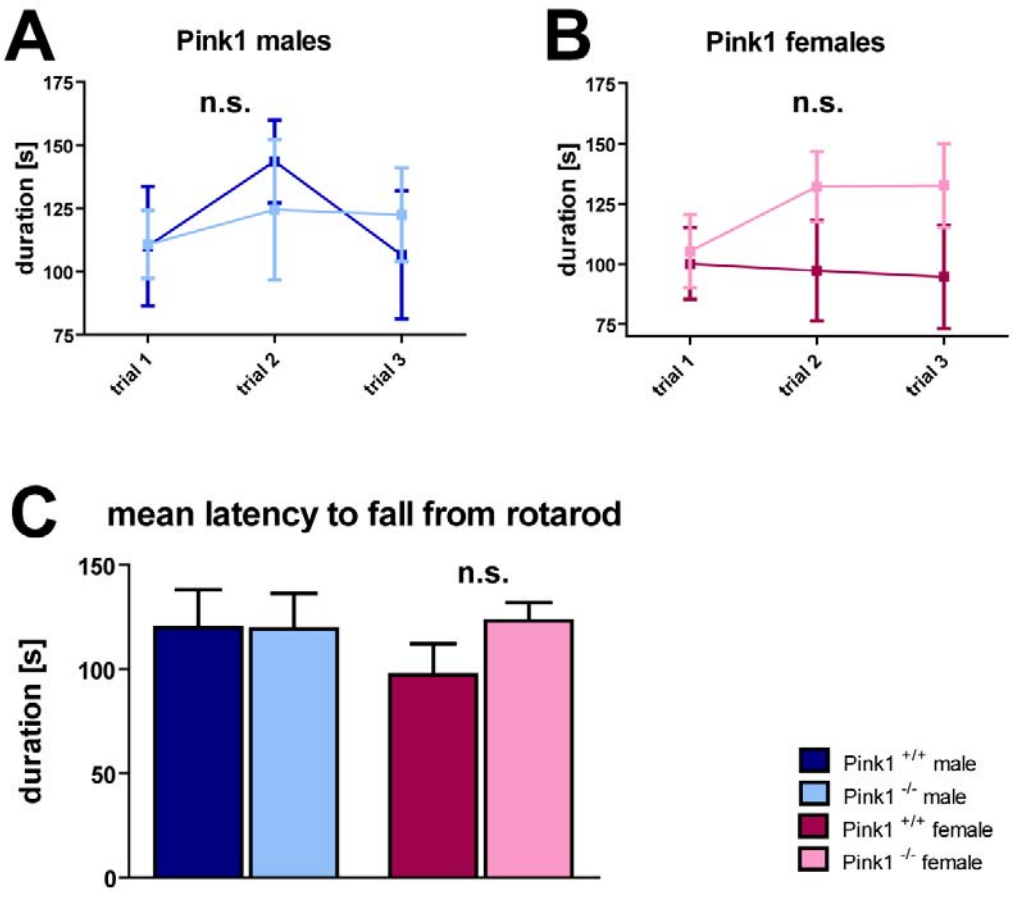

Figure 20: Pink1 knockout mice on the accelerated rotarod.
Pink1 males (**A**) and females (**B**) had three trials on the accelerating rotarod (RM-2-way ANOVA, n.s. $p > 0.05$). (**C**) shows the mean latency to fall from the rotating rod of all three trials. 2-factorial ANOVA revealed no significance for interaction, genotype or sex differences in the latency to fall from the accelerating rotarod (n.s. $p > 0.05$). Depicted are means with error bars representing SEM, n = 10-12.

Pink1 mutants did not differ from their wildtype littermates in the latency to fall from the rotating rod (males: Figure 20 A, repeated measures (RM) 2-way ANOVA, n.s. p = 0.499; females Figure 20 B, RM-2-way ANOVA, n.s. p = 0.514, and 7.4.2 Overview accelerating rotarod). Also evaluation of the mean latency to fall from the rotating rod (Figure 20 C) produced a p-value above 0.05 (2-way ANOVA, n.s. p = 0.367). Thus, Pink1 knockout mice did not show any disturbances in their balance in this test.

5.4.5.2 No depression-like behavior can be seen in Pink1 deficient mice

In addition to the known motoric dysfunctions in Parkinson's disease, many patients suffer from early-indicative features. The discussion and evaluation of these symptoms came up rather recently in the debate about PD. These manifestations include e.g. sleep disturbances, slowness in thinking, decreased motivation, cognitive impairments, and depression. To evaluate the behavior of Pink1 mutant mice in relation to the above mentioned symptoms, they were tested in the forced swim test, which can gives hints about depression-like behavior.

In the forced swim test, mice are placed in a beaker of water where they cannot escape, thus they are forced to swim (4.7.3 Forced swim test). Their behavior is divided into three forms, namely swimming, struggling, and floating (defined as immobility), and recorded. Although the graph looks like Pink1 mutant mice struggled less than the controls, 2-factorial ANOVA did not reveal p-values below 0.05 (Figure 21 B and 7.4.3 Overview forced swim test). Furthermore the time the animals spent swimming or floating did not differ between genotypes or genders (Figure 21 A, C and 7.4.3 Overview forced swim test).

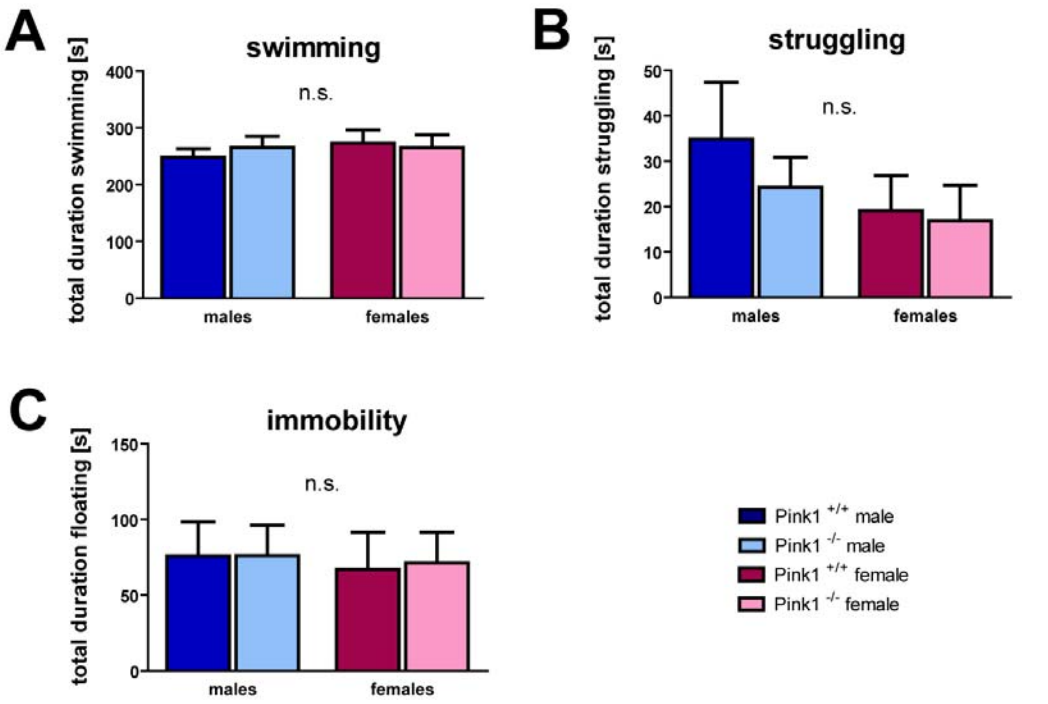

Figure 21: Pink1 mice did not show depression-like behavior in the forced swim test. Pink1 knockout and littermate control mice were put in a beaker filled with water and their behavior concerning swimming (**A**), struggling (**B**), and immobility (floating) (**C**) was recorded. Statistical analysis revealed no significance for interaction, gender or genotype (2-way ANOVA). Columns show means with error bars representing SEM (n = 10-12).

Another behavioral test that can give information about depression-like phenotypes is the tail suspension test. In this test mice are fixed on the tail, hanging upside down in the air, and their behavior concerning activity and immobility is recorded (4.7.4 Tail suspension test). Pink1 knockout females showed a tendency to a higher duration of immobility than their wildtype littermates, but statistical analysis via a 2-factorial ANOVA did not classify this difference significant. Likewise, no significant differences between male mutant and control mice could be detected. (Figure 22). Hence, in the tail suspension test, as well as in the forced swimming test, Pink1 deficient mice did not show any depression-like behavior.

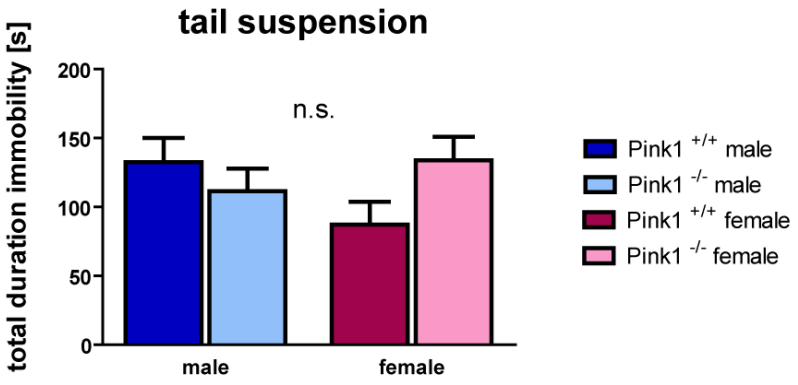

Figure 22: Pink1 knockout displayed no depression-like phenotype in the tail suspension test.
No significance could be determined for the total duration of immobility during tail suspension (2-way ANOVA, n.s. $p > 0.05$). Columns show means with error bars representing SEM (n = 10-12).

5.4.5.3 Ablation of Pink1 leads to cognitive dysfunctions

In addition to depression-like behavior, I wanted to assess another one of the early PD symptoms, which is cognitive impairment, in the Pink1 mutant mice. To assess their social behavior, Pink1 mice underwent a social discrimination test.

In the social discrimination test the animals undergo a sampling phase where they can explore and get to know another mouse. Later they are presented again with this now known mouse and another, novel mouse. Normally they should take more time to olfactorily investigate the unknown animal (4.7.5 Social discrimination test). While Pink1 wildtype male mice did distinguish between a known and an unknown mouse, their mutant littermates did not spend significantly more time exploring the unknown mouse, showing that they are not able to discriminate (RM 2-factorial ANOVA, interaction $p = 0.027$, followed by Bonferroni *post-hoc* test, $p < 0,01$ for familiar vs. novel subject in Pink1 wildtypes, $p > 0.05$ for fam. vs. novel subj. in Pink1 mutants, Figure 23 A, and 7.4.5 Overview social discrimination test). Further statistical evalutation of the test results revealed, that also the difference between the novel and the familiar subject showed a p-value below 0.05 which was considered significant (Figure 23 B, t-test, $p = 0.011$, see 7.4.5 Overview social discrimination test),

as well as the proportion of the novel subject within the sum of novel and familiar subjects (Figure 23 C, p = 0.027, see 7.4.5 Overview social discrimination test). Thus, Pink1 mutant mice are not able to discriminate between a familiar and an unknown mouse.

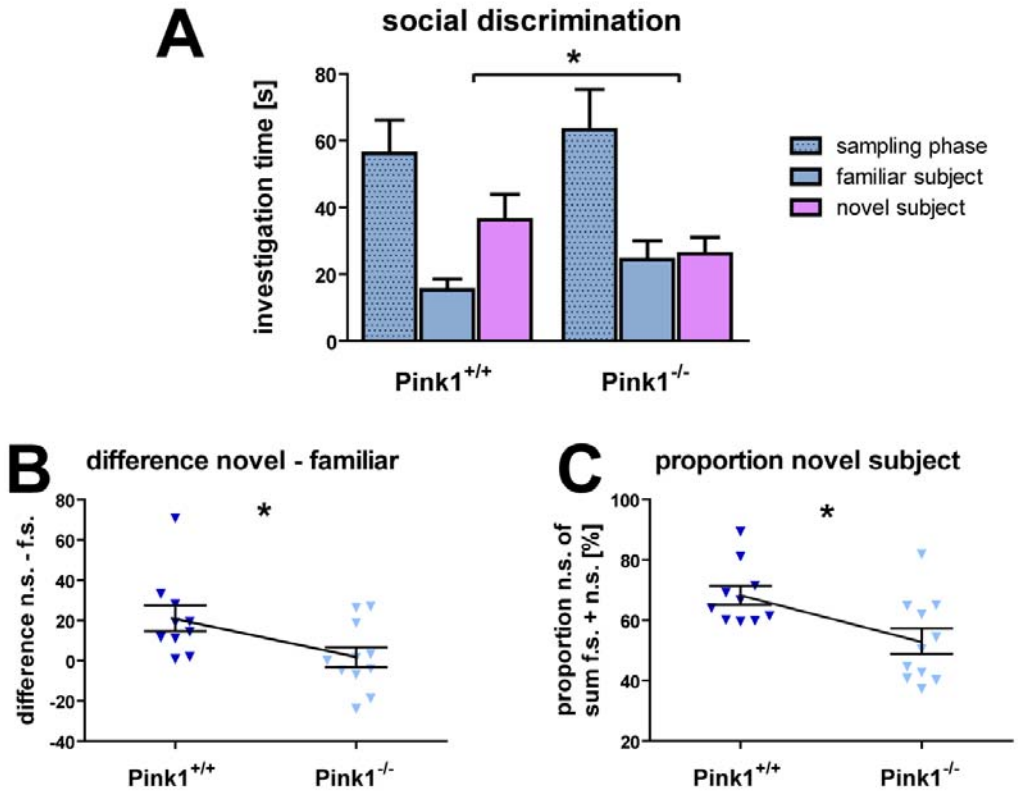

Figure 23: Pink1 ko mice cannot distinguish between familiar and novel mice.
Evalutation of social discrimination test. (**A**) The graph shows the time the test animals spent in olfactory investigation of another mouse during sampling phase and test phase. Repeated-measures 2-factorial ANOVA revealed significant interaction (*p = 0.027). Bonferroni *post-hoc* test showed that wildtype mice could discriminate (p < 0,01) while mutant could not (p > 0.05). (**B**) illustrates the difference between investigation time of unfamiliar and familiar mouse. An unpaired student's t-test revealed a p-value of *p = 0.011 for the difference of the means which is considered significant. (**C**) Proportion of investigating the unfamiliar within the sum of investigation time of familiar and unfamiliar animals. The difference between means of the two genotypes was considered significant as a p-value of *p = 0.027 was calculated using an unpaired student's t-test. Depicted are means, error bars show SEM, n = 10-12.

5.4.5.4 Memory function is normal in Pink1 mutants

One possible reason for the cognitive impairment of the Pink1 knockout mice could be a memory deficit. Thus the animals were tested in an object recognition test which assesses their ability to memorize. In the object recognition test, mice underwent three sampling phases with always the same object to explore. During the test phases which take place 3 hours and 24 hours after the sampling phases, they are presented with the known and a novel object, and the time they olfactorily explore each of the two objects is recorded. Pink1 knockout and wildtype littermate animals of both genders showed no memory deficits as they were able to discriminate between familiar and novel objects 3 hours (Figure 24 A and C) as well as 24 hours (Figure 24 B and D) after the sampling phases. Genders were pooled and repeated-measures 2-factorial ANOVA revealed statistically significant differences between the investigation time of familiar versus novel objects ($p < 0.0001$ after 3 hours, and $p = 0.0033$ after 24 hours), but not between the two genotypes or for interaction (Figure 24 and 7.4.6). Furthermore, the proportion of the novel object within the sum of novel and unknown object did not show significant genoptype differences ($p = 0.398$ after 3 hours, $p = 0.583$ after 24 hours, see 7.4.6 Overview object recognition test). Hence, Pink1 deficiency does not influence the ability of the mice to memorize; it neither affects short term nor long term memory. Thus, this test showed that the observed deficit in social behavior of Pink1 mutant mice is not caused by a memory dysfunction.

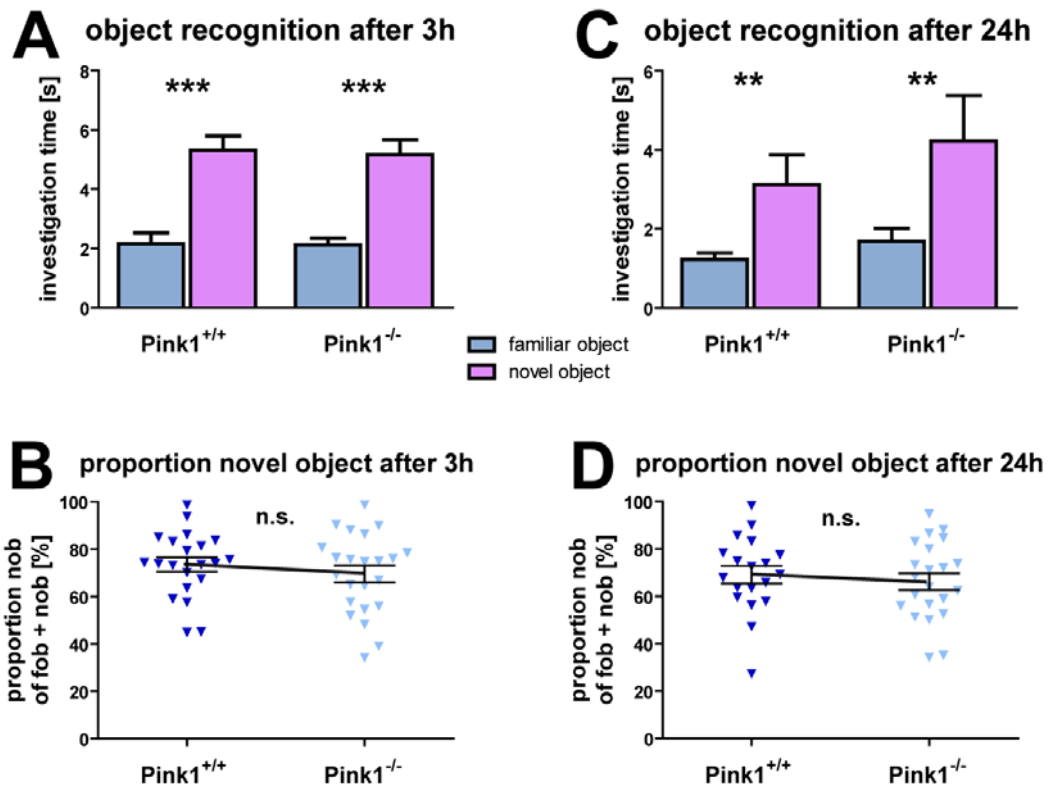

Figure 24: Pink1 knockout mice are able display no short term or long term memory deficit.
Object recognition test of Pink1 knockout and control mice, pooled genders, 3 hours (**A**) and 24 hours (**B**) after the sampling phases. Repeated measures 2-way ANOVA revealed no significant results for interaction or genotype, but a p-value of ***p < 0.0001 for the difference between familiar and novel objects 3 hours after sampling phases, and p-value of **p = 0.0033 for the discrimination between objects 24 hours after sampling phases. The proportion of the novel object within the sum of familiar and novel objects did not reveal statistically significant differences between knockout and control mice 3 hours after sampling phases (**C**) or 24 hours after (**D**) (2-tailed t-test, p = 0.398 for 3h and p = 0.583 for 24 h). Depicted are means with error bars representing SEM (pooled genders, n = 21-24).

5.4.5.5 Odor preference test

Another possible reason for the social impairment of Pink1 mutants could be a deficit in their smelling ability. In order to assess whether they are able to smell properly, Pink1 wildtype and mutant males underwent an odor preference test (4.7.7 Odor preference test). Usually the test animals are expected to spent more time on ofactorily exploring the used cage wood shavings (defined as odorous), than the fresh cage wood shavings (defined as non-odorous). It seems that Pink1 mutants and controls are capable of discriminating between odor and no odor (2-way ANOVA, p < 0.05,

considered not significant for Interaction, genotype, and odor vs. no odor, see 7.4.7 Overview odor preference test). But unexpectedly they explored the non-odorous object longer than the odorous one. This odor test is a very short, preliminary test. It does not allow to draw any conclusions about the detection limit of smells. Furthermore, it might not be sensitive enough to detect very small variances in test animals' smelling abilities. Thus, additional, more specific odor tests were performed.

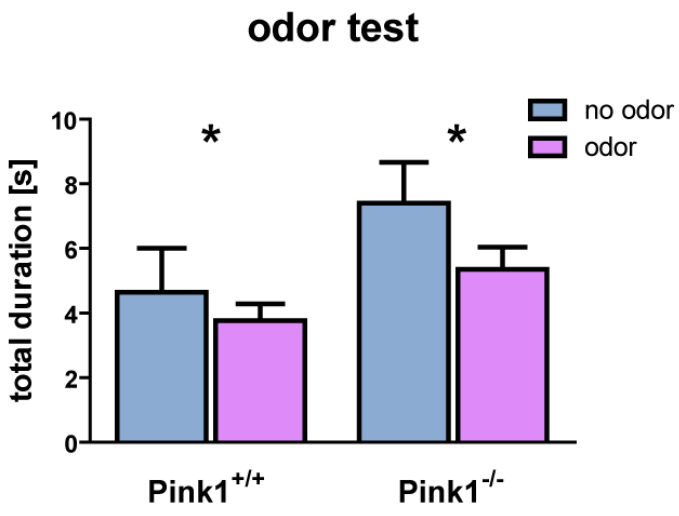

Figure 25: Odor preference test of Pink1 mice.
Depicted are the time Pink1 mutant and control mice spent with olfactorily exploring fresh cage wood shavings (no odor, blue bars) and used cage wood shavings (odor, lilac bars). Pink1 mutant mice seem to be able to distinguish between odor and no odor (*$p < 0.05$). But instead of sniffing longer on the odorous object, they spent more time on olfactorily exploring the odorless object.

5.4.5.6 Odor detection sensitivity

The odor preference test did not lead to satisfying results concerning the mice' smilling ability. Therefore they underwent two other tests concerning their smelling ability at the age of 24 months. One of these tests is the odor detection sensitivity test. Here the animals are trained to recognize and pick one specific odorant at any time. Between two different bowls, one containing cage wood shavings without any specific odor, the other one containing the odor the mouse was trained to in decreasing concentrations, the mouse needs to pick the right bowl. While the wildtype mice reached a binary dilution step of 27 (mean, SEM = 0.95), Pink1 knockout mice could only detect their trained odorant until 22 dilution steps (mean, SEM = 1.50. See also 7.4.8 Overview odor sensitivity test). Statistical evaluation via an unpaired t-test assuming

equal variances resulted in a p-value of p = 0.029, which is considered significant. Thus, Pink1 mutant mice show a significantly lower sensitivity in the detection of odor as the control animals.

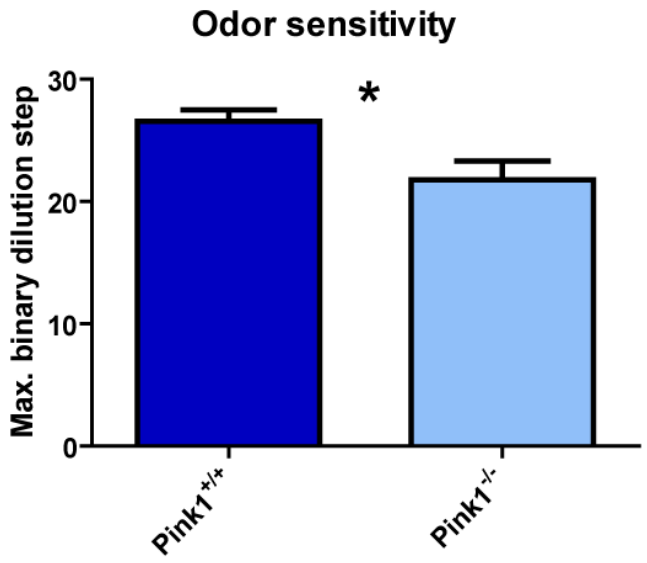

Figure 26: Odor sensitivity test.
Wildtype mice could detect the odorant until a maximum binary dilution step of 27 (mean), Pink1 knockouts only reached step 22 (mean). Graph showing means with SEM. The asterisk stands for a p-value below 0.05, considered significant.

5.4.5.7 Discrimination of binary mixtures of odorant

To further verify a dysfunctional olfactory system in Pink1 mutant mice, they went through another odor test. In this test the mice need to discriminate between two odors and find the one they were trained to. The two bowls contain different binary mixtures of the two odors. While every mouse is only trained to recognize one specific odor at any time, they vary between the two odors used from one animal to the other. Also in this test mice deficient of Pink1 showed smelling problems compaired to their wildtype littermates. At the binary mixtures of 100%, 70%, 55% and 53%, mice of both genotypes were still able to discriminate between the two odors and recognize their trained odor. At the control level of 50% binary mixtures, all mice behaved as expected, as the percentage of their correct choices should lie close to 50%.

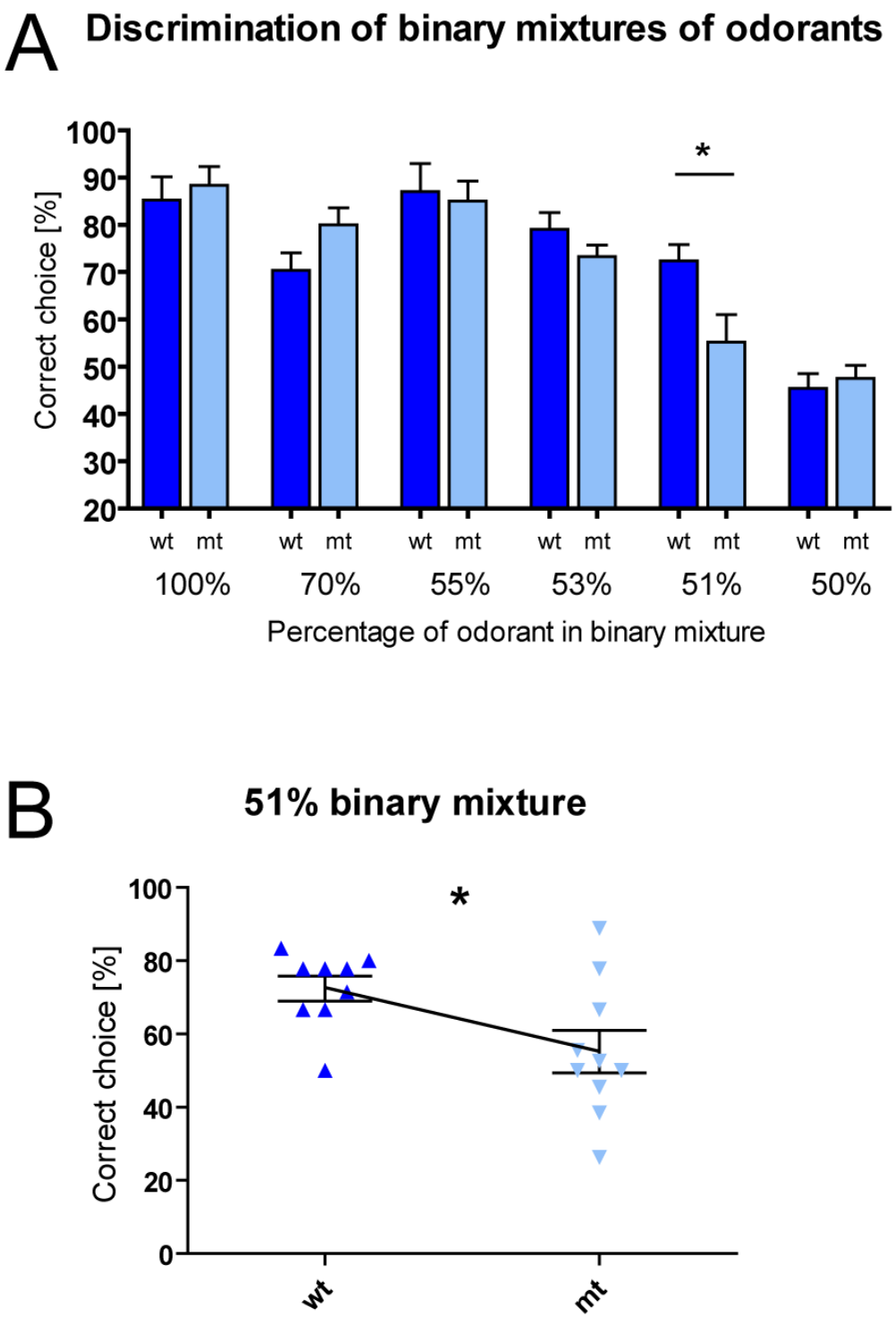

Figure 27: Discrimination of binary mixtures of odorant.
Percentage of correct choice in different percentages of odorant in binary mixture. Bars show means with error bars picturing SEM. (**A**). Scatter dot blot of 51% binary mixture showing means with error bars representing SEM (**B**). wt = wildtype,mt = Pink1 mutant mice. Asterisks indicating p = 0.024, considered significant.

But at a binary mixture of 51%, wildtype animals made the correct choice in 72% of the trials, while Pink1 mutant mice reached only 55% correct choices. Again the p-value was below 0.05 and considered significant ($p = 0.024$, unpaired t-test assuming equal variances. See also 7.4.9 Overview odor discrimination test). Consequently, Pink1 knockout mice show a decreased ability to discriminate between binary odorant mixtures when their concentrations are just above equal destribution of both odorants.

On the surface, Pink1 knockout mice seem have no olfactory problems compaired to their wildtype littermates. But when it comes to detection of very low concentrations of odorant, or discrimination of rather similar binary mixtures of odorant, their ability of olfaction seems to be impaired. This impairment is a presumable reason for their problems in social discrimination.

6 DISCUSSION

6.1 Pink1 expression in the mouse

6.1.1 Pink1 expression during embryonic development

In this work a detailed analysis of the expression of the PD associated gene *Pink1* was performed using radioactive *in situ* hybridization technique. This is the first study of the developmental expression pattern of *Pink1*. At the earliest stage of analysis, E7.5, no specific *Pink1* expression could be observed in the mouse embryo. This leads to the suggestion, that *Pink1* is not expressed during early embryonic development. *Pink1* expression was first detected around E9.0. At this stage, the gene is expressed ubiquitously throughout the whole embryo. The pattern of expression stays ubiquitously during development, but it starts to be specifically stronger in defined regions from E10.0. onwards (Figure 6). Regions of strong Pink1 expression during development are e.g. the developing heart, liver, and brain. These are areas which are particularly energy consuming. Since mitochondria are the cell organelles supporting cells with their required energy, and Pink1 was shown to localize to mitochondria (Silvestri *et al.*, 2005), this would support a role of Pink1 in mitochondrial function. Other areas of strong *Pink1* expression during embryonic development are the thalamus, and the hypothalamus, where *Pink1* is even more abundant. It should be considered that the time of onset of *Pink1* expression is around E 9.0, and it is particularly strongly expressed in developing neural tissue. These findings might imply Pink1 in specification and differentiation of neurons in the brain, which starts around E9.5-E10 in the mouse (Prakash & Wurst, 2004). In addition, I confirmed Pink1 expression in the mesencephalic flexure, which is the area where midbrain dopaminergic neurons, including those neurons predominantly affected by neurodegeneration in PD, arise from (Prakash & Wurst, 2004). Interestingly, the developmental expression pattern of Pink1 mainly resembles that of DJ-1 during development (Röthig *et al.*, submitted). Considering that *Pink1* and *DJ-1* were shown to be inherited in a digenic manner (Tang *et al.*, 2006), and both proteins localize to mitochondria (Silvestri *et al.*, 2005; Zhang *et al.*, 2005), this

finding allows the suggestion that these two PD related genes might function in the same or at least similar pathways.

6.1.2 Pink1 expression in the adult mouse brain

In the expression analysis of *Pink1* in the adult mouse brain I could confirm results of other studies, which report distinct areas of strong *Pink1* expression in the cortex, thalamus, hippocampus, substantia nigra, striatum, and pons (Blackinton *et al.*, 2007; Taymans *et al.*, 2006). Furthermore I could verify findings of strong *Pink1* expression in regions CA1-CA3 of the hippocampus, while in the dentate gyrus expression levels are strong, but not as intense (Blackinton *et al.*, 2007). Cerebellar *Pink1* expression manifested relatively weakly in the purkinje and granule cell layer compared to the molecular layer and the cerebellar nuclei, confirming findings of other groups (Taymans *et al.*, 2006). Again specific *Pink1* expression in the hypothalamus was detected, which I observed previously during development. This finding might be of interest with regard to PD, as a group of neurons in the zebrafish hypothalamus was found to be specifically vulnerable to MPTP treatment (Wen *et al.*, 2008). These neurons could also be specifically vulnerable to other parkinsonism-inducing incidents, hence anti-apoptotic factors such as Pink1 would be very important for them. Starting in later developmental stages and staying until adulthood, the thalamus manifested to be another region of marked *Pink1* expression. Defined thalamical nuclei as the anterior ventromedial thalamic nuclei around birth and the anterodorsal thalamic nucleus in the adult brain showed even more intense expression than other parts of the thalamus. In addition, I found high levels of *Pink1* in areas where other studies reported only mild expression, including the substantia nigra, dentate gyrus of the hippocampus, and superior and inferior colliculi (Taymans *et al.*, 2006). Most strikingly, in the PD related substantia nigra pars compacta, levels of *Pink1* are strikingly high, while the neighboring substantia nigra pars reticulata exhibits only moderate expression. In other studies in mouse brain, both regions of the substantia nigra showed medium Pink1 occurence (Taymans *et al.*, 2006). In rat brain the effect I observed was also seen, but

not as distinct (Taymans *et al.*, 2006). In my study, *Pink1* was found to be specifically strongly expressed in neuronal cells, while glia did not show specific signals, and *Pink1* was absent from endothelial cells (Figure 7 E). These results verify others from studies of *Pink1* mRNA in mouse, rat, and human brain, but there are also opposing findings of Pink1 protein in glial and endothelial cells (Gandhi *et al.*, 2006). It might be that expression of Pink1 protein depends on other factors than just the amount of mRNA, which would explain the differences between *Pink1* mRNA and Pink1 protein expression. The contradictory findings I observed could be explained by the different techniques used for expression analysis. In this approach, radioactive *in situ* hybridization was used, which is a very sensitive method, that can detect more distinct patterns than other methods. Furthermore, tissue of rat and human brain was investigated in some of these analyses, hence another reason for disagreements might be species differences in the expression of *Pink1*.

6.2 Generation of the Pink1 knockout mouse line

In 1997, *α-synuclein* was found to be the gene corresponding to *PARK1*-linked parkinsonism (Polymeropoulos *et al.*, 1997). This discovery demonstrated for the first time that a specific mutation can cause a well-defined form of parkinsonism. In addition, it led to the identification of α-synuclein as the main component of Lewy bodies, providing further insight in important factors in the underlying mechanisms of PD pathogenesis. In the following years, several other of the PD causing loci were mapped to yield specific genes. The discovery of these genes, the subsequent generation of genetically engineered animal models, and their analysis provides a great opportunity to investigate the mechnisam of neurodegeneration in PD. Animal models of parkinsonism represent an excellent possibility to accelerate the progress in this field. They allow an investigation in respect of underlying mechanisms of neuronal degeneration and dysfunction, factors that predispose to the disease. In addition, animal models also provide possibilities to modify disease progression. At the beginning of this research project, no Pink1

deficient animal models had been published. Therefore mice with a deletion of the PD-related gene *Pink1* were generated in this research project.

Complete knockout models can be embryonically lethal when the gene of interest either has a basic role in cellular or developmental biology. Embryonic lethality or the death of test animals early after birth limit the functional characterization of a gene of interest; they can even exclude it. In order to avoid this, conditional knockouts can be generated via specific systems as e.g. the Cre/loxP or flp/FRT system. A complete knockout can still be achieved from the conditional e.g. by crossing a the conditionally targeted mouse line with a line expressing Cre in the zygote or in all cells of the organism. At the beginning of this research project, no detailed information about Pink1 function was available. It was predicted from its amino acid sequence to contain a serine-threonine kinase domain and a mitochondrial targeting motif, and recombinant Pink1 was shown to colocalize with mitotracker, suggesting a mitochondrial localization (Valente *et al.*, 2004a). Hence it seemed possible that Pink1 executes an important function in mitochondria. Mitochondria are indispensable for every kind of cell because they generate the energy for all occuring cellular processes. Consequentially, embryonic lethality of Pink1 knockout mice appaered likely. Thus, the targeting strategy of Pink1 was planned to generate a conditional knockout. In contrast to conventional gene deletion, a conditional knockout mouse can be combined with any Cre expressing mouse line. This generates a knockout of the gene of interest at defined developmental stages. Another advantage of conditional mutagenesis is the possibility to study the function of a gene only in a determined kind of cell type.

After electroporation of the targeting construct DNA into ES cells, 3 clones out of 600 were found to be positive for homologous recombination, which is in the expected range of ca. 0.5% positive clones per electroporation. These clones had been verified by Southern blot screening using various probes and digestion enzymes to confirm the correct insertion of the targeting construct on the 3’- and 5’-end. But in the end two of these assumedly positive clones proved themselves negative, because they did not contain the second loxP site lying almost 2 kb further downstream than the rest of the recombinant

DNA (see Figure 10 C). Finally the remaining clone was found to be positive for complete homologous recombination and was used for injection into blastocysts to generate mice. The Pink1 conditional (floxed) mice were cross-bred with mice of a Cre deleter line to yield a complete knockout. *Pink1*$^{-/-}$ mice turned out to be viable as well as capable of reproduction. Therefore this project was continued with the analysis of the complete knockout mice. The finding that Pink1 expression in the wildtype mouse starts around E9.0, and shows remarkably strong signals in developing neural tissue lead to the hypothesis, that Pink1 might be important for neurogenesis in the developing brain (see 6.1.1 Pink1 expression during embryonic development). But Pink1 mutant mice proved to be viable throughout adulthood. Furthermore they show no obvious alterations of brain morphology. This indicates that Pink1 has no obvious and drastic effect on the development of the brain. Furthermore it does not seem to be relevant for neuronal cell survival.

6.3 Removal of *Pink1* exons 2 and 3 leads to Pink1 knockout

To verify the knockout of Pink1, RT-PCR on mouse brain RNA and RNA from MEF cells was performed. Primers were designed to lie in exons 1 and 4, spanning the two exons to be removed in the knockout. Bands of the expected size confirmed the knockout in samples with *Pink1*$^{-/-}$ genotype on the mRNA level. All band intensities of truncated mRNA were comparably weaker than the intensities of wildtype *Pink1* mRNA, suggesting only very low abundance of mutant mRNA as well. Thus, the removal of *Pink1* exons 2 and 3 as planned in the targeting construct leads to a Pink1 knockout.

6.4 Generation of mouse embryonic fibroblast cell lines

Working with mouse models provides a unique opportunity to study various processes in an animal organism that is highly homologous to the human organism. However, there are some disadvantages of this model system. Performing experiments in the mouse can be rather time consuming, because in the mouse one cycle of generation takes three months. Another option for

research is to perform cell culture experiments. Working *in vitro* is not an alternative to the mouse organism, but it provides an option of a quick, preliminary analysis which can then be confirmed and/or continued subsequently in the mouse model. In order to assess questions and obtain conclusions in a fast, preliminary way, I generated 56 mouse embryonic fibroblast cell lines from Pink1 knockout mice. To ensure the use of adequate controls, heterozygous animals were used for the breedings so that pairs of mutant and control cell lines were always originating from the same offspring. To keep these cell lines in culture over a long time range, selected pairs of MEF cell lines were immortalized. Immortalization of primary cell lines can be performed in several ways. While transfection with largeT Antigen can lead to side effects originating from the inserted DNA, the 3T3 method is based on spontaneous mutation of the cells, which can be of different origin in every single cell line. In this project I wanted to be aware of possible side effects, therefore I chose to use both method for immortalization of MEF cells in parallel.

6.5 Absence of Pink1 does not alter mitochondrial morphology or OPA1 processing

Pink1 seems to play a role in the regulation of mitochondrial function involved in PD pathogenesis. This hypothesis is supported by several studies that demonstrate mitochondrial localization of recombinant, tagged Pink1 in mammalian cell lines (Beilina *et al.*, 2005; Clark *et al.*, 2006; Gandhi *et al.*, 2006; Petit *et al.*, 2005; Valente *et al.*, 2004a), as well as endogenous Pink1 in *Drosophila* and human tissue (Clark *et al.*, 2006; Gandhi *et al.*, 2006). To find out more about the influence of Pink1 on mitochondrial dynamics, the mitochondrial morphology was analyzed in the presence and absence of Pink1. In three different pairs of Pink1 mutant and corresponding wildtype MEF cell lines no alterations of mitochondrial morphology could be observed (see 5.4.2.2 Pink1 deficiency does not lead to changes in mitochondrial morphology). Furthermore, the abundance of different isoforms of OPA1 was analyzed, because OPA1 gets proteolytically processed into smaller isoforms

when the mitochondrial membrane potential is disturbed. This effect directly connects changes in mitochondrial morphology with mitochondrial dysfunction (see 2.2.4 Pink1 and mitochondrial dynamics and (Duvezin-Caubet *et al.*, 2006). In this research project I could show that proteolytic processing of OPA1 is not changed in Pink1 mutant MEF cells compared to control cell lines (5.4.2.3 Ablation of Pink1 does not change OPA 1 (Optic Atrophy 1) processing). Most of the reported Pink1 deficient fly models e.g. exhibit rather severe phenotypes, including swollen or enlarged mitochondria (Clark *et al.*, 2006; Park *et al.*, 2006; Yang *et al.*, 2006). One reason for the observed findings in this project, contradicting to some published data, might be species differences. Despite the conservation of important constitutive cell processes in *Drosophila* and mammals, there are subtle but important differences between different organisms which might result in observations in mice, that are not relevant to human disease and vice versa (Muqit & Feany, 2002). The differences between a fly and the organism of a mammal would even be more pronounced. Thus, the differences between the reported, severe mitochondrial phenotypes in Pink1 deficient *Drosophila* models and the results of this work could result from species differences. Furthermore, different cell types likely have different energy requirements. In some *Drosophila* models of Pink1 deficiency, the drastic effect on mitochondrial structure was only demonstrated in muscle tissue (Clark *et al.*, 2006; Park *et al.*, 2006). Moreover, in several of the reported experiments, a knockdown strategy was used to generate a lack of Pink1 protein. Pink1 downregulation represents a rather acute model of protein deficiency, whereas knockout cells or organisms lack Pink1 from the moment they exist on. This can result in functional substitution of Pink1 by other proteins over a range of time, during which the cell or the organism deals with the situation even better over time and new equilibria of cellular processes are formed. This might not or only partially resemble the situation in acute knockdown models. This notion is supported by the fact that in primary cortical neurons after lentiviral mediated knockdown a mitochondrial fragmentation could be observed (Lutz *et al.*, 2009). However this phenotype vanishes with time suggesting the presence of compensatory mechanisms (Kloos, personal communication). In addition, clearly significant differences in mitochondrial morphology of Pink1 deficient HeLa cells and human fibroblasts

were only observed under low-glucose cirumstances (Exner *et al.*, 2007). In addition to Pink1 deficiency, the use of low glucose media represents another stressing factor for the cells. Another possible reason for the observed contradictory results could be that the influence of Pink1 deficiency on mitochondrial morphology might come into appearance only under stress conditions.

6.6 Pink1 and mitochondrial complex I activity

Evidence suggests impairment of the mitochondrial respiratory chain in sporadic and toxin induced PD. However the most suggestive link to mitochondrial dysfunction comes from the study of genetic forms of PD, where it was reported that pathogenic mutations in the mitochondrial protein Pink1 are sufficient to cause the disease (Valente *et al.*, 2004a; Valente *et al.*, 2004b). While several previous studies show compromised mitochondrial function in loss of Pink1 function animal models, the exact mode of action of Pink1 remained unclear. In a collaborative work was shown that Pink1 deficiency causes defects in reserve pool (RP) mobilization during intense stimulation. Furthermore a key defect in the electron transfer chain at the level of complex I caused by Pink1 loss of function was demonstrated in mouse brain, in *Drosophila* brain, and muscle enriched tissues (see 5.4.3 Parkinson's disease mutations in Pink1 affect Complex I activity in mitochondria). Moreover, this deficit is rescued when Pink1 is reintroduced. The lack of complex I activity could be an explanation for the phenotypes associated with Pink1 loss of function. Complex I loss can lead to a reduction of the mitochondrial electrochemical gradient and hence promote opening of the voltage dependent mitochondrial permeability transition pore (PTP), which can then cause an increase of cytochrome c release and thus cell death (Irwin *et al.*, 2003). Loss of complex I in synaptic mitochondria may also result in RP mobilization defects during intense stimulation. The RP defect observed in Pink1 mutants is very reminiscent to, albeit not as severe as that observed in Drp1 mutants (Verstreken *et al.*, 2005). Drp1 mediates mitochondrial fission and its overexpression in neurons results in excess synaptic mitochondria (Li

et al., 2004). Loss of Drp1 leads to depletion of synaptic mitochondria and decreased local mitochondrial ATP production which is critical for RP mobilization (Verstreken *et al.*, 2005). Consistent with this hypothesis, ATP levels in Pink1 mutant *Drosophila* and SH-SY5Y cells are reduced compared to controls (Clark *et al.*, 2006; Lutz *et al.*, 2009), which provides an explanation for the neuronal defects observed in Pink1 mutants. Moreover, feeding the synapses with ATP rescued the RP mobilization deficit. This indicates that energy demands requiring strong mitochondrial function are reduced in Pink1 mutant synapses. The observed results are also consistent with data on genetic interactions between Drp1 and Pink1. In some cases loss of Drp1 function worsened, while adding a copy of Drp1 alleviated Pink1 loss of function phenotypes (Poole *et al.*, 2008; Yang *et al.*, 2008). But other groups also reported a mitigation of Pink1 loss of function phenotypes upon expression of a dominant negative form of Drp1 (Lutz *et al.*, 2009). While some of these data indeed suggest a synergistic effect of Drp1 and Pink1 deficiency, they are still quite controversial, and they do not necessarily imply a direct role of Pink1 in mitochondrial fission. The impairment of complex I observed on collaboration could also be another explanation for the discrepancies between this work and others dealing with the effect of Pink1 on mitochondrial morphology. Any kind of mitochondrial dysfunction is accompanied by its fragmentation (Dimmer *et al.*, 2008; Rojo *et al.*, 2002). Thus, is seems very likely that the reported mitochondrial fragmentation and/or exceeding fission resulting from deficiency of Pink1 is an epiphenomenon of the primary mitochondrial dysfunction sustained by reduced complex I activity.

6.7 Ablation of Pink1 has no effect on the numbers of nigral dopaminergic neurons and levels of striatal dopamine

In order to have a closer look into the nigrostriatal system of Pink1 knockout mice, TH-positive substantia nigra neurons were examined. Pink1 mutants did not show any gross abnormalities in the neuronal structure and tissue organization in this area (see Figure 16). As in other Pink1 deficient mouse

models and most other models of familial PD (Abeliovich *et al.*, 2000; Andres-Mateos *et al.*, 2007; Chandran *et al.*, 2008; Chen *et al.*, 2005; Goldberg *et al.*, 2003; Goldberg *et al.*, 2005; Itier *et al.*, 2003; Kim *et al.*, 2005; Kitada *et al.*, 2007; Masliah *et al.*, 2000; Matsuoka *et al.*, 2001; Palacino *et al.*, 2004; Rathke-Hartlieb *et al.*, 2001; Von Coelln *et al.*, 2004; Yamaguchi & Shen, 2007; Zhou *et al.*, 2007) the number of dopaminergic neurons in the substantia nigra pars compacta is not reduced in the Pink1 knockout mouse model described in this work. To verify these findings, the amounts of dopamine and its metabolite DOPAC were measured in cortex, hippocampus, striatum, and ventral midbrain of Pink1 mutant and control mice. Most importantly with respect to PD, the absence of Pink1 did not change levels of dopamine or DOPAC in the striatum, as well as in other brain regions assessed. These results are in agreement with other results from Pink1 deficient mice (Kitada *et al.*, 2007; Zhou *et al.*, 2007). Consistent with the unaltered numbers of TH-positive nigral neurons and normal levels of striatal dopamine, Pink1 mutant mice did not show any deficits in the balance or the distance they traveled in the open field. Also they did as well as the controls on the accelerated rotarod. Thus, it looks like the nigrostriatal system of dopaminergic neurons is not affected in general by Pink1 deficiency. This effect was also observed in a variety of other familial PD mouse models (Abeliovich *et al.*, 2000; Goldberg *et al.*, 2003; Perez & Palmiter, 2005; Richfield *et al.*, 2002; Yamaguchi & Shen, 2007; Zhou *et al.*, 2007), as they showed an absence of motor dysfunctions. Since PD is an age-related disease, it seems likely that a variety of circumstances is needed to overcome a certain threshold upon which the death of nigral dopaminergic neurons is initiated. These circumstances could be a combination of genetic events, age-related factors, and environmental impacts, where the focus lies probably on the latter, as an aged triple knockout mouse model of PD genes Pink1, Parkin, and DJ-1 did not show nigral degeneration as well (Kitada *et al.*, 2009).

6.8 Pink1 deficient mice show slightly elevated levels of cortical serotonin

Neurodegeneration in PD can affect several neuronal systems in different areas of the brain. In addition to the specific degeneration of nigrostriatal dopaminergic neurons, the affected areas can include for instance the cortex and hippocampus, were the serotonergic dorsal raphe neurons and the noradrenergic neurons of the locus coeruleus project to (Leranth & Hajszan, 2007; Shen & Cookson, 2004). To find out whether any of these systems might be affected in Pink1 mutant mice, the contents of serotonin (5HT) and its metabolite 5-HIAA, and noradrenaline, were also measured in cortex, hippocampus, striatum, and ventral midbrain of Pink1 mutant and control mice. Most of the assessed neurotransmitters were not altered in any of the different brain regions. But interestingly, the HPLC analysis revealed that levels of serotonin were slightly, but significantly elevated in mutant mice (see 5.4.4.2 Quantitative analysis of catecholamines in Pink1 knockout brains revealed elevated cortical levels of serotonin (5HT)). Quantities of cortical 5-HIAA, a metabolite of 5HT, are not significantly lower in mutants than in wildtype animals. Thus, a deficit in serotonin turnover can be excluded as a cause for the elevated levels of 5HT. It was reported that serotonin by itself is involved in the regulation of dopamine release via actions on complex neuronal circuitries, both directly and indirectly (Di Matteo *et al.*, 2008). The increase of serotonin could be the cause of another to date unknown event in PD pathogenesis. Moreover, it might also stand in relation with the observed RP mobilization defects during intense stimulation. However, it should be taken into consideration that there is just a very slight difference between the serotonin levels in Pink1 mutant and wildtype mice. Thus, for a more accurate interpretation this experiment would need to be repeated with a higher number of animals. Furthermore, since PD is an age-related disease, it would also be very important to monitor this circumstance in aged animals and find out whether the effect increases with age.

6.9 Pink1 and early PD symptoms

In addition to the characteristic symptoms of Morbus Parkinson, non-motoric deficits were reported to be implicated in the disease as well. These include e.g. insomnia, depression, anxiety, olfactory dysfunction, slowness of thinking, dementia, hallucination, reduced motivation, and cognitive impairments (Hughes *et al.*, 2000; Juri *et al.*, 2008; Madeley *et al.*, 1991; Matuja & Aris, 2008; Mindham, 1970; Verbaan *et al.*, 2007; Verbaan *et al.*, 2008). Most of the abovementioned deficits emerge prior to the characteristic PD symptoms nigral degeneration and motor dysfunctions (Poewe, 2008). To assess some of these non-motor symptoms in Pink1 deficient mice, they underwent a battery of different behavioral tests. Open field, forced swimming and tail suspension tests revealed that Pink1 mutants do not display any anxiety phenotype or depression-like behavior. Another important early-indicative PD symptom is cognitive impairment. In the case of the Pink1 mutant mouse line generated in this project, this was assessed via a social discrimination test. I could show that mice lacking Pink1 cannot discriminate between a known and an unfamiliar mouse. One possible circumstance underlying this dysfunction could be dysfunctional memory. Therefore an object recognition test was carried out. In this test mutant mice performed as well as controls and showed, that they were able to discriminate between known and unknown objects even 24 hours after the sampling phase. This means, that Pink1 deficient mice show normal short-term and long-term memory. Hence, I could exclude an insufficiency in memory function as a possible cause for the social discrimination deficit. Another possible reason for this deficit could be an impairment in olfaction or olfactory discrimination. In order to assess this feature, Pink1 mice were tested in an odor preference test, which gave only very unsatisfying results, as it is very preliminary and not specific enough to reveal slight differences in olfaction. Thus the animals underwent two additional, more specific odor tests. The odor sensitivity test and odor discrimination test revealed that Pink1 knockout mice show no deficit when they need to discriminate between clear, strong odorants or have to detect high concentrations of odorant. But when it comes to a range where the maximum sensitivity of their olfactory system is needed, their ability of olfaction is impaired. Thus, Pink1 knockouts do show an olfactory

dysfunction. This impairment could be a possible cause for the observed phenotype in social discrimination. Furthermore, it was shown that olfactory bulbectomized rats show a lower rate of serotonin synthesis (van der Stelt *et al.*, 2005) and serotonin increases the excitatory response to odorous stimulation in moths (Kloppenburg *et al.*, 1999). Thus, it might also be possible that the beforementioned increase in cortical serotonin is an attempt of the organism to overcome olfactory deficits.

6.10 Conclusion and outlook

In this work a Pink1 (PARK6) conditional and complete knockout mouse line was successfully generated. A detailed expression analysis of Pink1 showed that it is ubiquitously expressed, with high occurance in the overall mouse brain, strong expression in the PD-implicated substantia nigra pars compacta, and specifically striking neuronal expression. These findings suggest that the Pink1 knockout mouse line is an adequate model for the study of Parkinson's disease. The complete Pink1 knockout mouse line proved to be viable and fertile and was therefore analyzed to find out more about the function of Pink1 in respect to the pathology of Parkinson's disease. Alterations of mitochondrial morphology have been observed in *Drosophila* and *in vitro* models before, but could not be detected in the Pink1 mutant mouse embryonic fibroblast cell lines generated in during this work. Possible explanations for this finding might be species differences in the function of Pink1 in mitochondria, a possible functional substitution of Pink1 because of the non-acuteness of this mouse model, or the possibility Pink1 does not have a direct impact on mitochondrial morphology. Changes in mitochondrial dynamics might rather be a secondary effect to the until now unknown primary functions of Pink1 in mitochondria. A collaborative analysis yielded the discovery of defects in RP mobilization upon intense stimulation and impaired complex I activity in the absence of Pink1. This provided genetic evidence that mutations found in a subset of autosomal recessive PD are similarly resulting from a similar central pathogenic event, the impairment of complex I activity. This impairment is likely the underlying

primary event of influences on mitochondrial dynamics, and thereby a reason for contradictory results in the area of mitochondrial morphology.

Up to now, no described rodent model for PD was capable of reproducing all key symptoms of the disease that can be found in human patients: slowly progressing motor dysfunctions combined with loss of striatal dopamine fibers and dopamine neuron loss in the substantia nigra accompanied by Lewy body pathology. Several toxins as for instance MPTP or rotenone are known to cause parkinsonian-like symptoms as well. In particular those substances with a high specificity for dopaminergic neurons induce many of the characteristic features of PD. But these are of less importance in the process of understanding the pathoaethiology of PD, since only very few PD cases are caused by toxins. It is rather suggested, that a combination of environmental and genetic factors might lead to the disease. Therefore it can be of particular interest to combine genetic and toxin-induced models. The study on Pink1 and mitochondrial morphology could be followed up e.g. with challenging experiments using substances as paraquat and rotenone, or by analyzing mitochondrial morphology and/or complex I under oxidative stress conditions. Furthermore, to be closer to the situation in the living brain, it is needed to assess mitochondrial morphology in neurons and in the mouse brain. This could be realized with primary neuronal cultures and knockdown of genes of interest via lentiviral injections into the brain of Pink1 knockout mice.

A characteristical PD-like phenotype with degeneration of dopaminergic neurons in the substantia nigra and altered levels of dopamine in the striatum and ventral midbrain could not be observed in Pink1 knockout mice. Confirming the missing organic phenotype, no impairment of motoric behavior could be detected in Pink1 mutant mice. An evaluation of the levels of specific neurotransmitters in different brain regions showed an increased amount of cortical serotonin in Pink1 deficient mice. This result could be connected with the dysfunctional RP mobilization, as serotonin can be involved in the regulation of dopamine release. Moreover, the upregulation of serotonin might also be an effort of the organism to overcome detected olfactory deficits. To further verify this finding and find out more about a possible connection to the vesicular dopamine release, it would be necessary to repeat this experiment

with a greater number of test animals and find out if the effect increases with age.

This work was the first study where Pink1 deficient mice were screened for cognitive impairment. Since this is one of the early-indicative symptoms of Parkinson's disease, which can arise a long time before the typical motoric symptoms, this is of particular interest for PD. The analysis of Pink1 mice revealed that Pink1 mutants do show deficits in social discrimination, which are not caused by memory defects, but rather by an impairment in olfaction. Many PD patients display non-motor defects that emerge considerably early in the progress of the disease. The cognitive impairment observed in Pink1 deficient mice verifies this mouse model as a very promising candidate for studies on early non-motor symptoms of Parkinson's disease. Nevertheless, it would be very important to find out more about the molecular events underlying the observed olfactory impairment in further studies.

The fact that Pink1 function in mice is non-essential for the survival of nigral neurons suggests that additional factors contribute to nigral degeneration, one of the main characteristics of PD. Furthermore, regarding all reported data about other PD mouse models, it appaers that the mere absence or genetic modification of one of the familial PD genes is not sufficient to induce PD characteristic symptoms as e.g. the death of nigral dopaminergic neurons and subsequent motor dysfunction in mice. Different factors implied in PD pathogenesis, as e.g. UPS impairment, oxidative stress, mitochondrial dysfunction, and problems in cytoskelettal transport, might all share one downstream target or pathway. If several of these critical factors occur simultaneously, vicious circles could be initiated. Thereby a threshold could be exceeded, which would subsequently lead to neuronal degeneration.

7 APPENDIX

7.1 Overview of generated MEF cell lines

cell line	breeding pair (male / female)	preparation date	genotype Pink1	immortalization
AR365/1	475 / 365	31.08.2006	+/-	
AR365/2	475 / 365	31.08.2006	+/-	
AR365/3	475 / 365	31.08.2006	+/+	
AR365/4	475 / 365	31.08.2006	+/-	
AR365/5	475 / 365	31.08.2006	+/+	
AR365/6	475 / 365	31.08.2006	+/-	
AR365/7	475 / 365	31.08.2006	+/-	
AR365/8	475 / 365	31.08.2006	+/+	
AR365/9	475 / 365	31.08.2006	+/-	
AR365/10	475 / 365	31.08.2006	+/-	
AR365/11	475 / 365	31.08.2006	+/-	
AR112/1	475 / 112	11.10.2006	l/+	
AR112/2	475 / 112	11.10.2006	-/-	
AR112/3	475 / 112	11.10.2006	+/-	
AR138/1	476 / 138	11.10.2006	+/-	
AR138/2	476 / 138	11.10.2006	+/-	
AR138/3	476 / 138	11.10.2006	+/-	
AR170/1	475 / 170	30.10.2006	+/-	
AR170/2	475 / 170	30.10.2006	+/-	
AR170/3	475 / 170	30.10.2006	+/-	
AR170/4	475 / 170	30.10.2006	-/-	
AR170/5	475 / 170	30.10.2006	-/-	
AR170/6	475 / 170	30.10.2006	-/-	largeT
AR170/7	475 / 170	30.10.2006	+/+	3T3 & SV40 largeT
AR170/8	475 / 170	30.10.2006	-/-	
AR170/9	475 / 170	30.10.2006	-/-	3T3
AR325/1	475 / 325	29.01.2007		
AR325/2	475 / 325	29.01.2007	+/+	

AR325/3	475 / 325	29.01.2007	+/-	
AR325/4	475 / 325	29.01.2007		
AR325/5	475 / 325	29.01.2007		
AR367/1	476 / 367	29.01.2007	+/+	
AR367/2	476 / 367	29.01.2007	+/+	
AR367/3	476 / 367	29.01.2007		
AR367/4	476 / 367	29.01.2007	+/-	
AR367/5	476 / 367	29.01.2007	-/-	largeT
AR367/6	476 / 367	29.01.2007	+/+	largeT
AR367/7	476 / 367	29.01.2007	+/-	
AR367/8	476 / 367	29.01.2007	+/+	
AR1.1	1357 / 1224	02.11.2007	+/+	
AR1.2	1357 / 1224	02.11.2007	l/+	
AR1.3	1357 / 1224	02.11.2007	l/+	
AR1.4	1357 / 1224	02.11.2007	+/+	
AR1.5	1357 / 1224	02.11.2007	l/+	
AR1.6	1357 / 1224	02.11.2007	l/+	
AR1.7	1357 / 1224	02.11.2007	l/+	
AR1.8	1357 / 1224	02.11.2007	l/+	
AR1.9	1357 / 1224	02.11.2007	+/+	
AR2.1	1360 / 1350	02.11.2007	l/+	
AR2.2	1360 / 1350	02.11.2007		
AR2.3	1360 / 1350	02.11.2007	+/+	largeT
AR2.4	1360 / 1350	02.11.2007	+/+	largeT
AR2.5	1360 / 1350	02.11.2007	l/l	
AR2.6	1360 / 1350	02.11.2007	+/+	largeT
AR2.7	1360 / 1350	02.11.2007	l/+	
AR2.8	1360 / 1350	02.11.2007	l/l	largeT

Table 3: Mouse embryonic fibroblast cell lines generated from E12-15 embryos.
Pink scripture stands for a *Pink1*$^{l/+}$ genotype, purple scripture for *Pink1*$^{l/l}$, light blue for *Pink1*$^{+/-}$, dark blue indicates a *Pink1*$^{-/-}$ genotype, and black scripture confers to wildtype *Pink1*$^{+/+}$ genotype.

7.2 Stereological countings of TH-positive nigral neurons

	6 months		19 months	
	wt	ko	wt	ko
mean	8958	7977	11250	10910
SEM	200.7	880.3	776.6	815.8
p-value	0.3164		0.7677	

Table 4: Coutings of TH-positive substantia nigra neurons in 6 months and 19 months old Pink1 mutant mice and littermate controls.
Means, SEMs, and p-value's (unpaired, two-tailed t-test), no significant reduction of TH-positive neurons could be found in Pink1 mutant mice.

7.3 Quantification of neurotransmitter contents via HPLC

neuro-transmitter		C wt	C ko	S wt	S ko	H wt	H ko	VMB wt	VMB ko
5HT	mean	0.29	0.35	0.33	0.37	0.33	0.3	0.71	0.76
	SEM	0.14	0.1	0.11	0.16	0.2	0.14	0.11	0.19
	p-value	**0.032**		0.191		0.461		0.183	
5'-HIAA	mean	0.31	0.34	0.54	0.57	0.73	0.59	1.09	1.09
	SEM	0.2	0.16	0.42	0.42	0.51	0.29	1.22	0.53
	p-value	0.341		0.635		0.082		0.982	
NA	mean	0.24	0.29	0.11	0.13	0.29	0.29	0.47	0.51
	SEM	0.06	0.19	0.11	0.19	0.08	0.16	0.11	0.16
	p-value	0.108		0.601		0.967		0.28	
DA	mean	0.12	0.22	7.33	7.7	-	-	0.22	0.21
	SEM	0.2	0.4	5.91	5.53	-	-	0.11	0.08
	p-value	0.2		0.733		-		0.538	
DOPAC	mean	-	-	0.4	0.5	-	-	0.11	0.11
	SEM	-	-	0.2	0.58	-	-	0.06	0.08
	p-value	-		0.313		-		0.941	

Table 5: Determination of 5HT, 5-HIAA, NA, DA, and DOPAC contents from cortex, hippocampus, striatum, and ventral midbrain of 6 months old Pink1 knockout and control mice via HPLC measurements.
5HT = 5 hydroxy trymptamin = serotonin; 5-HIAA = 5-hydroxyindole acetic acid; NA = noradrenalin; DA = dopamine; DOPAC = 3,4-dihydroxyphenylacetic acid; C = cortex; H = hippocampus; S = striatum; VMB = ventral midbrain. Unpaired, two-tailed t-test revealed significantly higher levels of serotonin in Pink1 mutant cortices.

7.4 Behavioral analysis

7.4.1 Overview open field test

Distance travelled [cm]	Pink1$^{+/+}$			Pink1$^{-/-}$			2-way ANOVA		
	Mean	SEM	n	Mean	SEM	n	p (I)	p (geno)	p (gen)
male	633.48	50.09	10	590.66	26.05	12	0.284	0.835	0.35
female	534.26	44.09	11	597.56	65.44	12			
Time [s] spent in 16% center	Pink1$^{+/+}$			Pink1$^{-/-}$			2-way ANOVA		
	Mean	SEM	n	Mean	SEM	n	p (I)	p (geno)	p (gen)
male	181.12	26.63	10	198.99	30.09	12	0.764	0.386	0.212
female	135.01	30.41	11	170.68	28.96	12			
Time [s] spent in 45% center	Pink1$^{+/+}$			Pink1$^{-/-}$			2-way ANOVA		
	Mean	SEM	n	Mean	SEM	n	p (I)	p (geno)	p (gen)
male	575.07	54.08	10	552.01	67.52	12	0.412	0.644	0.138
female	426.2	69.42	11	508.53	58.97	12			

Table 6: Open field test.
Showing means, standard errors of means (SEM), numbers of test animals (n) and results of statistical evaluation. P (I) = p-value for interaction; p (geno) = p-value for genotype; p (gen) = p-value for gender.

7.4.2 Overview accelerating rotarod

Latency to fall	Pink1$^{+/+}$			Pink1$^{-/-}$			2-way ANOVA		
	Mean	SEM	n	Mean	SEM	n	p (I)	p (geno)	p (gen)
male	119.86	18.32	7	119.14	17.29	7	0.367	0.393	0.534
female	97.27	14.97	11	123.33	8.78	12			
Duration on rotarod [s]	Pink1$^{+/+}$ males			Pink1$^{-/-}$ males			2-way ANOVA		
	Mean	SEM	n	Mean	SEM	n	p (I)	p (geno)	p (trial 1-3)
trial 1	110	23.61	7	110.71	13.53	7	0.499	0.973	0.248
trial 2	143.57	16.42	7	124.43	27.80	7			
trial 3	106.57	25.32	7	122.43	18.42	7			
Duration on rotarod [s]	Pink1$^{+/+}$ females			Pink1$^{-/-}$ females			2-way ANOVA		
	Mean	SEM	n	Mean	SEM	n	p (I)	p (geno)	p (trial 1-3)
trial 1	100.18	14.95	11	105.33	15.23	12	0.514	0.14	0.704
trial 2	97.18	20.84	11	132.08	14.57	12			
trial 3	94.55	21.34	11	132.5	17.41	12			
Duration on rotarod [s] genders combined	Pink1$^{+/+}$			Pink1$^{-/-}$			2-way ANOVA		
	Mean	SEM	n	Mean	SEM	n	p (I)	p (geno)	p (trial 1-3)
trial 1	104.0	12.58	18	107.32	10.6	19	0.492	0.272	0.329
trial 2	115.22	14.94	18	129.26	13.33	19			
trial 3	99.22	15.93	18	128.79	12.65	19			

Table 7: Overview of the accelerating rotarod test.
Shown are the combined latency to fall from the rod, and the duration the mice stayed on the rod during the three trials in means, standard errors of means (SEM), number of tested mice (n), and statistical evaluation of the data. P (I) = p-value for interaction; p (geno) = p-value for genotype; p (gen) = p-value for gender.

7.4.3 Overview forced swim test

Time [s] spent swimming	Pink1$^{+/+}$			Pink1$^{-/-}$			2-way ANOVA		
	Mean	SEM	n	Mean	SEM	n	p (I)	p (geno)	p (gen)
male	248.25	14.44	9	265.04	20.48	12	0.533	0.834	0.56
female	273.24	23.09	9	264.85	22.7	11			
Time [s] spent struggling	Pink1$^{+/+}$			Pink1$^{-/-}$			2-way ANOVA		
	Mean	SEM	n	Mean	SEM	n	p (I)	p (geno)	p (gen)
male	34.83	12.47	9	24.23	6.61	12	0.633	0.463	0.19
female	19.08	7.68	9	16.83	7.9	11			
Time [s] spent floating	Pink1$^{+/+}$			Pink1$^{-/-}$			2-way ANOVA		
	Mean	SEM	n	Mean	SEM	n	p (I)	p (geno)	p (gen)
male	75.99	22.39	9	76.01	20.35	11	0.924	0.923	0.756
female	67.0	24.64	9	71.25	20.4	12			

Table 8: Forced swim test.
Overview of the results showing means, SEM (standard error of means) and n (number of test animals) and subsequent statistical analysis of the times the test animals spent swimming, struggling, and floating. P (I) = p-value for interaction; p (geno) = p-value for genotype; p (gen) = p-value for gender.

7.4.4 Overview tail suspension test

Total immobility [s]	Pink1$^{+/+}$			Pink1$^{-/-}$			2-way ANOVA		
	Mean	SEM	n	Mean	SEM	n	p (I)	p (geno)	p (gen)
male	132.55	17.57	7	111.42	16.57	11	0.061	0.471	0.518
female	87.29	16.48	11	133.87	16.97	12			
Total activity [s]	Pink1$^{+/+}$			Pink1$^{-/-}$			2-way ANOVA		
	Mean	SEM	n	Mean	SEM	n	p (I)	p (geno)	p (gen)
male	227.17	17.56	7	247.99	16.55	11	0.062	0.467	0.516
female	272.31	16.46	11	225.78	16.97	12			

Table 9: Tail suspension test.
Overview of the results showing means, SEM (standard error of means) and n (number of test animals) and subsequent statistical analysis of the total times the test animals spent in immobility and activity. P (I) = p-value for interaction; p (geno) = p-value for genotype; p (gen) = p-value for gender.

7.4.5 Overview social discrimination test

Investi-gation time [s]	Pink1$^{+/+}$			Pink1$^{-/-}$			2-way ANOVA			Bonferroni p-value	
	Mean	SEM	n	Mean	SEM	n	p (I)	p (geno)	p (f.s./u.s)	Pink1$^{+/+}$	Pink1$^{-/-}$
f.s.	15.33	3.2	10	36.33	7.61	10	**0.027**	0.931	0.011	**p < 0.01**	**p > 0.05**
u.s.	24.39	5.62	11	26.08	4.94	11					

Table 10: Social discrimination test, Investigation time of familiar and unfamiliar subjects.
Overview of Investigation times of familiar and unfamiliar mice (=subjects) showing means, standard errors of means (SEM), number of test animals. Statistical analysis via 2-way ANOVA revealed a p-value of 0.027, which is considered significant. Hence a Bonferroni post test was performed. It displayed a $p < 0.01$ for wildtype animals, clearly showing that they can distinguish between familiar and unfamiliar mice, and $p > 0.05$ for mutant animals, which seemingly cannot discriminate. P (I) = p-value for interaction; p (geno) = p-value for genotype; p (f.s./u.s.) = p-value for familiar subject vs. unfamiliar subject.

Difference u.s. – f.s. [s]	Pink1$^{+/+}$	Pink1$^{-/-}$	t-test p-value	Proportion u.s. of (u.s. + f.s.) [%]	Pink1$^{+/+}$	Pink1$^{-/-}$	t-test p-value
Mean	21.01	1.69	**0.027**	Mean	68.26	53.07	**0.011**
SEM	6.39	5.02		SEM	3.16	4.21	

Table 11: Social discrimination test, difference between familiar and unfamiliar mice and proportion of time examining the unfamiliar of the sum of unfamiliar + familiar.
Overview showing means and standard errors of mean (SEM) and statistical evaluation via a t-test with equal variances showing $p < 0.05$, considered significant, for both calculations.

7.4.6 Overview object recognition test

Investigation time [s], 3 h after sampling phase	Pink1$^{+/+}$			Pink1$^{-/-}$			2-way ANOVA		
	Mean	SEM	n	Mean	SEM	n	p (I)	p (geno)	p (f.o./u.o.)
fam. object	2.16	0.36	21	2.12	0.22	23	0.882	0.825	< 0.0001
unfam. object	5.32	0.49	21	5.16	0.51	23			
Investigation time [s], 24 h after sampling phase	Pink1$^{+/+}$			Pink1$^{-/-}$			2-way ANOVA		
	Mean	SEM	n	Mean	SEM	n	p (I)	p (geno)	p (f.o./u.o.)
fam. object	1.23	0.17	18	1.69	0.32	22	0.651	0.329	0.0033
unfam. object	3.12	0.76	18	4.23	1.16	22			

Table 12: Object recognition test, investigation time of familiar and unfamiliar objects, 3 h and 24 h after the sampling phases.
Overview with means, standard errors of mean (SEM), number of test animals (n), and statistical analysis via 2-way ANOVA. P (I) = p-value for interaction; p (geno) = p-value for genotype; p (f.o./u.o.) = p-value for familiar object vs. unfamiliar object. P-values for f.o./u.o. are $p < 0.05$, considered significant, showing that all mice can discriminate between familiar and unfamiliar objects 3 h as well as 24 h after the sampling phases.

Proportion u.o.of (u.o. + f.o.) [%], 3 h after sampling phase	Pink1$^{+/+}$	Pink1$^{-/-}$	t-test p-value	Proportion u.o. of (u.o. + f.o.) [%], 24 h after sampling phase	Pink1$^{+/+}$	Pink1$^{-/-}$	t-test p-value
Mean	73.53	69.49	0.398	Mean	69.06	66.23	0.583
SEM	3.07	3.54		SEM	3.7	3.5	

Table 13: Object recognition test, proportion investigation time unfamiliar object of the sum of unfamiliar + familiar objects, 3 h and 24 h after sampling phases.
Overview with means, standard errors of mean (SEM), and statistical analysis via unpaired t-test with equal variances. P-values are both $p > 0.05$ considered not significant, also showing that wildtype and mutant mice are able to discriminate between familiar and unfamiliar objects.

7.4.7 Overview odor preference test

Total duration of investigation [s]	Pink1$^{+/+}$			Pink1$^{-/-}$			2-way ANOVA		
	Mean	SEM	n	Mean	SEM	n	p (I)	p (geno)	p (sp.od./no sp.od.)
no specific odor	4.65	1.36	9	7.41	1.26	11	0.376	0.113	**0.034**
specific odor	3.76	0.52	9	5.36	0.68	11			

Table 14: Odor preference test.
Overview with means, standard errors of mean (SEM), number of test animals (n), and statistical analysis via 2-way ANOVA. P (I) = p-value for interaction; p (geno) = p-value for genotype; p (sp.od./no sp.od.) = p-value for specific odor vs. no specific odor. P (sp.od./no sp.od) < 0.05, considered significant, shows that seemingly both genotypes can distinguish between an eppendorf cup filled with fresh cage wood shavings and one that is filled with used cage wood shavings.

7.4.8 Overview odor sensitivity test

Maximum binary dilution step reached	Pink1$^{+/+}$			Pink1$^{-/-}$			t-test
	Mean	SEM	n	Mean	SEM	n	p-value
	26.57	0.95	7	21.8	1.5	10	**0.029**

Table 15: Odor sensitivity test showing the maximum binary dilution step where mice can still detect the odor.
Overview with means, standard errors of mean (SEM), number of test animals (n), and statistical analysis via an unpaired t-test with equal variances. p < 0.05 is considered significant. The max. binary dilution step,m where the animals could still detect the odor, was significantly lower in Pink1 mutants than in controls.

7.4.9 Overview odor discrimination test

Correct choice	100%			70%			55%		
	$Pink1^{+/+}$	$Pink1^{-/-}$	p	$Pink1^{+/+}$	$Pink1^{-/-}$	p	$Pink1^{+/+}$	$Pink1^{-/-}$	p
Mean	85.19	88.33	0.623	70.37	80.0	0.078	87.04	85.0	0.78
SEM	4.97	3.97		3.7	3.56		5.91	4.27	
Correct choice	**53%**			**51%**			**50%**		
	$Pink1^{+/+}$	$Pink1^{-/-}$	p	$Pink1^{+/+}$	$Pink1^{-/-}$	p	$Pink1^{+/+}$	$Pink1^{-/-}$	p
Mean	79.01	73.29	0.194	72.38	55.18	**0.024**	45.37	47.5	0.618
SEM	3.56	2.43		3.4	5.82		3.14	2.79	

Table 16: Odor discrimination test.
Overview of Means, SEM (standard error of means), and p-values of unpaired t-test with equal variances. Mice were tested for the following binary mixing percentages of a trained odor: 100%, 70%, 55%, 53%, 51%, and 50%. At 51% binary mixing percentage p = 0.024, which is considered significant. Pink1 mutants made significantly less often the correct choice than wildtype controls when tested with a 51% mixture.

7.5 Index of figures and tables

Index of figures

Index of tables

7.6 Abbreviations

°C	degree Celsius
ψ_m	mitochondrial membrane potential
5-HIAA	5-hydroxyindole acetic acid
6-OHDA	6-hydroxydopamine
Ac	acetate
amp	ampicillin
ATP	adenosine triphosphate
a.u.	arbitrary units
BN-PAGE	Blue Native gel electrophoresis
bp	base pair(s)
cDNA	copy DNA
cko	conditional knockout
CMV	cytomegalovirus promotor
cpm	counts per minute
Cre	cyclization recombination enzyme, also called Cre recombinase
CsA	cyclosporin A
CTP	cytidine triphosphate
DA	dopamine
DAB	3,3'-diaminobenzidine
Dat	dopamine transporter
dATP	desoxy adenosine triphosphate
dCTP	desoxy cytidine triphosphate
DEPC	diethylpyrocarbonate
dGTP	desoxy guanosine triphosphate
DHBA	3,4-Dihydroxybenzylamine
DMEM	Dubecco's modified Eagle's medium
DMSO	dimethylsulfoxide
DNA	desoxyribonucleic acid
DNAse	desoxyribonuclease
dNTP	desoxy nucleoside triphosphate
DOPAC	3,4-dihydroxyphenylacetic acid
DsRed	tradename of the red fluorescent protein drFP583

Drp1	dynamin related protein 1
DTT	dithiothreitol
dTTP	desoxy thymidine trisphosphate
E	embryonic day
e.g.	exempli gratia (Latin), for example (English)
eGFP	enhanced green fluorecent protein
et al.	et alteres (Latin), and others (English)
EtBr	ethidium bromide
ETC	electron transport chain
EtOH	ethanole
flp	flipase recombination enzyme
FCS	fetal calf serum
FRT	flipase recognition target
g	gram
G418	Geneticin, an analogon of neomycin
GFP	green fluorescent protein
GTP	guanosine triphosphate
h	hour
h	human
hCG	human chorion gonadotropin
HPLC	High Performance Liquid Chromatography
HVA	homovanillic acid
i.p.	intraperitoneally
IHC	immunohistochemistry
IMM	inner mitochondrial membrane
IMS	mitochondrial intermembrane space
IRES	internal ribosomal entry site
ISH	in situ hybridization
k	kilo (10^3)
kb	kilobase
kDa	kilodalton
kg	kilogram
ko	knockout
l	liter
l	loxP / floxed

LB	lysogeny broth (Bertani, 2004)
LIF	leukemia inhibiting factor
loxP	locus of X-over P1
LTR	long terminal repeat
m	meter
m	milli (10^{-3})
M	molar (mol/l)
µ	micro (10^{-6})
mDsRed	mitochondrially targeted DsRed
MEF	mouse embryonic fibroblasts
min	minute
MPP^+	1-methyl-4-phenylpyridinium ion
MPTP	1-methyl-4-phenyl-tetrahydropyridine
mRNA	messenger ribonucleic acid
mtDNA	mitochondrial DNA
n	nano (10^{-9})
n	probe number
nm	nanometer
NMJ	neuromuscular junction
neo	neomycin
NTP	nucleoside triphosphate
OD	optical density
OMM	outer mitochondrial membrane
o.n.	over night
OPA1	optic atrophy 1
p	p-value for statistical analysis
P	postnatal day
PBS	phosphate buffered saline
PCR	Polymerase Chain Reaction
PD	Parkinson's Disease
PFA	para formaldehyde
pgk	phosphoglycerat kinase promotor
Pink1	P-TEN Induced Kinase 1
PMS	post-mitochondrial supernatant
PMSG	pregnant mare's serum gonadotropin

PNS	post-nuclear supernatant
PTEN	phosphate and tensin homologue
PTP	mitchondrial permeability transition pore
RM	repeated-measures
RNA	ribonucleic acid
RNAi	RNA interference
RNS	reactive nitrogen species
ROS	reactive oxygen species
RP	reserve pool of vesicles
RT-PCR	reverse transcriptase polymerase chain reaction
s	second
SDS	sodium dodecyle sulfate
SEM	standard error of means
siRNA	small interfering RNA
SV40	simian virus 40
TH	tyrosine hydroxylase
TMRM	tetramethylrhodamine methyl ester
TTX	tetrodotoxin
U	units (of enzyme)
UCH-L1	ubiquitin C-terminal hydroxylase 1 (PARK3)
UPS	ubiquitin-proteasome system
UTP	uridine triphosphate
wPRE	woodchuck hepatitis virus posttranscriptional regulatory element
wt	wildtype

7.7 Anatomical abbreviations

Vth	Vth cranial nerve, trigeminal nucleus
cb	cerebellum
cbn	cerebellar nuclei
cx	cortex
drg	dorsal root ganglia

h	heart
hb	hindbrain
hip	hippocampus
hth	hypothalamus
li	liver
mb	midbrain
ob	olfactory bulb
pcx	piriform cortex
pn	pontine nuclei
sc	superior colliculus
sn	substantia nigra
snpc	substantia nigra pars compacta
snpr	substantia nigra pars reticulata
str	striatum
th	thalamus
VTA	ventral tegmental area

8 REFERENCES

Abbas, N., Lucking, C. B., Ricard, S. & other authors (1999). A wide variety of mutations in the parkin gene are responsible for autosomal recessive parkinsonism in Europe. French Parkinson's Disease Genetics Study Group and the European Consortium on Genetic Susceptibility in Parkinson's Disease. *Hum Mol Genet* **8**, 567-574.

Abeliovich, A., Schmitz, Y., Farinas, I. & other authors (2000). Mice lacking alpha-synuclein display functional deficits in the nigrostriatal dopamine system. *Neuron* **25**, 239-252.

Abou-Sleiman, P. M., Muqit, M. M., McDonald, N. Q. & other authors (2006a). A heterozygous effect for PINK1 mutations in Parkinson's disease? *Ann Neurol* **60**, 414-419.

Abou-Sleiman, P. M., Muqit, M. M. & Wood, N. W. (2006b). Expanding insights of mitochondrial dysfunction in Parkinson's disease. *Nat Rev Neurosci* **7**, 207-219.

Adra, C. N., Boer, P. H. & McBurney, M. W. (1987). Cloning and expression of the mouse pgk-1 gene and the nucleotide sequence of its promoter. *Gene* **60**, 65-74.

Andres-Mateos, E., Perier, C., Zhang, L. & other authors (2007). DJ-1 gene deletion reveals that DJ-1 is an atypical peroxiredoxin-like peroxidase. *Proc Natl Acad Sci U S A* **104**, 14807-14812.

Ansari, K. A. & Johnson, A. (1975). Olfactory function in patients with Parkinson's disease. *J Chronic Dis* **28**, 493-497.

Beilina, A., Van Der Brug, M., Ahmad, R., Kesavapany, S., Miller, D. W., Petsko, G. A. & Cookson, M. R. (2005). Mutations in PTEN-induced putative kinase 1 associated with recessive parkinsonism have differential effects on protein stability. *Proc Natl Acad Sci U S A* **102**, 5703-5708.

Belin, A. C. & Westerlund, M. (2008). Parkinson's disease: a genetic perspective. *FEBS J* **275**, 1377-1383.

Bertani, G. (2004). Lysogeny at mid-twentieth century: P1, P2, and other experimental systems. *J Bacteriol* **186**, 595-600.

Betarbet, R., Sherer, T. B., MacKenzie, G., Garcia-Osuna, M., Panov, A. V. & Greenamyre, J. T. (2000). Chronic systemic pesticide exposure reproduces features of Parkinson's disease. *Nat Neurosci* **3**, 1301-1306.

Biskup, S., Moore, D. J., Celsi, F. & other authors (2006). Localization of LRRK2 to membranous and vesicular structures in mammalian brain. *Ann Neurol* **60**, 557-569.

Blackinton, J. G., Anvret, A., Beilina, A., Olson, L., Cookson, M. R. & Galter, D. (2007). Expression of PINK1 mRNA in human and rodent brain and in Parkinson's disease. *Brain Res* **1184**, 10-16.

Bogaerts, V., Theuns, J. & van Broeckhoven, C. (2008). Genetic findings in Parkinson's disease and translation into treatment: a leading role for mitochondria? *Genes Brain Behav* **7**, 129-151.

Bonifati, V., Rizzu, P., van Baren, M. J. & other authors (2003). Mutations in the DJ-1 gene associated with autosomal recessive early-onset parkinsonism. *Science* **299**, 256-259.

Bossy-Wetzel, E., Schwarzenbacher, R. & Lipton, S. A. (2004). Molecular pathways to neurodegeneration. *Nat Med* **10 Suppl**, S2-9.

Braak, H., Del Tredici, K., Rub, U., de Vos, R. A., Jansen Steur, E. N. & Braak, E. (2003). Staging of brain pathology related to sporadic Parkinson's disease. *Neurobiol Aging* **24**, 197-211.

Brinkley, B. R., Barham, S. S., Barranco, S. C. & Fuller, G. M. (1974). Rotenone inhibition of spindle microtubule assembly in mammalian cells. *Exp Cell Res* **85**, 41-46.

Cappelletti, G., Maggioni, M. G. & Maci, R. (1999). Influence of MPP+ on the state of tubulin polymerisation in NGF-differentiated PC12 cells. *J Neurosci Res* **56**, 28-35.

Cappelletti, G., Pedrotti, B., Maggioni, M. G. & Maci, R. (2001). Microtubule assembly is directly affected by MPP(+)in vitro. *Cell Biol Int* **25**, 981-984.

Cappelletti, G., Surrey, T. & Maci, R. (2005). The parkinsonism producing neurotoxin MPP+ affects microtubule dynamics by acting as a destabilising factor. *FEBS Lett* **579**, 4781-4786.

Casarejos, M. J., Menendez, J., Solano, R. M., Rodriguez-Navarro, J. A., Garcia de Yebenes, J. & Mena, M. A. (2006). Susceptibility to rotenone is increased in neurons from parkin null mice and is reduced by minocycline. *J Neurochem* **97**, 934-946.

Castello, P. R., Drechsel, D. A. & Patel, M. (2007). Mitochondria are a major source of paraquat-induced reactive oxygen species production in the brain. *J Biol Chem* **282**, 14186-14193.

Chan, D. C. (2006). Mitochondria: dynamic organelles in disease, aging, and development. *Cell* **125**, 1241-1252.

Chance, B., Williams, G. R. & Hollunger, G. (1963). Inhibition of electron and energy transfer in mitochondria. I. Effects of Amytal, thiopental, rotenone, progesterone, and methylene glycol. *J Biol Chem* **238**, 418-431.

Chandran, J. S., Lin, X., Zapata, A. & other authors (2008). Progressive behavioral deficits in DJ-1-deficient mice are associated with normal nigrostriatal function. *Neurobiol Dis* **29**, 505-514.

Chen, L., Cagniard, B., Mathews, T. & other authors (2005). Age-dependent motor deficits and dopaminergic dysfunction in DJ-1 null mice. *J Biol Chem* **280**, 21418-21426.

Chinta, S. J., Kumar, M. J., Hsu, M., Rajagopalan, S., Kaur, D., Rane, A., Nicholls, D. G., Choi, J. & Andersen, J. K. (2007). Inducible alterations of glutathione levels in adult dopaminergic midbrain neurons result in nigrostriatal degeneration. *J Neurosci* **27**, 13997-14006.

Clark, I. E., Dodson, M. W., Jiang, C., Cao, J. H., Huh, J. R., Seol, J. H., Yoo, S. J., Hay, B. A. & Guo, M. (2006). Drosophila pink1 is required for mitochondrial function and interacts genetically with parkin. *Nature* **441**, 1162-1166.

Darios, F., Corti, O., Lucking, C. B. & other authors (2003). Parkin prevents mitochondrial swelling and cytochrome c release in mitochondria-dependent cell death. *Hum Mol Genet* **12**, 517-526.

de Rijk, M. C., Launer, L. J., Berger, K. & other authors (2000). Prevalence of Parkinson's disease in Europe: A collaborative study of population-based cohorts. Neurologic Diseases in the Elderly Research Group. *Neurology* **54**, S21-23.

Deng, H., Dodson, M. W., Huang, H. & Guo, M. (2008). The Parkinson's disease genes pink1 and parkin promote mitochondrial fission and/or inhibit fusion in Drosophila. *Proc Natl Acad Sci U S A* **105**, 14503-14508.

Dexter, D. T., Carter, C. J., Wells, F. R., Javoy-Agid, F., Agid, Y., Lees, A., Jenner, P. & Marsden, C. D. (1989a). Basal lipid peroxidation in substantia nigra is increased in Parkinson's disease. *J Neurochem* **52**, 381-389.

Dexter, D. T., Wells, F. R., Lees, A. J., Agid, F., Agid, Y., Jenner, P. & Marsden, C. D. (1989b). Increased nigral iron content and alterations in other metal ions occurring in brain in Parkinson's disease. *J Neurochem* **52**, 1830-1836.

Di Matteo, V., Di Giovanni, G., Pierucci, M. & Esposito, E. (2008). Serotonin control of central dopaminergic function: focus on in vivo microdialysis studies. *Prog Brain Res* **172**, 7-44.

Di Monte, D. A., Chan, P. & Sandy, M. S. (1992). Glutathione in Parkinson's disease: a link between oxidative stress and mitochondrial damage? *Ann Neurol* **32 Suppl**, S111-115.

Dimmer, K. S., Navoni, F., Casarin, A., Trevisson, E., Endele, S., Winterpacht, A., Salviati, L. & Scorrano, L. (2008). LETM1, deleted in Wolf-Hirschhorn syndrome is required for normal mitochondrial morphology and cellular viability. *Hum Mol Genet* **17**, 201-214.

Doty, R. L., Deems, D. A. & Stellar, S. (1988). Olfactory dysfunction in parkinsonism: a general deficit unrelated to neurologic signs, disease stage, or disease duration. *Neurology* **38**, 1237-1244.

Duvezin-Caubet, S., Jagasia, R., Wagener, J. & other authors (2006). Proteolytic processing of OPA1 links mitochondrial dysfunction to alterations in mitochondrial morphology. *J Biol Chem* **281**, 37972-37979.

Ebner, K., Wotjak, C. T., Landgraf, R. & Engelmann, M. (2002). Forced swimming triggers vasopressin release within the amygdala to modulate stress-coping strategies in rats. *Eur J Neurosci* **15**, 384-388.

Exner, N., Treske, B., Paquet, D. & other authors (2007). Loss-of-function of human PINK1 results in mitochondrial pathology and can be rescued by parkin. *J Neurosci* **27**, 12413-12418.

Farrer, M., Chan, P., Chen, R. & other authors (2001). Lewy bodies and parkinsonism in families with parkin mutations. *Ann Neurol* **50**, 293-300.

Feng, J. (2006). Microtubule: a common target for parkin and Parkinson's disease toxins. *Neuroscientist* **12**, 469-476.

Fornai, F., di Poggio, A. B., Pellegrini, A., Ruggieri, S. & Paparelli, A. (2007). Noradrenaline in Parkinson's disease: from disease progression to current therapeutics. *Curr Med Chem* **14**, 2330-2334.

Forno, L. S. (1996). Neuropathology of Parkinson's disease. *J Neuropathol Exp Neurol* **55**, 259-272.

Frazier, A. E., Kiu, C., Stojanovski, D., Hoogenraad, N. J. & Ryan, M. T. (2006). Mitochondrial morphology and distribution in mammalian cells. *Biol Chem* **387**, 1551-1558.

Galter, D., Westerlund, M., Carmine, A., Lindqvist, E., Sydow, O. & Olson, L. (2006). LRRK2 expression linked to dopamine-innervated areas. *Ann Neurol* **59**, 714-719.

Gandhi, S., Muqit, M. M., Stanyer, L. & other authors (2006). PINK1 protein in normal human brain and Parkinson's disease. *Brain* **129**, 1720-1731.

Gautier, C. A., Kitada, T. & Shen, J. (2008). Loss of PINK1 causes mitochondrial functional defects and increased sensitivity to oxidative stress. *Proc Natl Acad Sci U S A* **105**, 11364-11369.

Giasson, B. I., Duda, J. E., Murray, I. V., Chen, Q., Souza, J. M., Hurtig, H. I., Ischiropoulos, H., Trojanowski, J. Q. & Lee, V. M. (2000). Oxidative damage linked to neurodegeneration by selective alpha-synuclein nitration in synucleinopathy lesions. *Science* **290**, 985-989.

Giasson, B. I., Duda, J. E., Quinn, S. M., Zhang, B., Trojanowski, J. Q. & Lee, V. M. (2002). Neuronal alpha-synucleinopathy with severe movement disorder in mice expressing A53T human alpha-synuclein. *Neuron* **34**, 521-533.

Goldberg, M. S., Fleming, S. M., Palacino, J. J. & other authors (2003). Parkin-deficient mice exhibit nigrostriatal deficits but not loss of dopaminergic neurons. *J Biol Chem* **278**, 43628-43635.

Goldberg, M. S., Pisani, A., Haburcak, M. & other authors (2005). Nigrostriatal dopaminergic deficits and hypokinesia caused by inactivation of the familial Parkinsonism-linked gene DJ-1. *Neuron* **45**, 489-496.

Gotz, M. E., Freyberger, A. & Riederer, P. (1990). Oxidative stress: a role in the pathogenesis of Parkinson's disease. *J Neural Transm Suppl* **29**, 241-249.

Haque, M. E., Thomas, K. J., D'Souza, C. & other authors (2008). Cytoplasmic Pink1 activity protects neurons from dopaminergic neurotoxin MPTP. *Proc Natl Acad Sci U S A* **105**, 1716-1721.

Hastings, T. G., Lewis, D. A. & Zigmond, M. J. (1996). Role of oxidation in the neurotoxic effects of intrastriatal dopamine injections. *Proc Natl Acad Sci U S A* **93**, 1956-1961.

Hattori, N., Tanaka, M., Ozawa, T. & Mizuno, Y. (1991). Immunohistochemical studies on complexes I, II, III, and IV of mitochondria in Parkinson's disease. *Ann Neurol* **30**, 563-571.

Hegde, R., Srinivasula, S. M., Zhang, Z. & other authors (2002). Identification of Omi/HtrA2 as a mitochondrial apoptotic serine protease that disrupts inhibitor of apoptosis protein-caspase interaction. *J Biol Chem* **277**, 432-438.

Higashi, S., Biskup, S., West, A. B. & other authors (2007). Localization of Parkinson's disease-associated LRRK2 in normal and pathological human brain. *Brain Res* **1155**, 208-219.

Hughes, T. A., Ross, H. F., Musa, S., Bhattacherjee, S., Nathan, R. N., Mindham, R. H. & Spokes, E. G. (2000). A 10-year study of the incidence of and factors predicting dementia in Parkinson's disease. *Neurology* **54**, 1596-1602.

Irwin, W. A., Bergamin, N., Sabatelli, P. & other authors (2003). Mitochondrial dysfunction and apoptosis in myopathic mice with collagen VI deficiency. *Nat Genet* **35**, 367-371.

Itier, J. M., Ibanez, P., Mena, M. A. & other authors (2003). Parkin gene inactivation alters behaviour and dopamine neurotransmission in the mouse. *Hum Mol Genet* **12**, 2277-2291.

Jefferson, M. (1973). James Parkinson, 1775-1824. *Br Med J* **2**, 601-603.

Jellinger, K. A. (2003). Parkinson disease with old-age onset. *Arch Neurol* **60**, 1814-1815.

Jensen, F., Koprowski, H. & Ponten, J. A. (1963). Rapid Transformation of Human Fibroblast Cultures by Simian Virus. *Proc Natl Acad Sci U S A* **50**, 343-348.

Jones, J. M., Datta, P., Srinivasula, S. M. & other authors (2003). Loss of Omi mitochondrial protease activity causes the neuromuscular disorder of mnd2 mutant mice. *Nature* **425**, 721-727.

Juri, C., Viviani, P. & Chana, P. (2008). Features associated with the development of non-motor manifestations in Parkinson's disease. *Arq Neuropsiquiatr* **66**, 22-25.

Kim, R. H., Smith, P. D., Aleyasin, H. & other authors (2005). Hypersensitivity of DJ-1-deficient mice to 1-methyl-4-phenyl-1,2,3,6-tetrahydropyrindine (MPTP) and oxidative stress. *Proc Natl Acad Sci U S A* **102**, 5215-5220.

Kitada, T., Pisani, A., Porter, D. R. & other authors (2007). Impaired dopamine release and synaptic plasticity in the striatum of PINK1-deficient mice. *Proc Natl Acad Sci U S A* **104**, 11441-11446.

Kitada, T., Tong, Y., Gautier, C. A. & Shen, J. (2009). Absence of nigral degeneration in aged parkin/DJ-1/PINK1 triple knockout mice. *J Neurochem*.

Klein, R. L., Dayton, R. D., Henderson, K. M. & Petrucelli, L. (2006). Parkin is protective for substantia nigra dopamine neurons in a tau gene transfer neurodegeneration model. *Neurosci Lett* **401**, 130-135.

Kloppenburg, P., Ferns, D. & Mercer, A. R. (1999). Serotonin enhances central olfactory neuron responses to female sex pheromone in the male sphinx moth manduca sexta. *J Neurosci* **19**, 8172-8181.

Koprowski, H., Ponten, J., Jensen, F., Ravdin, R. G., Moorhead, P. & Saksela, E. (1963). Transformation of cultures of human tissue infected with simian virus SV40. *Acta Unio Int Contra Cancrum* **19**, 362-367.

Kuroda, Y., Mitsui, T., Kunishige, M., Shono, M., Akaike, M., Azuma, H. & Matsumoto, T. (2006). Parkin enhances mitochondrial biogenesis in proliferating cells. *Hum Mol Genet* **15**, 883-895.

Laemmli, U. K. (1970). Cleavage of structural proteins during the assembly of the head of bacteriophage T4. *Nature* **227**, 680-685.

Lee, H. J., Khoshaghideh, F., Lee, S. & Lee, S. J. (2006). Impairment of microtubule-dependent trafficking by overexpression of alpha-synuclein. *Eur J Neurosci* **24**, 3153-3162.

Lee, M. K., Stirling, W., Xu, Y. & other authors (2002). Human alpha-synuclein-harboring familial Parkinson's disease-linked Ala-53 --> Thr mutation causes neurodegenerative disease with alpha-synuclein aggregation in transgenic mice. *Proc Natl Acad Sci U S A* **99**, 8968-8973.

Leranth, C. & Hajszan, T. (2007). Extrinsic afferent systems to the dentate gyrus. *Prog Brain Res* **163**, 63-84.

Leroy, E., Boyer, R. & Polymeropoulos, M. H. (1998). Intron-exon structure of ubiquitin c-terminal hydrolase-L1. *DNA Res* **5**, 397-400.

Li, Z., Okamoto, K., Hayashi, Y. & Sheng, M. (2004). The importance of dendritic mitochondria in the morphogenesis and plasticity of spines and synapses. *Cell* **119**, 873-887.

Liu, M. J., Liu, M. L., Shen, Y. F., Kim, J. M., Lee, B. H., Lee, Y. S. & Hong, S. T. (2007). Transgenic mice with neuron-specific overexpression of HtrA2/Omi suggest a neuroprotective role for HtrA2/Omi. *Biochem Biophys Res Commun* **362**, 295-300.

Lotharius, J. & Brundin, P. (2002). Pathogenesis of Parkinson's disease: dopamine, vesicles and alpha-synuclein. *Nat Rev Neurosci* **3**, 932-942.

Lutz, A. K., Exner, N., Fett, M. E. & other authors (2009). Loss of parkin or PINK1 function increases Drp1-dependent mitochondrial fragmentation. *J Biol Chem* **284**, 22938-22951.

Madeley, P., Biggins, C. A., Boyd, J. L. & Mindham, R. H. (1991). Cognitive impairments and depression in Parkinson's disease. *J Neurol Neurosurg Psychiatry* **54**, 941.

Maingay, M., Romero-Ramos, M. & Kirik, D. (2005). Viral vector mediated overexpression of human alpha-synuclein in the nigrostriatal dopaminergic neurons: a new model for Parkinson's disease. *CNS Spectr* **10**, 235-244.

Manning-Bog, A. B., Caudle, W. M., Perez, X. A. & other authors (2007). Increased vulnerability of nigrostriatal terminals in DJ-1-deficient mice is mediated by the dopamine transporter. *Neurobiol Dis* **27**, 141-150.

Marshall, L. E. & Himes, R. H. (1978). Rotenone inhibition of tubulin self-assembly. *Biochim Biophys Acta* **543**, 590-594.

Martins, L. M., Iaccarino, I., Tenev, T. & other authors (2002). The serine protease Omi/HtrA2 regulates apoptosis by binding XIAP through a reaper-like motif. *J Biol Chem* **277**, 439-444.

Martins, L. M., Morrison, A., Klupsch, K. & other authors (2004). Neuroprotective role of the Reaper-related serine protease HtrA2/Omi revealed by targeted deletion in mice. *Mol Cell Biol* **24**, 9848-9862.

Masliah, E., Rockenstein, E., Veinbergs, I., Mallory, M., Hashimoto, M., Takeda, A., Sagara, Y., Sisk, A. & Mucke, L. (2000). Dopaminergic loss and inclusion body formation in alpha-synuclein mice: implications for neurodegenerative disorders. *Science* **287**, 1265-1269.

Matsuoka, Y., Vila, M., Lincoln, S. & other authors (2001). Lack of nigral pathology in transgenic mice expressing human alpha-synuclein driven by the tyrosine hydroxylase promoter. *Neurobiol Dis* **8**, 535-539.

Matuja, W. B. & Aris, E. A. (2008). Motor and non-motor features of Parkinson's disease. *East Afr Med J* **85**, 3-9.

McLean, P. J., Kawamata, H., Ribich, S. & Hyman, B. T. (2000). Membrane association and protein conformation of alpha-synuclein in intact neurons. Effect of Parkinson's disease-linked mutations. *J Biol Chem* **275**, 8812-8816.

McNaught, K. S. & Jenner, P. (2001). Proteasomal function is impaired in substantia nigra in Parkinson's disease. *Neurosci Lett* **297**, 191-194.

McNaught, K. S., Olanow, C. W., Halliwell, B., Isacson, O. & Jenner, P. (2001). Failure of the ubiquitin-proteasome system in Parkinson's disease. *Nat Rev Neurosci* **2**, 589-594.

Mills, R. D., Sim, C. H., Mok, S. S., Mulhern, T. D., Culvenor, J. G. & Cheng, H. C. (2008). Biochemical aspects of the neuroprotective mechanism of PTEN-induced kinase-1 (PINK1). *J Neurochem* **105**, 18-33.

Mindham, R. H. (1970). Psychiatric symptoms in Parkinsonism. *J Neurol Neurosurg Psychiatry* **33**, 188-191.

Mitsumoto, A. & Nakagawa, Y. (2001). DJ-1 is an indicator for endogenous reactive oxygen species elicited by endotoxin. *Free Radic Res* **35**, 885-893.

Mizuno, Y., Ohta, S., Tanaka, M., Takamiya, S., Suzuki, K., Sato, T., Oya, H., Ozawa, T. & Kagawa, Y. (1989). Deficiencies in complex I subunits of the respiratory chain in Parkinson's disease. *Biochem Biophys Res Commun* **163**, 1450-1455.

Mizuno, Y., Hattori, N., Kubo, S. & other authors (2008). Review. Progress in the pathogenesis and genetics of Parkinson's disease. *Philos Trans R Soc Lond B Biol Sci* **363**, 2215-2227.

Moore, D. J., West, A. B., Dawson, V. L. & Dawson, T. M. (2005). Molecular pathophysiology of Parkinson's disease. *Annu Rev Neurosci* **28**, 57-87.

Morais, V. A., Verstreken, P., Roethig, A. & other authors (2009). Parkinson's disease mutations in PINK1 result in decreased Complex I activity and deficient synaptic function. *EMBO Molecular Medicine* **1**, 99-111.

Muqit, M. M. & Feany, M. B. (2002). Modelling neurodegenerative diseases in Drosophila: a fruitful approach? *Nat Rev Neurosci* **3**, 237-243.

Muqit, M. M., Abou-Sleiman, P. M., Saurin, A. T. & other authors (2006). Altered cleavage and localization of PINK1 to aggresomes in the presence of proteasomal stress. *J Neurochem* **98**, 156-169.

Murakami, T., Moriwaki, Y., Kawarabayashi, T. & other authors (2007). PINK1, a gene product of PARK6, accumulates in alpha-synucleinopathy brains. *J Neurol Neurosurg Psychiatry* **78**, 653-654.

Nakabeppu, Y., Tsuchimoto, D., Yamaguchi, H. & Sakumi, K. (2007). Oxidative damage in nucleic acids and Parkinson's disease. *J Neurosci Res* **85**, 919-934.

Neumann, M., Muller, V., Gorner, K., Kretzschmar, H. A., Haass, C. & Kahle, P. J. (2004). Pathological properties of the Parkinson's disease-associated protein DJ-1 in alpha-synucleinopathies and tauopathies: relevance for multiple system atrophy and Pick's disease. *Acta Neuropathol* **107**, 489-496.

Nunnari, J., Marshall, W. F., Straight, A., Murray, A., Sedat, J. W. & Walter, P. (1997). Mitochondrial transmission during mating in Saccharomyces cerevisiae is determined by mitochondrial fusion and fission and the intramitochondrial segregation of mitochondrial DNA. *Mol Biol Cell* **8**, 1233-1242.

Okamoto, K. & Shaw, J. M. (2005). Mitochondrial morphology and dynamics in yeast and multicellular eukaryotes. *Annu Rev Genet* **39**, 503-536.

Olanow, C. W. (2007). The pathogenesis of cell death in Parkinson's disease--2007. *Mov Disord* **22 Suppl 17**, S335-342.

Orth, M. & Schapira, A. H. (2002). Mitochondrial involvement in Parkinson's disease. *Neurochem Int* **40**, 533-541.

Palacino, J. J., Sagi, D., Goldberg, M. S., Krauss, S., Motz, C., Wacker, M., Klose, J. & Shen, J. (2004). Mitochondrial dysfunction and oxidative damage in parkin-deficient mice. *J Biol Chem* **279**, 18614-18622.

Park, J., Lee, S. B., Lee, S. & other authors (2006). Mitochondrial dysfunction in Drosophila PINK1 mutants is complemented by parkin. *Nature* **441**, 1157-1161.

Park, J., Lee, G. & Chung, J. (2009). The PINK1-Parkin pathway is involved in the regulation of mitochondrial remodeling process. *Biochem Biophys Res Commun* **378**, 518-523.

Perez, F. A. & Palmiter, R. D. (2005). Parkin-deficient mice are not a robust model of parkinsonism. *Proc Natl Acad Sci U S A* **102**, 2174-2179.

Perry, T. L., Godin, D. V. & Hansen, S. (1982). Parkinson's disease: a disorder due to nigral glutathione deficiency? *Neurosci Lett* **33**, 305-310.

Petit, A., Kawarai, T., Paitel, E. & other authors (2005). Wild-type PINK1 prevents basal and induced neuronal apoptosis, a protective effect abrogated by Parkinson disease-related mutations. *J Biol Chem* **280**, 34025-34032.

Plun-Favreau, H., Klupsch, K., Moisoi, N. & other authors (2007). The mitochondrial protease HtrA2 is regulated by Parkinson's disease-associated kinase PINK1. *Nat Cell Biol* **9**, 1243-1252.

Poewe, W. (2008). Non-motor symptoms in Parkinson's disease. *Eur J Neurol* **15 Suppl 1**, 14-20.

Polymeropoulos, M. H., Lavedan, C., Leroy, E. & other authors (1997). Mutation in the alpha-synuclein gene identified in families with Parkinson's disease. *Science* **276**, 2045-2047.

Poole, A. C., Thomas, R. E., Andrews, L. A., McBride, H. M., Whitworth, A. J. & Pallanck, L. J. (2008). The PINK1/Parkin pathway regulates mitochondrial morphology. *Proc Natl Acad Sci U S A* **105**, 1638-1643.

Prakash, N. & Wurst, W. (2004). Specification of midbrain territory. *Cell Tissue Res* **318**, 5-14.

Pridgeon, J. W., Olzmann, J. A., Chin, L. S. & Li, L. (2007). PINK1 Protects against Oxidative Stress by Phosphorylating Mitochondrial Chaperone TRAP1. *PLoS Biol* **5**, e172.

Ramirez, A., Heimbach, A., Grundemann, J. & other authors (2006). Hereditary parkinsonism with dementia is caused by mutations in ATP13A2, encoding a lysosomal type 5 P-type ATPase. *Nat Genet* **38**, 1184-1191.

Rathke-Hartlieb, S., Kahle, P. J., Neumann, M., Ozmen, L., Haid, S., Okochi, M., Haass, C. & Schulz, J. B. (2001). Sensitivity to MPTP is not increased in Parkinson's disease-associated mutant alpha-synuclein transgenic mice. *J Neurochem* **77**, 1181-1184.

Ren, Y., Liu, W., Jiang, H., Jiang, Q. & Feng, J. (2005). Selective vulnerability of dopaminergic neurons to microtubule depolymerization. *J Biol Chem* **280**, 34105-34112.

Richfield, E. K., Thiruchelvam, M. J., Cory-Slechta, D. A., Wuertzer, C., Gainetdinov, R. R., Caron, M. G., Di Monte, D. A. & Federoff, H. J. (2002). Behavioral and neurochemical effects of wild-type and mutated human alpha-synuclein in transgenic mice. *Exp Neurol* **175**, 35-48.

Rochet, J. C., Outeiro, T. F., Conway, K. A., Ding, T. T., Volles, M. J., Lashuel, H. A., Bieganski, R. M., Lindquist, S. L. & Lansbury, P. T. (2004). Interactions among alpha-synuclein, dopamine, and biomembranes: some clues for understanding neurodegeneration in Parkinson's disease. *J Mol Neurosci* **23**, 23-34.

Rojo, M., Legros, F., Chateau, D. & Lombes, A. (2002). Membrane topology and mitochondrial targeting of mitofusins, ubiquitous mammalian homologs of the transmembrane GTPase Fzo. *J Cell Sci* **115**, 1663-1674.

Rubinsztein, D. C. (2006). The roles of intracellular protein-degradation pathways in neurodegeneration. *Nature* **443**, 780-786.

Saigoh, K., Wang, Y. L., Suh, J. G. & other authors (1999). Intragenic deletion in the gene encoding ubiquitin carboxy-terminal hydrolase in gad mice. *Nat Genet* **23**, 47-51.

Schapira, A. H., Cooper, J. M., Dexter, D., Jenner, P., Clark, J. B. & Marsden, C. D. (1989). Mitochondrial complex I deficiency in Parkinson's disease. *Lancet* **1**, 1269.

Schapira, A. H. (2007). Mitochondrial dysfunction in Parkinson's disease. *Cell Death Differ* **14**, 1261-1266.

Schiesling, C., Kieper, N., Seidel, K. & Kruger, R. (2008). Review: Familial Parkinson's disease--genetics, clinical phenotype and neuropathology in relation to the common sporadic form of the disease. *Neuropathol Appl Neurobiol* **34**, 255-271.

Schmidt-Supprian, M. & Rajewsky, K. (2007). Vagaries of conditional gene targeting. *Nat Immunol* **8**, 665-668.

Schober, A. (2004). Classic toxin-induced animal models of Parkinson's disease: 6-OHDA and MPTP. *Cell Tissue Res* **318**, 215-224.

Schuermann, M. (1990). An expression vector system for stable expression of oncogenes. *Nucleic Acids Res* **18**, 4945-4946.

Schwenk, F., Baron, U. & Rajewsky, K. (1995). A cre-transgenic mouse strain for the ubiquitous deletion of loxP-flanked gene segments including deletion in germ cells. *Nucleic Acids Res* **23**, 5080-5081.

Serpell, L. C., Berriman, J., Jakes, R., Goedert, M. & Crowther, R. A. (2000). Fiber diffraction of synthetic alpha-synuclein filaments shows amyloid-like cross-beta conformation. *Proc Natl Acad Sci U S A* **97**, 4897-4902.

Setsuie, R., Wang, Y. L., Mochizuki, H. & other authors (2007). Dopaminergic neuronal loss in transgenic mice expressing the Parkinson's disease-associated UCH-L1 I93M mutant. *Neurochem Int* **50**, 119-129.

Shen, J. & Cookson, M. R. (2004). Mitochondria and dopamine: new insights into recessive parkinsonism. *Neuron* **43**, 301-304.

Shimura-Miura, H., Hattori, N., Kang, D., Miyako, K., Nakabeppu, Y. & Mizuno, Y. (1999). Increased 8-oxo-dGTPase in the mitochondria of substantia nigral neurons in Parkinson's disease. *Ann Neurol* **46**, 920-924.

Silvestri, L., Caputo, V., Bellacchio, E., Atorino, L., Dallapiccola, B., Valente, E. M. & Casari, G. (2005). Mitochondrial import and enzymatic activity of PINK1 mutants associated to recessive parkinsonism. *Hum Mol Genet* **14**, 3477-3492.

Smith, A. G., Heath, J. K., Donaldson, D. D., Wong, G. G., Moreau, J., Stahl, M. & Rogers, D. (1988). Inhibition of pluripotential embryonic stem cell differentiation by purified polypeptides. *Nature* **336**, 688-690.

Spillantini, M. G., Schmidt, M. L., Lee, V. M., Trojanowski, J. Q., Jakes, R. & Goedert, M. (1997). Alpha-synuclein in Lewy bodies. *Nature* **388**, 839-840.

Strauss, K. M., Martins, L. M., Plun-Favreau, H. & other authors (2005). Loss of function mutations in the gene encoding Omi/HtrA2 in Parkinson's disease. *Hum Mol Genet* **14**, 2099-2111.

Taira, T., Saito, Y., Niki, T., Iguchi-Ariga, S. M., Takahashi, K. & Ariga, H. (2004). DJ-1 has a role in antioxidative stress to prevent cell death. *EMBO Rep* **5**, 213-218.

Tanaka, K., Suzuki, T., Hattori, N. & Mizuno, Y. (2004). Ubiquitin, proteasome and parkin. *Biochim Biophys Acta* **1695**, 235-247.

Tang, B., Xiong, H., Sun, P. & other authors (2006). Association of PINK1 and DJ-1 confers digenic inheritance of early-onset Parkinson's disease. *Hum Mol Genet* **15**, 1816-1825.

Taymans, J. M., Van den Haute, C. & Baekelandt, V. (2006). Distribution of PINK1 and LRRK2 in rat and mouse brain. *J Neurochem* **98**, 951-961.

Terzioglu, M. & Galter, D. (2008). Parkinson's disease: genetic versus toxin-induced rodent models. *FEBS J*.

Todaro, G. J. & Green, H. (1963). Quantitative studies of the growth of mouse embryo cells in culture and their development into established lines. *J Cell Biol* **17**, 299-313.

Unoki, M. & Nakamura, Y. (2001). Growth-suppressive effects of BPOZ and EGR2, two genes involved in the PTEN signaling pathway. *Oncogene* **20**, 4457-4465.

Valente, E. M., Abou-Sleiman, P. M., Caputo, V. & other authors (2004a). Hereditary early-onset Parkinson's disease caused by mutations in PINK1. *Science* **304**, 1158-1160.

Valente, E. M., Salvi, S., Ialongo, T. & other authors (2004b). PINK1 mutations are associated with sporadic early-onset parkinsonism. *Ann Neurol* **56**, 336-341.

van der Stelt, H. M., Breuer, M. E., Olivier, B. & Westenberg, H. G. (2005). Permanent deficits in serotonergic functioning of olfactory bulbectomized rats: an in vivo microdialysis study. *Biol Psychiatry* **57**, 1061-1067.

Vande Walle, L., Lamkanfi, M. & Vandenabeele, P. (2008). The mitochondrial serine protease HtrA2/Omi: an overview. *Cell Death Differ* **15**, 453-460.

Vekrellis, K., Rideout, H. J. & Stefanis, L. (2004). Neurobiology of alpha-synuclein. *Mol Neurobiol* **30**, 1-21.

Verbaan, D., Marinus, J., Visser, M., van Rooden, S. M., Stiggelbout, A. M., Middelkoop, H. A. & van Hilten, J. J. (2007). Cognitive impairment in Parkinson's disease. *J Neurol Neurosurg Psychiatry* **78**, 1182-1187.

Verbaan, D., van Rooden, S. M., Visser, M., Marinus, J. & van Hilten, J. J. (2008). Nighttime sleep problems and daytime sleepiness in Parkinson's disease. *Mov Disord* **23**, 35-41.

Vercammen, L., Van der Perren, A., Vaudano, E., Gijsbers, R., Debyser, Z., Van den Haute, C. & Baekelandt, V. (2006). Parkin protects against neurotoxicity in the 6-hydroxydopamine rat model for Parkinson's disease. *Mol Ther* **14**, 716-723.

Verstreken, P., Ly, C. V., Venken, K. J., Koh, T. W., Zhou, Y. & Bellen, H. J. (2005). Synaptic mitochondria are critical for mobilization of reserve pool vesicles at Drosophila neuromuscular junctions. *Neuron* **47**, 365-378.

Vila, M. & Przedborski, S. (2004). Genetic clues to the pathogenesis of Parkinson's disease. *Nat Med* **10 Suppl**, S58-62.

Von Coelln, R., Thomas, B., Savitt, J. M., Lim, K. L., Sasaki, M., Hess, E. J., Dawson, V. L. & Dawson, T. M. (2004). Loss of locus coeruleus neurons

and reduced startle in parkin null mice. *Proc Natl Acad Sci U S A* **101**, 10744-10749.

Vu, P. K. & Sakamoto, K. M. (2000). Ubiquitin-mediated proteolysis and human disease. *Mol Genet Metab* **71**, 261-266.

Wang, D., Qian, L., Xiong, H. & other authors (2006). Antioxidants protect PINK1-dependent dopaminergic neurons in Drosophila. *Proc Natl Acad Sci U S A* **103**, 13520-13525.

Wang, H. L., Chou, A. H., Yeh, T. H., Li, A. H., Chen, Y. L., Kuo, Y. L., Tsai, S. R. & Yu, S. T. (2007). PINK1 mutants associated with recessive Parkinson's disease are defective in inhibiting mitochondrial release of cytochrome c. *Neurobiol Dis* **28**, 216-226.

Wen, L., Wei, W., Gu, W., Huang, P., Ren, X., Zhang, Z., Zhu, Z., Lin, S. & Zhang, B. (2008). Visualization of monoaminergic neurons and neurotoxicity of MPTP in live transgenic zebrafish. *Dev Biol* **314**, 84-92.

Williams, R. L., Hilton, D. J., Pease, S. & other authors (1988). Myeloid leukaemia inhibitory factor maintains the developmental potential of embryonic stem cells. *Nature* **336**, 684-687.

Wilson, P. O., Barber, P. C., Hamid, Q. A., Power, B. F., Dhillon, A. P., Rode, J., Day, I. N., Thompson, R. J. & Polak, J. M. (1988). The immunolocalization of protein gene product 9.5 using rabbit polyclonal and mouse monoclonal antibodies. *Br J Exp Pathol* **69**, 91-104.

Yamaguchi, H. & Shen, J. (2007). Absence of dopaminergic neuronal degeneration and oxidative damage in aged DJ-1-deficient mice. *Mol Neurodegener* **2**, 10.

Yamazaki, K., Wakasugi, N., Tomita, T., Kikuchi, T., Mukoyama, M. & Ando, K. (1988). Gracile axonal dystrophy (GAD), a new neurological mutant in the mouse. *Proc Soc Exp Biol Med* **187**, 209-215.

Yang, Y., Gehrke, S., Imai, Y. & other authors (2006). Mitochondrial pathology and muscle and dopaminergic neuron degeneration caused by inactivation of Drosophila Pink1 is rescued by Parkin. *Proc Natl Acad Sci U S A* **103**, 10793-10798.

Yang, Y., Ouyang, Y., Yang, L., Beal, M. F., McQuibban, A., Vogel, H. & Lu, B. (2008). Pink1 regulates mitochondrial dynamics through interaction with the fission/fusion machinery. *Proc Natl Acad Sci U S A* **105**, 7070-7075.

Yoritaka, A., Hattori, N., Uchida, K., Tanaka, M., Stadtman, E. R. & Mizuno, Y. (1996). Immunohistochemical detection of 4-hydroxynonenal protein adducts in Parkinson disease. *Proc Natl Acad Sci U S A* **93**, 2696-2701.

Youdim, M. B., Ben-Shachar, D. & Riederer, P. (1989). Is Parkinson's disease a progressive siderosis of substantia nigra resulting in iron and melanin induced neurodegeneration? *Acta Neurol Scand Suppl* **126**, 47-54.

Zhang, L., Shimoji, M., Thomas, B. & other authors (2005). Mitochondrial localization of the Parkinson's disease related protein DJ-1: implications for pathogenesis. *Hum Mol Genet* **14**, 2063-2073.

Zhivotovsky, B. & Kroemer, G. (2004). Apoptosis and genomic instability. *Nat Rev Mol Cell Biol* **5**, 752-762.

Zhou, H., Falkenburger, B. H., Schulz, J. B., Tieu, K., Xu, Z. & Xia, X. G. (2007). Silencing of the Pink1 gene expression by conditional RNAi does not induce dopaminergic neuron death in mice. *Int J Biol Sci* **3**, 242-250.

Zimprich, A., Biskup, S., Leitner, P. & other authors (2004). Mutations in LRRK2 cause autosomal-dominant parkinsonism with pleomorphic pathology. *Neuron* **44**, 601-607.

Danksagung

Mein Dank gilt an erster Stelle Herrn Prof. Dr. Wolfgang Wurst, der mir die Möglichkeit gab, das Projekt dieser Dissertation an seinem Institut durchzuführen. Ich habe dadurch umfangreiche Kenntnisse im Gebiet der molekularen Neurogenetik erlangt. Ebenfalls dankbar bin ich für seine vielfältigen Ideen, die meine Begeisterung für die Wissenschaft ebenso gesteigert haben, wie seine konstruktive Kritik. Frau Dr. Daniela Vogt Weisenhorn danke ich für ihre exzellente Betreuung in wissenschaftlichen Fragen und allen anderen Belangen während meiner Doktorarbeit. Die konstruktiven Diskussionen mit ihr haben wesentlich zu meiner Motivation beigetragen, meine wissenschaftliche und analytische Denkweise angeregt, meine Argumentationsfähigkeit geschult und mir gezeigt, wie wichtig es ist, immer wieder ‚über den Tellerrand hinauszuschauen'. Sowohl praktisch wie auch theoretisch habe ich sehr viel von ihr gelernt, worüber ich sehr dankbar bin. Ich bin ebenfalls sehr dankbar für die mir gewährten Freiräume in der Planung, Gestaltung und Durchführung meiner Dissertation, die meine Kreativität und meine Selbstständigkeit gefördert haben.

Weiterhin gilt mein Dank Herrn Prof. Dr. Gierl und Herrn Prof. Dr. Schneitz für ihre Bereitschaft, meine Dissertation zu beurteilen und die Promotionsprüfung durchzuführen. Herrn Dr. Ralf Kühn danke ich für die Planung der targeting Strategie und seine beratende Unterstützung in genetischen Fragen. Ebenso danke ich Barbara Di Benedetto für die Vorarbeit und Zusammenarbeit bei der Klonierung des Konstrukts. Herzlicher Dank an die technischen Angestellten des Instituts, besonders Ira, Susanne Bourier, Miriam, Helga, und allen voran Annerose Kurz-Drexler für ihre Unterstützung und Hilfsbereitschaft bei zahlreichen Experimenten. Mein Dank gilt außerdem dem Injektionsteam um Susi und Adrianne, sowie dem Team von Dr. Sabine Hölter-Koch, besonders Lisa Glasl, ohne die aus meine positiven Klonen keine Mäuse geworden wären bzw. diese auch nicht verhaltenstechnisch hätten analysiert werden können. Ebenfalls danke ich allen Tierpflegern in der DoBe und Quarantäne, die sich um ‚meine Mäuse' gekümmert haben, für ihre Hilfe. Ich möchte auch allen Kollegen des IDG für die angenehme und freundschaftliche Arbeitsatmosphäre danken. Weiterhin danke ich den ‚Neurodegenerationists'

Florian, Trang, Jingzhong, Weiqian, Cordula, Betti und Karina für ihre praktische Hilfe und zahlreiche Gespräche, Anregungen und Diskussionen. Ich danke den ‚Mädels vom mittleren Labor' und den Leuten vom ‚hinteren Büro' für die lustige Atmosphäre, ihr Engagement und ihre Hilfsbereitschaft. Persönlich möchte ich besonders meiner Kollegin Patricia Steuber-Buchberger für zahlreiche wissenschaftliche und nicht-wissenschaftliche Gespräche, ihre Hilfsbereitschaft und ihre Freundschaft danken.

Meiner Familie und meinen Freunden danke ich ganz besonders, dass sie mich durch ihren Rückhalt und ihren Zuspruch immer bestärkt haben. Ein dickes Dankeschön geht an meine Mama, die mir in den ganzen Jahren meines Studiums und meiner Promotion immer zur Seite stand, für ihre Geduld mit ‚meiner Wissenschaft', ihre Motivation und ihre uneingeschränkte Unterstützung. Ihr habt mir alle sehr geholfen, meinen Weg erfolgreich zu gehen!

Erklärung

Ich erkläre an Eides statt, dass ich die der Fakultät für

Ernährung, Landnutzung und Umwelt

der Technischen Universität München zur Promotionsprüfung

vorgelegte Arbeit mit dem Titel:

Generation and analysis of a Pink1 deficient mouse model for Parkinson's disease

in Institut für Entwicklungsgenetik, Helmholtz Zentrum München

.....
(Institut, Klinik, Krankenhaus, Abteilung)

unter der Anleitung und Betreuung durch

.....

Prof. Dr. Wolfgang Wurst

.....

ohne sonstige Hilfe erstellt und bei der Abfassung nur die gemäß § 6 Abs. 5 angegebenen Hilfsmittel benutzt habe.

(**X**) Ich habe die Dissertation in dieser oder ähnlicher Form in keinem anderen Prüfungsverfahren als Prüfungsleistung vorgelegt.

( ) Die vollständige Dissertation wurde in .....
..... veröffentlicht. Die Fakultät für
..... hat der Vorveröffentlichung zugestimmt.

(**X**) Ich habe den angestrebten Doktorgrad noch nicht erworben und bin nicht in einem früheren Promotionsverfahren für den angestrebten Doktorgrad endgültig gescheitert.

( ) Ich habe bereits am ..... bei der Fakultät für .....
der Hochschule .....
unter Vorlage einer Dissertation mit dem Thema .....
.....
die Zulassung zur Promotion beantragt mit dem Ergebnis:
.....

Die Promotionsordnung der Technischen Universität München ist mir bekannt.

München, den ....
Unterschrift